

Contents

Glossary	xiii
Acronyms	xv
1 Introduction and Literature Review	1
1.1 Cancer Research in the Post-Genomic Era	1
1.1.1 Cancer is a Global Health Issue	2
1.1.1.1 The Genetics and Molecular Biology of Cancers	3
1.1.2 The genomic Revolution in Cancer Research	4
1.1.2.1 High-Throughput Technologies	4
1.1.2.2 Bioinformatics and Genomic Data	6
1.1.3 Genomics Projects	6
1.1.3.1 The Cancer Genome Project	6
1.1.3.2 The Cancer Genome Atlas Project	7
1.1.4 Genomic Cancer Medicine	9
1.1.4.1 Cancer Genes and Driver Mutations	9
1.1.4.2 Precision Cancer Medicine	10
1.1.4.3 Molecular Diagnostics and Pan-Cancer Medicine	10
1.1.4.4 Targeted Therapeutics and Pharmacogenomics	10
1.1.5 Systems and Network Biology	11
1.1.5.1 Network Medicine and Polypharmacology	13
1.2 A Synthetic Lethal Approach to Cancer Medicine	14
1.2.1 Synthetic Lethal Genetic Interactions	14
1.2.2 Synthetic Lethal Concepts in Genetics	15
1.2.3 Synthetic Lethality in Model Systems	16
1.2.3.1 Synthetic Lethal Pathways and Networks	16
1.2.3.2 Evolution of Synthetic Lethality	17
1.2.4 Synthetic Lethality in Cancer	18
1.2.5 Clinical Impact of Synthetic Lethality in Cancer	19
1.2.6 High-throughput Screening for Synthetic Lethality	21
1.2.6.1 Synthetic Lethal Screens	22
1.2.7 Computational Prediction of Synthetic Lethality	25
1.2.7.1 Bioinformatics Approaches to Genetic Interactions	25
1.2.7.2 Comparative Genomics	26
1.2.7.3 Analysis and Modelling of Protein Data	29
1.2.7.4 Differential Gene Expression	31

1.2.7.5	Data Mining and Machine Learning	32
1.2.7.6	Mutually Exclusive Bimodality	35
1.2.7.7	Rationale for Further Development	36
1.3	E-cadherin as a Synthetic Lethal Target	36
1.3.1	The <i>CDH1</i> gene and its Biological Functions	36
1.3.1.1	Cytoskeleton	37
1.3.1.2	Extracellular and Tumour Micro-environment	37
1.3.1.3	Cell-Cell Adhesion and Signalling	37
1.3.2	<i>CDH1</i> as a Tumour (and Invasion) Suppressor	38
1.3.2.1	Breast Cancers and Invasion	38
1.3.3	Hereditary Diffuse Gastric Cancer and Lobular Breast Cancer	38
1.3.4	Cell Line Models of <i>CDH1</i> Null Mutations	40
1.4	Summary and Research Direction of Thesis	40
1.4.1	Thesis Aims	42
2	Methods and Resources	43
2.1	Bioinformatics Resources for Genomics Research	43
2.1.1	Public Data and Software Packages	43
2.1.1.1	Cancer Genome Atlas Data	44
2.1.1.2	Reactome and Annotation Data	45
2.2	Data Handling	45
2.2.1	Normalisation	45
2.2.2	Sample Triage	46
2.2.3	Metagenes and the Singular Value Decomposition	46
2.2.3.1	Candidate Triage and Integration with Screen Data . .	48
2.3	Techniques	49
2.3.1	Statistical Procedures and Tests	49
2.3.2	Gene Set Over-representation Analysis	50
2.3.3	Clustering	50
2.3.4	Heatmap	50
2.3.5	mMdelling and Simulations	51
2.3.5.1	Receiver Operating Characteristic (Performance) . .	52
2.3.6	Resampling Analysis	52
2.4	Pathway Structure Methods	53
2.4.1	Network and Graph Analysis	53
2.4.2	Sourcing Graph Structure Data	54
2.4.3	Constructing Pathway Subgraphs	54
2.4.4	Network Analysis Metrics	55
2.5	Implementation	56
2.5.1	Computational Resources and Linux Utilities	56
2.5.2	R Language and Packages	57
2.5.3	High Performance and Parallel Computing	60

3 Methods Developed During Thesis	62
3.1 A Synthetic Lethal Detection Methodology	62
3.2 Synthetic Lethal Simulation and Modelling	64
3.2.1 A Model of Synthetic Lethality in Expression Data	65
3.2.2 Simulation Procedure	69
3.3 Detecting Simulated Synthetic Lethal Partners	71
3.3.1 Binomial Simulation of Synthetic Lethality	72
3.3.2 Multivariate Normal Simulation of Synthetic Lethality	74
3.3.2.1 Multivariate Normal Simulation with Correlated Genes	76
3.3.2.2 Specificity with Query-Correlated Pathways	83
3.4 Graph Structure Methods	86
3.4.1 Upstream and Downstream Gene Detection	86
3.4.1.1 Permutation Analysis for Statistical Significance	87
3.4.1.2 Hierarchy Based on Biological Context	87
3.4.2 Simulating Gene Expression from Graph Structures	88
3.5 Customised Functions and Packages Developed	93
3.5.1 Synthetic Lethal Interaction Prediction Tool	93
3.5.2 Data Visualisation	94
3.5.3 Extensions to the iGraph Package	96
3.5.3.1 Sampling Simulated Data from Graph Structures	96
3.5.3.2 Plotting Directed Graph Structures	96
3.5.3.3 Computing Information Centrality	97
3.5.3.4 Testing Pathway Structure with Permutation Testing .	97
3.5.3.5 Metapackage to Install iGraph Functions	98
4 Synthetic Lethal Analysis of Gene Expression Data	99
4.1 Synthetic Lethal Genes in Breast Cancer	100
4.1.1 Synthetic Lethal Pathways in Breast Cancer	102
4.1.2 Expression Profiles of Synthetic Lethal Partners	103
4.1.2.1 Subgroup Pathway Analysis	106
4.2 Comparing Synthetic Lethal Gene Candidates	109
4.2.1 Primary siRNA Screen Candidates	109
4.2.2 Comparison with Correlation	109
4.2.3 Comparison with Primary Screen Viability	111
4.2.4 Comparison with Secondary siRNA Screen Validation	113
4.2.5 Comparison to Primary Screen at Pathway Level	115
4.2.5.1 Resampling Genes for Pathway Enrichment	117
4.2.6 Integrating Synthetic Lethal Pathways and Screens	120
4.3 Metagene Analysis	122
4.3.1 Pathway Expression	123
4.3.2 Somatic Mutation	125
4.3.3 Synthetic Lethal Pathway Metagenes	129
4.3.4 Synthetic Lethality in Breast Cancer	130
4.4 Replication in Stomach Cancer	131
4.5 Discussion	132
4.5.1 Strengths of the SLIPT Methodology	132

4.5.2	Synthetic Lethal Pathways for E-cadherin	133
4.5.3	Replication and Validation	135
4.5.3.1	Integration with short interfering RNA (siRNA) Screening	135
4.5.3.2	Replication across Tissues	136
4.6	Summary	136
5	Synthetic Lethal Pathway Structure	138
5.1	Synthetic Lethal Genes in Reactome Pathways	138
5.1.1	The PI3K/AKT Pathway	139
5.1.2	The Extracellular Matrix	141
5.1.3	G Protein Coupled Receptors	144
5.1.4	Gene Regulation and Translation	144
5.2	Network Analysis of Synthetic Lethal Genes	145
5.2.1	Gene Connectivity and Vertex Degree	146
5.2.2	Gene Importance and Centrality	147
5.2.2.1	Information Centrality	147
5.2.2.2	PageRank Centrality	149
5.3	Relationships between Synthetic Lethal Genes	151
5.3.1	Hierarchical Pathway Structure	151
5.3.1.1	Contextual Hierarchy of PI3K	151
5.3.1.2	Testing Contextual Hierarchy of Synthetic Lethal Genes	151
5.3.2	Upstream or Downstream Synthetic Lethality	155
5.3.2.1	Measuring Structure of Candidates within PI3K	155
5.3.2.2	Resampling for Synthetic Lethal Pathway Structure . .	157
5.4	Discussion	159
5.5	Summary	161
6	Simulation and mMdelling of Synthetic Lethal Pathways	163
6.1	Synthetic Lethal Detection Methods	164
6.1.1	Performance of SLIPT and χ^2 across Quantiles	164
6.1.1.1	Correlated Query Genes affects Specificity	168
6.1.2	Alternative Synthetic Lethal Detection Strategies	170
6.1.2.1	Correlation for Synthetic Lethal Detection	170
6.1.2.2	Testing for Bimodality with BiSEp	172
6.2	Simulations with Graph Structures	173
6.2.1	Performance over Graph Structures	174
6.2.1.1	Simple Graph Structures	174
6.2.1.2	Constructed Graph Structures	176
6.2.2	Performance with Inhibitions	179
6.2.3	Synthetic Lethality across Graph Structures	184
6.2.4	Performance within a Simulated Human Genome	188
6.3	Simulations in More Complex Graph Structures	192
6.3.1	Simulations over Pathway-based Graphs	193
6.3.2	Pathway Structures in a Simulated Human Genome	196
6.4	Discussion	199

6.4.1	Simulation Procedure	199
6.4.2	Comparing Methods with Simulated Data	200
6.4.3	Design and Performance of SLIPT	201
6.4.4	Simulations from Graph Structures	203
6.5	Summary	204
7	Discussion	206
7.1	Synthetic Lethality and <i>CDH1</i> Biology	206
7.1.1	Established Functions of <i>CDH1</i>	207
7.1.2	The Molecular Role of <i>CDH1</i> in Cancer	207
7.2	Significance	208
7.2.1	Synthetic Lethality in the Genomic Era	208
7.2.2	Clinical Interventions based on Synthetic Lethality	210
7.3	Future Directions	211
7.4	Conclusions	213
	Bibliography	215
A	Sample Quality	239
A.1	Sample Correlation	239
A.2	Replicate Samples in The Cancer Genome Atlas (TCGA) Breast	241
B	Software Used for Thesis	245
C	Mutation Analysis in Breast Cancer	254
C.1	Synthetic Lethal Genes and Pathways	254
C.2	Synthetic Lethal Expression Profiles	257
C.3	Comparison to Primary Screen	260
C.3.1	Resampling Analysis	262
C.4	Compare Synthetic Lethal Interaction Prediction Tool (SLIPT) genes .	264
C.5	Metagene Analysis	266
C.6	Expression of Somatic Mutations	267
C.7	Metagene Expression Profiles	270
D	Intrinsic Subtyping	273
E	Stomach Expression Analysis	275
E.1	Synthetic Lethal Genes and Pathways	275
E.2	Comparison to Primary Screen	279
E.2.1	Resampling Analysis	281
E.3	Metagene Analysis	283
F	Synthetic Lethal Genes in Pathways	285
G	Pathway Connectivity for Mutation SLIPT	293
H	Information Centrality for Gene Essentiality	297

I Pathway Structure for Mutation SLIPT	300
J Performance of SLIPT and χ^2	303
J.1 Correlated Query Genes affects Specificity	309
K Simulations on Graph Structures	315
K.0.1 Simulations from Inhibiting Graph Structures	316
K.1 Simulation across Graph Structures	319
K.2 Simulations from Complex Graph Structures	323
K.2.1 Simulations from Complex Inhibiting Graphs	326
K.3 Simulations from Pathway Graph Structures	332

List of Figures

1.1	Synthetic genetic interactions	15
1.2	Synthetic lethality in cancer	19
2.1	Read count density	47
2.2	Read count sample mean	47
3.1	Framework for synthetic lethal prediction	63
3.2	Synthetic lethal prediction adapted for mutation	64
3.3	A model of synthetic lethal gene expression	66
3.4	Modelling synthetic lethal gene expression	67
3.5	Synthetic lethality with multiple genes	68
3.6	Simulating gene function	70
3.7	Simulating synthetic lethal gene function	70
3.8	Simulating synthetic lethal gene expression	71
3.9	Performance of binomial simulations	73
3.10	Comparison of statistical performance	73
3.11	Performance of multivariate normal simulations	75
3.12	Simulating expression with correlated gene blocks	77
3.13	Simulating expression with correlated gene blocks	78
3.14	Synthetic lethal prediction across simulations	79
3.15	Performance with correlations	80
3.16	Comparison of statistical performance with correlation structure	81
3.17	Performance with query correlations	82
3.18	Statistical evaluation of directional criteria	84
3.19	Performance of directional criteria	85
3.20	Simulated graph structures	89
3.21	Simulating expression from a graph structure	90
3.22	Simulating expression from graph structure with inhibitions	92
3.23	Demonstration of violin plots with custom features	95
3.24	Demonstration of annotated heatmap	95
3.25	Simulating graph structures	97
4.1	Synthetic lethal expression profiles of analysed samples	105
4.2	Comparison of SLIPT to siRNA	109
4.3	Compare SLIPT and siRNA genes with correlation	110
4.4	Compare SLIPT and siRNA genes with correlation	111
4.5	Compare SLIPT and siRNA genes with viability	112

4.6	Compare SLIPT genes with siRNA viability	113
4.7	Resampled intersection of SLIPT and siRNA candidates	117
4.8	Pathway metagene expression profiles	124
4.9	Expression profiles for constituent genes of PI3K	126
4.10	Expression profiles for estrogen receptor related genes	127
4.11	Somatic mutation against the PI3K metagene	128
5.1	synthetic lethality in the PI3K cascade	140
5.2	synthetic lethality in Elastic Fibre Formation	142
5.3	Synthetic lethality in Fibrin Clot Formation	143
5.4	Synthetic lethality and vertex degree	146
5.5	Synthetic lethality and centrality	149
5.6	Synthetic lethality and PageRank	150
5.7	Hierarchical structure of PI3K	152
5.8	Hierarchy score in PI3K against synthetic lethality in PI3K	153
5.9	Structure of synthetic lethality in PI3K	155
5.10	Structure of synthetic lethality resampling in PI3K	156
6.1	Performance of χ^2 and SLIPT across quantiles	166
6.2	Performance of χ^2 and SLIPT across quantiles with more genes	167
6.3	Performance of χ^2 and SLIPT across quantiles with query correlation .	168
6.4	Performance of χ^2 and SLIPT across quantiles with query correlation and more genes	169
6.5	Performance of negative correlation and SLIPT	171
6.6	Simple graph structures	174
6.7	Performance of simulations on a simple graph	175
6.8	Performance of simulations is similar in simple graphs	177
6.9	Performance of simulations on a pathway	178
6.10	Performance of simulations on a simple graph with inhibition	180
6.11	Performance is higher on a simple inhibiting graph	181
6.12	Performance of simulations on a constructed graph with inhibition . . .	182
6.13	Performance is affected by inhibition in graphs	184
6.14	Detection of synthetic lethality within a graph structure	186
6.15	Performance of simulations including a simple graph	189
6.16	Performance on a simple graph improves with more genes	190
6.17	Performance on an inhibiting graph improves with more genes	192
6.18	Performance of simulations on the PI3K cascade	195
6.19	Performance of simulations including the PI3K cascade	197
6.20	Performance on pathways improves with more genes	198
A.1	Correlation profiles of removed samples	239
A.2	Correlation analysis and sample removal	240
A.3	Replicate excluded samples	241
A.4	Replicate samples with all remaining	242
A.5	Replicate samples with some excluded	243
C.1	Synthetic lethal expression profiles of analysed samples	258

C.2	Comparison of mtSLIPT to siRNA	260
C.3	Compare mtSLIPT and siRNA genes with correlation	264
C.4	Compare mtSLIPT and siRNA genes with correlation	264
C.5	Compare mtSLIPT and siRNA genes with siRNA viability	265
C.6	Somatic mutation against PIK3CA metagene	267
C.7	Somatic mutation against PI3K protein	268
C.8	Somatic mutation against AKT protein	269
C.9	Pathway metagene expression profiles	270
C.10	Expression profiles for p53 related genes	271
C.11	Expression profiles for BRCA related genes	272
E.1	Synthetic lethal expression profiles of stomach samples	277
E.2	Comparison of SLIPT in stomach to siRNA	279
F.1	Synthetic lethality in the PI3K/AKT pathway	285
F.2	Synthetic lethality in the PI3K/AKT pathway in cancer	286
F.3	Synthetic lethality in the Extracellular Matrix	287
F.4	Synthetic lethality in the GPCRs	288
F.5	Synthetic lethality in the GPCR Downstream	289
F.6	Synthetic lethality in the Translation Elongation	290
F.7	Synthetic lethality in the Nonsense-mediated Decay	291
F.8	Synthetic lethality in the 3' UTR	292
G.1	Synthetic lethality and vertex degree	293
G.2	Synthetic lethality and centrality	294
G.3	Synthetic lethality and PageRank	295
H.1	Information centrality distribution	299
I.1	Synthetic lethality and heirarchy score in PI3K	300
I.2	Heirarchy score in PI3K against synthetic lethality in PI3K	301
I.3	Structure of synthetic lethality in PI3K	301
I.4	Structure of synthetic lethality resampling	302
J.1	Performance of χ^2 and SLIPT across quantiles	303
J.2	Performance of χ^2 and SLIPT across quantiles	305
J.3	Performance of χ^2 and SLIPT across quantiles with more genes	307
J.4	Performance of χ^2 and SLIPT across quantiles with query correlation	309
J.5	Performance of χ^2 and SLIPT across quantiles with query correlation	311
J.6	Performance of χ^2 and SLIPT across quantiles with query correlation and more genes	313
K.1	Performance of simulations on a simple graph	315
K.2	Performance of simulations on an inhibiting graph	316
K.3	Performance of simulations on a constructed graph with inhibition	317
K.4	Performance of simulations on a constructed graph with inhibition	318
K.5	Detection of synthetic lethality within a graph structure	319
K.6	Detection of synthetic lethality within an inhibiting graph	321

K.7	Detection of synthetic lethality within an inhibiting graph	322
K.8	Performance of simulations on a branching graph	323
K.9	Performance of simulations on a complex graph	324
K.10	Performance of simulations on a large graph	325
K.11	Performance of simulations on a branching graph with inhibition	326
K.12	Performance of simulations on a branching graph with inhibition	327
K.13	Performance of simulations on a complex graph with inhibition	328
K.14	Performance of simulations on a complex graph with inhibition	329
K.15	Performance of simulations on a large constructed graph with inhibition	330
K.16	Performance of simulations on a large constructed graph with inhibition	331
K.17	Performance of simulations on the $G_{\alpha i}$ signalling pathway	332
K.18	Performance of simulations including the $G_{\alpha i}$ signalling pathway	333

List of Tables

1.1	Methods for predicting genetic interactions	26
1.2	Methods for predicting synthetic lethality in cancer	27
1.3	Methods used by Wu <i>et al.</i> (2014)	28
2.1	Excluded samples by batch and clinical characteristics.	46
2.2	Computers used during thesis	56
2.3	Linux utilities and applications used during thesis	57
2.4	R installations used during thesis	58
2.5	R Packages used during thesis	58
2.6	R packages developed during thesis	60
4.1	Candidate synthetic lethal gene partners of <i>CDH1</i> from SLIPT	101
4.2	Pathways for <i>CDH1</i> partners from SLIPT	103
4.3	Pathways for clusters of <i>CDH1</i> partners from SLIPT	107
4.4	ANOVA for synthetic lethality and correlation with <i>CDH1</i>	111
4.5	Comparing SLIPT genes against secondary siRNA screen	114
4.6	Pathways for <i>CDH1</i> partners from SLIPT and siRNA	116
4.7	Pathways for <i>CDH1</i> partners from SLIPT	119
4.8	Pathways for <i>CDH1</i> partners from SLIPT and siRNA primary screen	121
4.9	Candidate synthetic lethal metagenes against <i>CDH1</i> from SLIPT	130
5.1	ANOVA for synthetic lethality and vertex degree	147
5.2	ANOVA for synthetic lethality and information centrality	149
5.3	ANOVA for synthetic lethality and PageRank centrality	151
5.4	ANOVA for synthetic lethality and PI3K hierarchy	154
5.5	Resampling for pathway structure of synthetic lethal detection methods	158
B.1	Complete list of R packages used during this thesis	245
C.1	Candidate synthetic lethal gene partners of <i>CDH1</i> from mtSLIPT	255
C.2	Pathways for <i>CDH1</i> partners from mtSLIPT	256
C.3	Pathways for clusters of <i>CDH1</i> partners from mtSLIPT	259
C.4	Pathways for <i>CDH1</i> partners from mtSLIPT and siRNA	261
C.5	Pathways for <i>CDH1</i> partners from mtSLIPT	262
C.6	Pathways for <i>CDH1</i> partners from mtSLIPT and siRNA primary screen	263
C.7	Candidate synthetic lethal metagenes against <i>CDH1</i> from mtSLIPT	266
D.1	Comparison of intrinsic subtypes	273

E.1	Synthetic lethal gene partners of <i>CDH1</i> from SLIPT in stomach cancer	275
E.2	Pathways for <i>CDH1</i> partners from SLIPT in stomach cancer	276
E.3	Pathways for clusters of <i>CDH1</i> partners in stomach SLIPT	278
E.4	Pathways for <i>CDH1</i> partners from SLIPT and siRNA	280
E.5	Pathways for <i>CDH1</i> partners from SLIPT in stomach cancer	281
E.6	Pathways for <i>CDH1</i> partners from SLIPT in stomach and siRNA	282
E.7	Synthetic lethal metagenes against <i>CDH1</i> in stomach cancer	283
G.1	ANOVA for synthetic lethality and vertex degree	296
G.2	ANOVA for synthetic lethality and information centrality	296
G.3	ANOVA for synthetic lethality and PageRank centrality	296
H.1	Information centrality for genes and molecules in the Reactome network	298
I.1	ANOVA for synthetic lethality and PI3K hierarchy	300
I.2	Resampling for pathway structure of synthetic lethal detection methods	302

Glossary

allele	A gene variant with a specific sequence and phenotype.
bioinformatics	Statistical or computational approaches to biological data or research tools.
centrality	A network metric which identifies important <i>vertices</i> .
copy number	The number of copies of DNA, typically two copies for diploid organisms but subject to variation.
E-cadherin	Epithelial cadherin (calcium-dependent adhesion), a cell-adhesion protein encoded by <i>CDH1</i> .
edge or link	A relationship connecting a pair of elements of a graph structure or network, may be weighted or directional.
essential	A gene which is required to be functional or expressed for a cell or organism to be viable, grow or develop.
gene expression	A measure of the relative expression of each gene from the mRNA extracted from (pooled) cells.
genome	An analysis of all of the DNA sequence in the genome.
genomic	An approach or technology designed to generate or use data from all genes in the genome.
graph or network	A mathematical structure modelling or depicting the relationships between elements.
information centrality	A network <i>centrality</i> metric which uses the impact of removing a <i>vertex or node</i> on connections in the network.

metagene	A consistent signal of expression for a collection of genes such as a biological pathway, derived from singular value decomposition.
microarray	A high-throughput technique to measure presence or abundance of nucleic acid sequences from binding to probes.
mutant	A variant or dysfunctional phenotype arising from a mutation in a gene.
mutation	A change in DNA sequence that disrupts gene function.
PageRank centrality	A network centrality metric which uses eigenvectors with a scaling factor (Brin and Page, 1998).
pathway	A series of biomolecules that produces a particular product or biological function.
RNA-Seq	Transcriptome data from sequencing RNA.
shortest path	A path with the fewest possible edges which connects two particular vertices .
small world	A property of a network which is highly connected and has a low characteristic path length, derived from the mean shortest path length across all pairs of nodes.
somatic mutation	A mutation that occurs in somatic cells, during a patient's lifespan.
synthetic lethal	Genetic interactions where inactivation of multiple genes is inviable (or deleterious) which are viable if inactivated separately.
treatment	Medical procedures for a disease to improve patient outcomes.
vertex or node	An element of a graph structure or network.
wild-type	A natural phenotype of a trait or the normally functional allele which encodes it.

Acronyms

ANOVA	Analysis of Variance.
AUROC	Area Under the Receiver Operating Characteristic (curve).
BioPAX	Biological Pathway Exchange.
CRAN	comprehensive R archive network.
DNA	Deoxyribonucleic Acid.
ER	Estrogen Receptor.
FDR	False Discovery Rate.
HPC	High Performance Computing.
mtSLIPT	Synthetic Lethal Interaction Prediction Tool (against mutation).
NeSI	New Zealand eScience Infrastructure.
PAM50	Prediction Analysis of Microarray 50.
RNA	Ribonucleic Acid.
ROC	Reciever Operating Characteristic (curve).
RSEM	RNA-Seq by Expectation Maximization (normalisation).
siRNA	Short Interfering RNA.
SLIPT	Synthetic Lethal Interaction Prediction Tool.
Slurm	Simple Linux Utility for Resource Management.
TCGA	The Cancer Genome Atlas (genomics project).

Chapter 2

Methods and Resources

In this Chapter, I will outline the various existing resources and methods utilised throughout this project. This includes public data repositories, stable and development releases of software packages (mostly for the R programming environment), and implementation of [bioinformatics](#) methods and statistical concepts with Shell or R scripts developed for this purpose. Methods and packages developed specifically for this project will be covered in more detail along with preliminary data to demonstrate and support their use in Chapter 3.

2.1 Bioinformatics Resources for Genomics Research

2.1.1 Public Data and Software Packages

Various [bioinformatics](#) resources, such as databases and methods, have become integral parts of genetics and [genomics](#) research. Reference [genomes](#), genotyped variants, [gene expression](#), and epigenetics profiles are among the most commonly used resources. [Gene expression](#) data in particular is widely available from many [microarray](#) and [RNA-Seq](#) studies, from repositories such as Gene Expression Omnibus (GEO) (Clough and Barrett, 2016), caArray (Heiskanen *et al.*, 2014), and ArrayExpress (Rustici *et al.*, 2013). Such profiles are excellent resources to examine the changes of [gene expression](#) occurring in cancers and the variation between samples. These [microarray](#) initiatives have set a precedent for data sharing, data mining, and the wider benefits of publicly available data for enabling the scientific community to further utilise the data rather than a single research group or consortium (Rung and Brazma, 2013). The practice of integrating findings from publicly available [genomics](#) data with the research questions and experimental results of individual research groups has carried over into [RNA-Seq](#)

datasets including the large-scale cancer genomics projects (Zhang *et al.*, 2011). This thesis is one such example of an investigation enabled by this wider movement and tools developed in various disciplines to generate, process, and disseminate genomic-scale data.

Along with databases, it is also becoming common practice for bioinformatics researchers to release their code as open-source or provide a software package to enable replication of the findings or further applications of the methods (Stajich and Lapp, 2006). This is part of a wider movement in software and data analysis with many tools to facilitate such work being released for use in Linux or the R programming environment (R Core Team, 2016). In addition to the R packages hosted on comprehensive R archive network (CRAN) (CRAN, 2017), the Bioconductor repositories (Gentleman *et al.*, 2004) also contain many packages specifically for applications in bioinformatics, and the GitHub site hosts many packages in various stages of development and early release. Packages from these various sources have been used throughout this project and cited where-ever possible. Several R packages have been developed during this thesis project and either publicly released on GitHub or prepared to accompany a publication.

2.1.1.1 Cancer Genome Atlas Data

Molecular profile data from normal and tumour samples was downloaded from publicly available sources, using the TCGA (TCGA, 2012) and the International Cancer Genomes Consortium (ICGC) web portals (Zhang *et al.*, 2011). These include gene expression (RNA-Seq), somatic mutation mutations, and anonymous clinical data. These versions downloaded were on the 6th of August 2015 (Release 19) and the 2nd of May 2016 (Release 20) for breast and stomach cancer respectively via the ICGC data portal (<https://dcc.icgc.org/>).

Performing a genomic alignment in remains a challenge in bioinformatics and methods to do so may yet be improved (Chen and Tompa, 2010). However, the statistical and biological aspects of bioinformatics are the focus of this thesis, comparing alignment methods is outside the scope of these investigations. The TCGA project (TCGA, 2012) used widely adopted tools: “Bowtie” for alignment (Langmead *et al.*, 2009), “mapsplice” to detect splice sites (Wang *et al.*, 2010), and the Reads Per Kilobase per Million mapped reads (RPKM) approach to qualify reads per transcript as a measure of gene expression (Mortazavi *et al.*, 2008). These are widely acceptable tools for processing RNA-Seq data which were used to produce the raw counts of mapped reads (tier 1) and normalised expression data (tier 3) publicly available from TCGA.

Raw count and RNA-Seq by Expectation Maximization (RSEM) normalised TCGA expression data from Illumina RNA-Seq protocols were available from 1177 breast samples (113 normal, 1057 primary tumour, and 7 metastases) for 20,501 genes. TCGA breast somatic mutation mutation data for 981 samples (976 primary tumours and 5 metastases) across 25,836 genes were available including 969 samples (964 primary tumours and 5 metastases) with corresponding RNA-Seq expression data and 19,166 genes mapped from Ensembl identifiers to gene symbols, of which 16,156 had corresponding gene expression information. Unless otherwise stated, the raw counts were used for further processing rather than the RSEM normalised data (provided by TCGA tier 3). For the purposes of this analysis somatic mutation mutations were reported if they were detected to non-synonymous substitutions, frameshifts, or truncations (by premature stop codons) which would likely disrupt the wild-type gene function.

Raw count TCGA expression data (TCGA tier 1) from Illumina RNA-Seq was also available for 450 stomach samples (35 normal, 415 primary tumour) for 20,501 genes. TCGA stomach mutation data was also available for 289 samples across 25807 genes, corresponding to 19436 genes with expression data.

2.1.1.2 Reactome and Annotation Data

Unless otherwise specified, pathway analysis was performed for human pathway annotation from the Reactome database (version 52) with pathway gene sets derived from the reactome.db R package. Entrez identifiers were mapped to gene symbols or aliases to match to TCGA expression and mutation data using the org.Hs.eg.db R package. Further pathway analysis used breast cancer gene signatures from Gatza and colleagues (Gatza *et al.*, 2011; Gatza *et al.*, 2014). These gene symbols were matched to the relevant dataset and used to construct a matrix of category membership using the safe R package (Barry, 2016).

2.2 Data Handling

2.2.1 Normalisation

Apart from the Prediction Analysis of Microarray 50 (PAM50) subtyping procedure (Parker *et al.*, 2009), which required RSEM normalised data (J.S. Parker personal communication), the analysis of the RNA-Seq data presented here was based on raw read count data. Raw read counts were log-scaled; samples removed for consistency (based on a Euclidean distance correlation matrix as described in Section 2.2.2); and the final dataset was TMM normalised (Robinson and Oshlack, 2010) then processed

using the `voom` function (Law *et al.*, 2014) in the `limma` R package (Ritchie *et al.*, 2015). Protein expression data generated from RPPA was normalised to dilution curves using the `SuperCurve` R package (Ju *et al.*, 2015; Neeley *et al.*, 2009).

2.2.2 Sample Triage

The `TCGA` breast RNA-Seq data were assessed for batch effects using a correlation matrix of the log-transformed raw counts for which a heatmap (Euclidean distance, complete linkage) is shown in Figure A.2. While no major batch effects were detectable between the samples, 9 samples were excluded due to poor correlation with the remaining samples, as detailed in Table 2.1. These samples showed unusual density plots compared to the rest of the dataset, and exhibited low mean read count in Figures 2.1 and 2.2. A heatmap showing key clinical properties of these excluded samples and their correlation with the remainder of the samples is shown in Figure A.1, and a full correlation heatmap (Figure A.2) shows these samples as relatively poorly correlated outliers in the bottom rows and left columns. In addition to the clustering analysis (in Appendix A.1), replicate tumour samples were also examined for sample quality in Appendix A.2. After removal of these samples, the `TCGA` dataset used for analysis consisted of the remaining 1168 samples (from 1040 patients): 1049 tumour samples, 112 normal tissue for matched samples, and 7 metastases.

Table 2.1: Excluded samples by batch and clinical characteristics.

Tissue Source	Type	Batch	Plate	Patient	Samples	p53	Subtype	Treatment (History)	Clinical Subtypes (Stage)
A7 Christiana	Tumour	47	A227	A0DB	1 of 3	NA	Luminal A	Mastectomy (no)	Estrogen receptor (ER) ⁺ Ductal (2)
A7 Christiana	Tumour	96	A220	A13D	1 of 3	Wildtype	Luminal A	Mastectomy (no)	ER ⁺ Ductal (2)
A7 Christiana	Tumour	96	A227	A13E	1 of 3	NA	Basal	Lumpectomy (no)	ER ⁻ Ductal (2)
A7 Christiana	Tumour	142	A277	A26E	1 of 3	NA	Basal	Lumpectomy (no)	ER ⁺ Ductal (2)
A7 Christiana	Tumour	47	A277	A0DC	1 of 2	NA	Luminal A	Mastectomy (yes)	ER ⁺ Lobular (3)
A7 Christiana	Tumour	142	A220	A26I	1 of 2	Mutant	Basal	Lumpectomy (yes)	ER ⁻ Ductal (2)
AC Intl Genomics	Tumour	177	A18M	A2QH	2 of 2	Mutant	Basal	Radical Mastectomy (no)	ER ⁻ Metaplastic (2)
AC Intl Genomics	Tumour	177	A220	A2QH	2 of 2	Mutant	Basal	Radical Mastectomy (no)	ER ⁻ Metaplastic (2)
GI ABS IUPUI	Normal	177	A16F	A2C8	1 of 1	NA	Luminal A	Radical Mastectomy and Neoadjuvant (no)	ER ⁺ Ductal (2)

Similarly, a correlation matrix of log-transformed raw counts was used to evaluate sample quality for `TCGA` stomach RNA-Seq. A tumour sample (patient 4294) was removed due to similar quality concerns leaving a final dataset for 449 samples (from 417 patients): 414 tumour samples and 35 normal tissue samples.

2.2.3 Metagenes and the Singular Value Decomposition

A “metagene” offers a consistent signal of pathway (expression) activation or inactivation by dimension reduction of a matrix, avoiding negatively correlated genes averaging out the signal of a mean-based centroid (Huang *et al.*, 2003). Constructing these path-

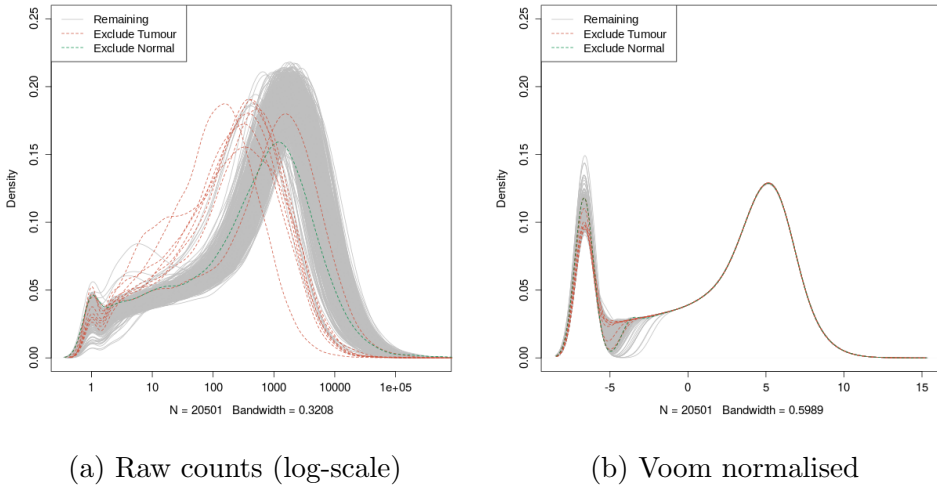


Figure 2.1: **Read count density.** Sample density plots of raw counts on log-scale and voom normalised showing samples removed due to quality concerns.

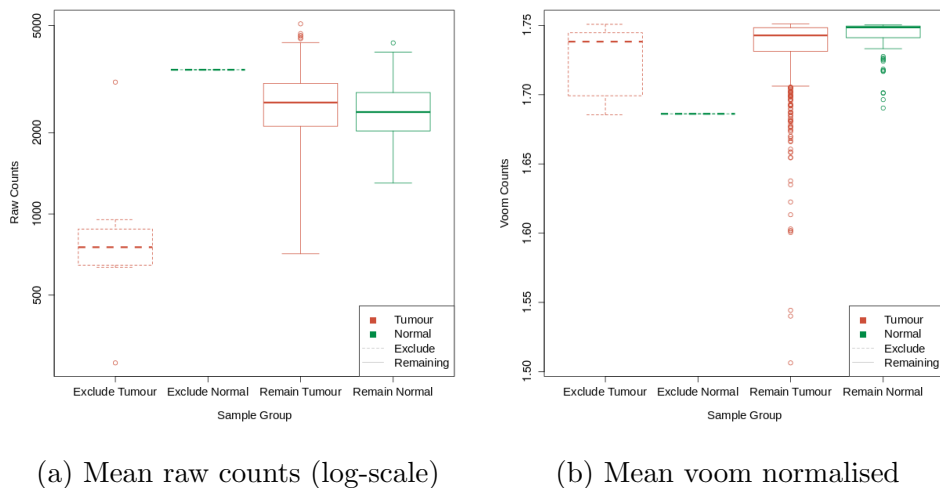


Figure 2.2: **Read count sample mean.** Boxplots of sample means for raw counts on log-scale and voom normalised show removed tumour samples with low mean read count.

`way metagenes` used gene sets for Reactome and Gatza signatures (Gatza *et al.*, 2011, 2014) as specified above (see Section 2.1.1.2). The singular-value decomposition was performed ($X = U^T DV$ where X is the data matrix of the gene set with genes \times samples) and the leading eigenvector (first column of V) corresponding to the largest singular value was used as a `metagene` for the `pathway` gene set. To ensure consistent directionality of `metagene` signals, the median of the gene set in each sample was calculated and correlated against the `metagene` with the (arbitrary) `metagene` sign adjusted as needed to conform with the majority of the gene set (i.e., positive correlation between `metagene` and the median-based centroid). To ensure that genes and `pathways` were weighted equally, `metagenes` were derived from a z-transformed dataset of `gene expression` and samples were scaled (by fractional ranking) for each `metagene` so that they were comparable on a [0, 1] scale.

2.2.3.1 Candidate Triage and Integration with Screen Data

Candidate triage in combination with the experimental data was intended to integrate findings of the `SLIPT` analysis with an ongoing experiment project (Chen *et al.*, 2014; Telford *et al.*, 2015). The first procedure to compare the `SLIPT` gene candidates for *CDH1* with an `siRNA` experimental screen (Telford *et al.*, 2015) was a direct comparison of the overlapping candidates, presented in a Venn diagram and tested with the χ^2 test. Since these candidates modestly overlapped at the gene level (even when excluding genes not contained in both datasets), further gene set over-representation analysis was performed for pathways specific to each detection approach and the intersection of the two.

The `pathway` composition of the intersection was further verified by a permutation resampling analysis (as described in Section 2.3.6): the same number of genes detected by `SLIPT` were sampled randomly from the universe of genes tested by both approaches. These samplings were performed over 1 million iterations and the `pathway` over-representation was compared for each of the 1652 reactome `pathways`. These over-representation scores (χ^2) were compared the observed over-representation in the intersection of the `SLIPT` candidates, with the proportion of resamplings with higher χ^2 values used for empirical p-values of `pathway` composition. The χ^2 test was used as an appropriation of Fisher's exact test on a hypergeometric distribution for resampling to computationally scale `pathway` over-representation tests across iterations. Pathways for which no resamplings were occurred as high as the observed were reported as $p < 10^{-6}$. These empirical p-values were adjusted for multiple comparisons (False discovery rate (FDR)). Intersection size was not assumed to be constant across resam-

plings so similarly with the proportion of resamplings with higher or lower intersection size were used to evaluate significance of enrichment or depletion respectively (of **siRNA** candidate among **SLIPT** candidate genes).

2.3 Techniques

Various statistical, computational, and **bioinformatics** techniques were performed throughout this thesis. This section describes these techniques and gives the parameters used unless otherwise specified. Where relevant, the R package implementation which provided the technique will be acknowledged.

2.3.1 Statistical Procedures and Tests

As described in sections 2.3.4 and 2.2.3, the z-transform has been used to generate z-scores in various analyses in this thesis. Each row of dataset (x) is transformed into a scores (z) using the mean (μ) and standard deviation (σ) of the data such that:

$$z = \frac{x - \mu(x)}{\sigma(x)}$$

This generates data where each row (gene) has a mean of 0 and standard deviation of 1. Where plotted as a heatmap, any data more than 3 standard deviations above or below the mean is plotted as 3 or -3 respectively.

Empirical Bayes differential **expression** analysis was performed using the **limma** R package (Ritchie *et al.*, 2015). Where specified, the Fisher's exact test, χ^2 test, and correlation were used to measure associations between variables (as implemented in the **stats** R package (R Core Team, 2016)). Unless otherwise specified, Pearson correlation was used for correlation analyses (r) and coefficient of determination (R^2). Where these comparisons are discussed in more detail, Fisher's exact test and χ^2 tests are supported by a table or Venn diagram, rendered with the **limma** R package (Ritchie *et al.*, 2015). In some analyses, correlation is further supported by a scatter plot and a line of best fit derived by least squares linear regression.

The **t.test** function (R Core Team, 2016) has also been used to implement the t-test to compare pairs of data. Where relevant, an **analysis of variance (ANOVA)** has been performed to report significance of multivariate predictors of outcomes, or least squares linear regression performed for the adjusted coefficient of determination (R^2) and F-statistic p-value to evaluate the fit of the predictor variables. For some analyses these are supported by boxplot or violinplot visualisation (rendered in R).

Multiple comparisons are adjusted by the Benjamini-Hochberg procedure to control the **FDR** unless otherwise specified (Benjamini and Hochberg, 1995). This procedure

adjusts p-values to achieve an average of the proportion of false-positives among significant tests below a threshold, α . The more stringent Holm-Bonferroni (Holm) procedure (Holm, 1979) was also applied in some cases to adjust for multiple comparisons and control the family-wise error rate which adjusts p-values so that the probability that any one of the tests is a false-positive (type-1 error) below a threshold, α .

2.3.2 Gene Set Over-representation Analysis

Gene set enrichment over-representation was performed to test whether there is an enrichment of a gene set (e.g., a biological [pathway](#)) among a group of input genes. Such input genes may be predicted [synthetic lethal](#) candidates or a subset defined by clustering (in Section 2.3.3) or comparison with experimental candidates (see Section 2.2.3.1). Initially, these tests were performed using the GeneSetDB web tool (Araki *et al.*, 2012) hosted by the University of Auckland on the Reactome [pathways](#) (Croft *et al.*, 2014). Since the GeneSetDB tool used an older version of Reactome (version 40), it was difficult to directly compare with the results of other analysis (see sections 2.2.3.1 and 2.3.6) performed on version 52 (as described in Section 2.1.1.2). Thus an implementation of the hypergeometric test in R (R Core Team, 2016) was used to test for over-representation against Reactome (version 52) [pathways](#). Pathways containing less than 10 genes or more than 500 (as performed in GeneSetDB by Araki *et al.*, 2012) were excluded before adjusting for multiple comparisons.

2.3.3 Clustering

Clustering analysis when performed uses unsupervised hierarchical clustering with complete linkage (distance calculated from the furthest possible pairing). For correlation matrices or multivariate normal parameters (e.g., Σ), the distance metric used was Euclidean distance. For empirical or simulated gene and [pathway expression](#) data correlation distance was used, calculated by $distance = 1 - cor(t(x))$ where cor is Pearson correlation and $t(x)$ is the transpose of the [expression](#) matrix.

2.3.4 Heatmap

Standardised z-scores of the data were used to plot heatmaps on an appropriate scale. Raw (log-scale) read counts or voom normalised counts per gene (as specified) were plotted as normalised z-scores on a $[-3, +3]$ blue-red scale. Similarly, correlations were plotted on a $[-1, +1]$ blue-red scale. These heatmaps were performed using the linkage and distance specified for the clustering performed in Section 2.3.3. The `gplots` R package (Warnes *et al.*, 2015) was used to generate many of the heatmaps throughout

this thesis, along with a customised heatmap function (released as `heatmap.2x`). Where clearly specified, data have been split into subsets with clustering performed separately on each subset with these plotted alongside each other.

2.3.5 mMdelling and Simulations

Statistical modelling and simulations have been used to test various `synthetic lethal` detection procedures on simulated data. This involves constructing a statistical model of how `synthetic lethality` would appear in (continuous normally distributed) `gene expression` data. Where presented (in Section 3.2.1), the assumptions of the model are stated clearly. The model allows sampling from a multivariate normal distribution (using the `mvtnorm` R package (Genz and Bretz, 2009; Genz *et al.*, 2016)) to generate simulated data with known underlying `synthetic lethal` partners (detailed in Section 3.2.2). We can test whether statistical procedures, including those developed in this thesis (presented in Section 3.1), are capable of detecting them upon this simulated data. This multivariate normal simulation procedure also enables the inclusion of correlation structure which is either given as correlated blocks of genes or derived from `pathway` structures (as detailed in Section 3.4.2).

If this multivariate normal distribution was sampled once and the procedure to add known `synthetic lethal` partners was performed, it generates a simulated dataset. Performing this simulation procedure and testing with a `synthetic lethal` detection procedure iteratively, these simulations can be used to assess the statistical performance of the detection procedure. The number of iterations (`Reps`) will be given for each simulation result. Typically, these are performed 1000 or 10,000 times depending on computational feasibility of doing so on larger datasets.

Several measures of statistical performance were used to assess the simulations. The following measures used the final classification of the detection procedure, statistical significance for χ^2 , significance and directional criteria met for `SLIPT` (see Section 3.1), and an arbitrary threshold: < -0.2 and $> +0.2$ for negative correlation and correlation respectively. Sensitivity (or “true positive rate”) was measured as the proportion of known `synthetic lethal` partners predicted to be `synthetic lethal`. Specificity (or “true negative rate”) was measured as the proportion of known non-synthetic lethal partners predicted not to be `synthetic lethal`. The “false positive rate” was measured here as the proportion of known non-synthetic lethal partners out of all putative partners predicted by the detection procedure. Statistical “accuracy” is the proportion of true predictions

for a detection procedure, which is both the correctly predicted known synthetic lethal partners and correctly negative known non-synthetic lethal partners.

2.3.5.1 Receiver Operating Characteristic (Performance)

A more general procedure to measure the statistical performance of a simulation is the Receiver Operating Characteristic (ROC) curve which does not assume a threshold for classification of synthetic lethality but demonstrates the trade-off of sensitivity and specificity (Akobeng, 2007; Fawcett, 2006; Zweig and Campbell, 1993). These curves (implemented with the `ROCR` R package (Sing *et al.*, 2005)) plot the True Positive Rate (sensitivity) against the False Positive Rate (1–specificity) as the prediction threshold is varied. An ideal detection method will have a true positive rate of 1 and a false positive rate of 0, hence the Area Under the receiver operating characteristic (ROC) curve (AUC or area under ROC (AUROC)) is a measure of statistical performance for a detection procedure accounting for this trade-off. AUROC values are typically range from 0.5 the value expected by random chance to 1 for an optimal detection method, however it is possible for an AUROC below 0.5 for a poor detection method that performs worse than random chance. In cancer biology, an AUROC of approximately 0.8 is a predictive biomarker suitable for publication (Hajian-Tilaki, 2013) but predictors with lower AUROC values may still be informative depending on the context. In this thesis, the AUROC values varies widely across simulation parameters and a primarily used for comparisons across these parameters, although they can also be used to refine thresholds for optimal classification.

2.3.6 Resampling Analysis

Resampling analyses (e.g., “permutation” analysis) are used to statistically test the significance of an observation without assuming the underlying distribution of expected test statistics Collingridge (2013). Instead these are derived from randomly shuffling test statistics or randomly sampling predicted candidates. For the purposes of this thesis, this involved randomly sampling genes from those tested to be analysed as putative synthetic lethal candidates. This was performed both for testing the significance of pathway composition in the intersection with experimental gene candidates (Section 2.2.3.1) and for assessing the significance of pathway structure among synthetic lethal candidates (Section 3.4.1.1).

These were analysed to compare the observed synthetic lethal genes against values derived from randomly sampling the same number of genes as observed by synthetic lethal from among the genes tested. Sampling iteratively across many resampling pro-

cedures, these resampling-based values form a null distribution that would be observed if the null hypothesis were true. Thus the proportion of resampling-based values across these iterations that are greater than or equal to that observed, forms an empirically derived p-value to test significance.

Resampling was performed for comparison (in Section 2.2.3.1) with fixed experimental screen candidates (Telford *et al.*, 2015) both resampling the number of genes overlapping with the screen candidates and test statistics for pathway enrichment. Resampling analysis was also applied to shortest paths and network metrics (in Section 3.4.1.1) to test significance of directional relationships between synthetic lethal candidate genes within pathway structures.

The number of iterations determines the accuracy of these p-values. For pathway composition (in Section 2.2.3.1), a million iterations were performed using high performance computing (as detailed in Section 2.5.3) to provide sufficient accuracy after adjusting for multiple comparisons across pathways. For the purposes of network analysis (in Section 3.4.1.1), a thousand iterations were sufficient to reject the null hypothesis for the majority of pathways tested before adjusting for multiple comparisons, and thus further iterations were not performed.

2.4 Pathway Structure Methods

2.4.1 Network and Graph Analysis

Networks are important in considering the structure of relationships in molecular biology, including gene regulation, kinase cellular signalling, and metabolic pathways (Barabási and Oltvai, 2004). Network theory is an interdisciplinary field which combines the approaches of computer science with the metrics and fundamental principles of graph theory, an area of pure mathematics dealing with relationships between sets of discrete elements. The vast amounts of molecular and cellular data from high-throughput technologies have enabled the application of network-based and genomes-wide bioinformatics analysis to examine the complexity of a cell at the molecular level and understand aberrations in cancer. This thesis uses various metrics and analysis procedures developed in Graph and Network theory to analyse graph structure of biological pathways. Where feasible, these have been implemented using the igraph R package with such procedures described below (Csardi and Nepusz, 2006). Custom R functions to perform more complex analysis and visualisation of iGraph data objects will be described later.

Graph theory is a branch of pure mathematics which deals with the properties of sets of discrete objects (referred to as a ‘node’ or ‘vertex’) with some pairs are joined (by a ‘link’ or an ‘edge’). While a seemingly reductionist abstraction to mathematically study relationships, graph theory serves has applications in a wide range of studies including life sciences. Network theory is the sub-discipline of graph theory which deals with networks which has become popular due to the vast potential for applications of networks (van Steen, 2010).

Applications vary depending on the situation modelled, particularly in how the edges between vertices are defined, whether they are directed or weighted, and whether multiple redundant edges between a pair of vertices (referred to as ‘parallel edges’) or edges connecting a vertex to itself (referred to as ‘loops’) are permitted in the model. Networks are defined such that the edges represent a relationship between the vertices and may be directed, weighted, or contain parallel edges or loops depending on the application (van Steen, 2010). Unless otherwise stated, graph structures and networks in thesis will be unweighted and have no parallel edges or loops. Where a directional relationship is known or modelled, it will be represented with a directed edge in a directed graph.

2.4.2 Sourcing Graph Structure Data

Pathway Commons interaction data was sourced using Biological pathway exchange (BioPAX) with the paxtools-4.3.0 Java application on October 6th 2015 (Cerami *et al.*, 2011; Demir *et al.*, 2013). This utility was used to source ‘sif’ format interaction data into R (R Core Team, 2016), from which the human Reactome (version 52) dataset of interactions was imported (Croft *et al.*, 2014), matching those used for pathway enrichment analysis. These interactions were used to construct an adjacency matrix for the Reactome network and subnetworks corresponding to each relevant biological pathway.

2.4.3 Constructing Pathway Subgraphs

Subgraphs for each relevant pathway were constructed by matching the nodes in the complete Reactome network to the pathway gene sets (as derived in Section 2.1.1.2). A subgraph with adjacent nodes was constructed by adding nodes which have an edge with a gene in the pathway gene set. The pathways these adjacent nodes belong to were added to form a “meta-pathway” to account for the possibility for nodes within the pathway being linked by the surrounding graph structure.

2.4.4 Network Analysis Metrics

The existing network analysis measures applied in this thesis (as described below) used an implementation in the `igraph` R package where it was available (Csardi and Nepusz, 2006). Otherwise, custom features were developed for analysis of iGraph objects in R and released as `igraph.extensions` (as described in Section 3.5.3).

Vertex degree is the number of `edges` a `node` has and is a fundamental measure of the importance and connectivity of a network (van Steen, 2010). More connected `nodes`, such as network hubs, will have a higher `vertex` degree relative to other `nodes`. For the purposes of this thesis, `vertex` degree ignored `edge` direction with loops (edges with itself) and double `edges` to the same `node` excluded.

A fundamental concept in network analysis is a “`shortest path`”, that is the shortest route via `edges` between any two particular `nodes` in a network. These are computed by Dijkstra’s algorithm (Dijkstra, 1959) in the `igraph` R package (Csardi and Nepusz, 2006). Where applicable paths will only use directed `edges` in a particular direction. Shortests paths are a useful measure of how close `nodes` are in a network. This is used to compute `information centrality`, and for further analysis of `pathway` structure (as described in Section 3.4.1).

Network `centrality` is an alternative measure of the importance or influence of a `node` to the `graph` structure (Borgatti, 2005). Various strategies are used to derive centrality, typically based on how connected the `node` is or the impact of `node` removal on the connectivity of the network. One of the most notable is the “`PageRank`” algorithm, a refinement of eigenvector `centrality` based on the eigenvectors of the adjacency matrix (Brin and Page, 1998). This is implemented in the `igraph` R package (Csardi and Nepusz, 2006).

Another network `centrality` measure that has been previously applied to biological protein interaction networks (Kranthi *et al.*, 2013) is the “`information centrality`”. The `information centrality` of a `node` is the relative impact on efficiency (transmission of information via shortest paths) of the network when the `node` is removed. That is the `centrality` (C) (Kranthi *et al.*, 2013) for `node` n in graph G is defined as:

$$C_n = \frac{E(G) - E(G')}{E(G)}$$

where G' is the subgraph with the `node` removed and E is the efficiency (Latora and Marchiori, 2001) derived from `shortest paths` (d_{ij} between `nodes` i and j) as:

$$E(G) = \frac{2}{N(N-1)} \sum_{i < j \in G} \frac{1}{d_{ij}}$$

The efficiency of the network can be derived from [shortest paths](#) implemented in the [igraph](#) R package and the iterative network [centrality](#) computation of each [node](#) has been released as an R package ([info.central](#)) and included in the [igraph.extensions](#) package.

2.5 Implementation

2.5.1 Computational Resources and Linux Utilities

Several computers were used to process and store data during this thesis (as summarised in Table 2.2), running different versions of Linux operating systems, including a personal laptop computer, laboratory desktop machine, departmental server, and the New Zealand eScience Infrastructure Intel Pan high-performance computing cluster (a supercomputer based at the University of Auckland). Each of these systems support a 64-bit architecture. Current workflows on local machines use Elementary OS (based on the Ubuntu versions given in Table 2.2) and interacting with these via ZSH shell. However, Ubuntu OS and the Bourne Again SHell (bash) were used at the inception of this project and bash is continues to be used for running scripts. Various Linux applications and command-line utilities were used on these machines (as summarised in Table 2.3). As such, the workflows developed in this project should be backwards-compatible with Ubuntu Linux (and other derivatives). The majority of novel methodology and implementations were performed in R which is a cross-platform language, packages developed in R will be available for users of Linux, Mac, and Windows machines.

Table 2.2: Computers used during thesis

	Viao Laptop	Lab Machine	Biochem Server	NeSI Pan Cluster
Operating System (OS)	Elementary OS Freya 0.3.2	Elementary OS Loki 0.4	Red Hat Enterprise Maipo 7.2	Cent OS Final 6.4
Upstream OS	Ubuntu LTS Trusty 14.04	Ubuntu LTS Xenial 16.04		
Linux Kernel	3.19.0-65-generic	4.4.0-36-generic	3.10.0-327.36.2.el7.x86_64	2.6.32-504.16.2.el6.x86_64
Shell: bash	4.3.11(1)	4.3.46(1)	4.2.46(1)	4.2.1(1)
Shell: zsh	5.0.2	5.1.1	5.0.2	5.2

Table 2.3: Linux utilities and applications used during thesis

		Viao Laptop	Lab Machine	Biochem Server	NeSI Pan Cluster
	OS	Elementary OS Freya 0.3.2	Elementary OS Loki 0.4	Red Hat Enterprise Maipo 7.2	Cent OS Final 6.4
	Linux Kernel	3.19.0-65-generic	4.4.0-36-generic	3.10.0-327.36.2.el7.x86_64	2.6.32-504.16.2.el6.x86_64
Scripting	Shell bash	4.3.11(1)	4.3.46(1)	4.2.46(1)	4.2.1(1)
	Shell zsh	5.0.2	5.1.1	5.0.2	5.2
Programming	Python	2.7.6	2.7.12	2.7.5	
	Java	1.8.0_101	9-ea	1.8.0_101	
	C++	4.8.4	5.4.0	4.8.5	4.4.7
Text Editor	nano	2.2.6	2.5.3	2.3.1	2.0.9
	kile (L ^A T _E X)	2.1.3	2.1.3		
Version Control	git	1.9.1	2.11.0	1.7.1	1.8.3.1
Shell Utilities	sed	4.4.2	4.4.2	4.4.2	4.4.1
	grep	2.16-1	2.25-1	2.20	2.6.3
	nohup	8.21	8.25	8.22	8.4
Typesetting	TeX	3.1415926	3.14159265		
	TeXLive (L ^A T _E X)	2013	2015		
	PDFTeX	2.5-1	2.6		
	pandoc	1.12.2.1	1.16.0.2		
Remote Computing	Slurm scheduler				16.05.6
	OpenSSH	7.2p2	7.2p2	6.6.1	5.3p1
	OpenSSL	1.0.2g	1.0.2g	1.0.01e-fips	1.0.01e-fips
	rsync	3.1.0p31	3.1.1p31	3.0.9p30	
	Globus Online Transfer			3.1	3.1
	Cisco AnyConnect VPN		3.1.05170		
Image Processing	Inkscape	0.48.4	0.91		
	GIMP	2.8.10	2.8.16		
	ImageMagick	6.7.7.10-6			

2.5.2 R Language and Packages

The R programming language has been used for the majority of this thesis. Current R installations across the machines used are given in Table 2.4. Local machines currently run the latest version of the R (at the time of writing) and remote machines run the versions and modules as managed by the system administrator.

Various scripts and packages in this thesis were developed or run in previous versions of RStudio and R but these run without error in the current version of R (and the older versions on remote machines). The R packages which were used throughout this thesis (as detailed in Table 2.5 with versions specified) were installed from the [comprehensive R archive network \(CRAN\)](#) ([CRAN, 2017](#)), Bioconductor ([Gentleman *et al.*, 2004](#), version 3.4; BiocInstaller 1.24.0), or GitHub. These packages were not updated when they would change the functionality of scripts or functions in packages, in particular imported data from annotation packages (used to define gene sets) have been saved as local files to continue using stable versions of these [pathway](#) data (across machines).

This is a summary of the key packages which (in addition to their dependencies) have been used throughout this project. Where a package implementation has been central to the methods applied, they are described in more detail in the relevant section. A full table of packages used in this thesis can be found in Appendix B (Table B.1). The R packages developed during this thesis are given in Table 2.6 with the relevant sections describing their implementation and use where appropriate, in addition to further details on these functions in Section 3.5.

Table 2.4: R installations used during thesis

		Viao Laptop	Lab Machine	Biochem Server	NeSI Pan Cluster
	OS	Elementary OS Freya 0.3.2	Elementary OS Loki 0.4	Red Hat Enterprise Maipo 7.2	Cent OS Final 6.4
Programming	R	3.3.2	3.3.2	3.3.1	3.3.0-intel (module)
Development	RStudio	1.0.136	1.0.136	1.0.136 (server)	

Table 2.5: R Packages used during thesis

Package	Version Used	Built	Repository
colorspace	1.3-2	3.3.1	CRAN
curl	2.3	3.3.1	CRAN
data.table	1.9.6	3.3.1	CRAN
dendextend	1.4.0	3.3.2	CRAN
DBI	0.5-1	3.3.1	CRAN
devtools	1.12.0	3.3.1	CRAN
dplyr	0.5.0	3.3.1	CRAN
ggplot2	2.2.1	3.3.1	CRAN
git2r	0.18.0	3.3.1	CRAN
gplots	3.0.1	3.3.1	CRAN
gtools	3.5.0	3.3.1	CRAN
igraph	1.0.1	3.3.1	CRAN
matrixcalc	1.0-3	3.3.1	CRAN
mclust	5.2.2	3.3.1	CRAN
mvtnorm	1.0-6	3.3.1	CRAN
org.Hs.eg.db	3.1.2	3.1.2	Bioconductor
openssl	0.9.6	3.3.1	CRAN
plyr	1.8.4	3.3.1	CRAN
purrr	0.2.2	3.3.1	CRAN

reactome.db	1.52.1	3.2.1	Bioconductor
RColorBrewer	1.1-2	3.3.1	CRAN
Rcpp	0.12.9	3.3.1	CRAN
ROCR	1.0-7	3.3.1	CRAN
roxygen2	6.0.1	3.3.2	CRAN
shiny	1.0.0	3.3.1	CRAN
snow	0.4-2	3.3.1	CRAN
testthat	1.0.2	3.3.2	CRAN
tidyverse	1.1.1	3.3.2	GitHub (hadley)
sm	2.2-5.4	3.3.1	CRAN
Unicode	9.0.0-1	3.3.2	CRAN
vioplot	0.2	3.3.1	CRAN
viridis	0.3.4	3.3.2	CRAN
xml2	1.1.1	3.3.2	CRAN
xtable	1.8-2	3.3.1	CRAN
zoo	1.7-14	3.3.1	CRAN
graphics	3.3.2	3.3.2	base
grDevices	3.3.2	3.3.2	base
cluster	2.0.5	3.3.1	base
graphics	3.3.2	3.3.2	base
grDevices	3.3.2	3.3.2	base
Matrix	1.2-8	3.3.1	base
stats	3.3.2	3.3.2	base

Table 2.6: R packages developed during thesis

Package Name	Description and GitHub Repository	Section
<code>slipt</code>	Synthetic lethal detection by SLIPT (to accompany publication) https://github.com/TomKellyGenetics/slipt	3.1
visualisation	<code>vioplotx</code> Customised violin plots (based on <code>vioplot</code>) https://github.com/TomKellyGenetics/vioplotx	3.4
	<code>heatmap.2x</code> Customised heatmaps (based on <code>gplots</code>) https://github.com/TomKellyGenetics/heatmap.2x	
igraph.extensions	<code>igraph.extensions</code> Meta-package to install the follow iGraph functions https://github.com/TomKellyGenetics/igraph.extensions	3.5.3
	<code>plot.igraph</code> Custom plotting of directed graphs https://github.com/TomKellyGenetics/plot.igraph	2.4.4
	<code>info.centrality</code> Computing information centrality from network efficiency https://github.com/TomKellyGenetics/info.centrality	3.4.2
	<code>pathway.structure.permutation</code> Testing pathway structure with resampling analysis https://github.com/TomKellyGenetics/pathway.structure.permutation	3.4.1.1
	<code>graphsim</code> Generating simulated expression from graph structures https://github.com/TomKellyGenetics/graphsim	3.4.2

2.5.3 High Performance and Parallel Computing

Another enabling technology for bioinformatics is parallel computing, performing independent operations in separate cores: this “multithreading” is widely used to increase the time to compute results. Bioinformatics is particularly amenable to this since performing multiple iterations of a simulation or testing separate genes is often “embarrassingly parallel”, being completely independent of the results of each other. As such parallel computing is offered by many high-performance “supercomputers” including national research infrastructure.

The New Zealand eScience Infrastructure (NeSI) is a High Performance Computing (HPC) organisation providing the Intel Pan cluster hosted by the University of Auckland (NeSI, 2017). The Pan cluster used throughout this thesis project to optimise and perform computations which would have otherwise been infeasible in the timeframe of thesis. Such technological developments and infrastructure initiatives have enabled bioinformatics research including this project. High performance computing on the Pan cluster was used extensively in this project including for resampling analysis (in sections 2.3.6 and 3.4.1.1), calculating information centrality (in Section 2.4.4), and in simulations (in sections 2.3.5, 3.2, and 3.4.2)

Scripts and data were transferred between the Pan cluster and University of Otago computing resources by `rsync` or the Globus file transfer service (Globus, 2017). R scripts (R Core Team, 2016) were run in parallel with the “simple network of workstations” `snow` R package Tierney *et al.* (2015). This utilised the “message passing interface” (Yu, 2002) when it was feasible with memory requirements to run in par-

allel across multiple compute [nodes](#), otherwise SOCKS was used to access multiple cores within an instance of R and pass input data to them. R jobs were submitted to queue for available resources and run on the Pan cluster via the [Simple Linux Utility for Resource Management \(Slurm\)](#) workload manager ([Slurm, 2017](#)). When running R scripts across many parameters or for memory-intensive jobs, Slurm array job submission and independent submission of different parameters via shell commands with arguments passed to R. In some cases, this submission was automated across a range of parameters with Bash scripts.

Chapter 3

Methods Developed During Thesis

In this Chapter, I will outline the rationale and development of various methods used throughout this thesis to examine [synthetic lethality](#) in gene expression data, graph structures, models and simulations. Fristly, the [Synthetic Lethal Interaction Prediction Tool \(SLIPT\)](#), a [bioinformatics](#) approach to triage of [synthetic lethal](#) candidate genes, will be described. This is one of the main research outputs of this thesis project, which was supported by comparisons to an experimental screen from a related project and performance on simulated data. These supporting findings will be covered in further chapters but some simulation data is given here to support the use and design of [SLIPT](#). This includes the construction of a statistical model of [synthetic lethality](#) in (continuous multivariate Gaussian) [gene expression](#) data, which enables testing [SLIPT](#) upon simulated data with known [synthetic lethal](#) partners. Another key component of this simulation pipeline is the generation of simulated data from a known [graph](#) structure or simulated biological pathway. The development of this simulation procedure and other statistical [treatment](#) of graph and [network](#) structures will also be covered. Various R packages have been developed to support this project, including the [slipt](#) package to implement the [SLIPT](#) methodology. Additional R packages for handling [graph](#) structures, simulations, and custom plotting features will be described as research outputs of this thesis, methods applied throughout, and contributions of open-source software.

3.1 A Synthetic Lethal Detection Methodology

The [SLIPT](#) methodology identifies [gene expression](#) patterns consistent with [synthetic lethal](#) interactions, between a query gene and a panel of candidate interacting partners. Gene expression was scored “low”, “medium”, or “high”, sorting samples by tertiles

($1/3$ -quantiles) for each gene. Genes with insufficient expression across all samples were excluded by requiring that the first tertile of raw counts is above zero. A χ^2 test was then performed between the query gene and each candidate partner. The p-values for the χ^2 test were corrected for multiple testing using False discovery rate (FDR) error control to reduce false positives (Benjamini and Hochberg, 1995). Significance was called for FDR adjusted $p < 0.05$. A synthetic lethal interaction was predicted (as shown in Figure 3.1) when (i) the χ^2 test was significant; (ii) observed low-query, low-candidate samples were less frequent than expected; and (iii) observed low-query, high-candidate and high-query, low-candidate samples were more frequent than expected.

The synthetic lethal prediction procedure was also performed with somatic mutation mutation data for the query gene. This was intended for a query gene known which is recurrently mutated, with the majority of mutations disrupting gene function (e.g., null or frameshift mutations). A synthetic lethal interaction was predicted (as shown in Figure 3.2) when (i) the χ^2 test was significant; (ii) observed mutant-query, low-candidate samples were less frequent than expected; and (iii) observed mutant-query,

		Candidate Gene		
		Low	Medium	High
Query Gene (e.g. CDH1)	Low	Observed less than expected		Observed more than expected
	Medium			
	High	Observed more than expected		

Figure 3.1: Framework for synthetic lethal prediction. SLIPT was designed to identify candidate interacting genes from gene expression data using the χ^2 test against a query gene. Samples are sorted into low, medium, and high expression quantiles for each gene to test for a directional shift. A sample being low in both genes of a synthetic lethal pair is unlikely, since loss of both genes will be deleterious, and is expected to be statistically under-represented in a gene expression dataset. We expect a corresponding (symmetric) increase in frequency of sample with low-high gene pairs. Synthetic lethal candidate (exprSL) partners of a gene are identified by running this procedure on all possible partner genes, selecting those with an FDR-adjusted χ^2 -derived $p < 0.05$, and meeting the directional criteria. Since synthetic lethal genes are partners of each other, commutatively, the symmetric direction criteria were defined such that detected synthetic lethal genes are partners of each other.

		Candidate Gene		
		Low	Medium	High
Query Gene (e.g. <i>CDH1</i>)	Mutation	Observed less than expected		→ Observed more than expected
	Wild-type	↓ Observed more than expected		

Figure 3.2: **Synthetic lethal prediction adapted for mutation.** SLIPT was also adapted to identify candidate interacting genes using (somatic mutation) mutation data of the query gene in the χ^2 test. Samples are sorted into low, medium, and high expression quantiles for each candidate gene and tested for a directional shift against mutation status of the query gene. A sample having low expression or mutation for the synthetic lethal pair is expected to be unlikely with a corresponding increase in frequency of sample with mutant-high or wild-type-low gene pairs. Synthetic lethal candidate (mtSL) partners of a gene were identified from running this procedure on all possible partner genes, selecting those with an FDR-adjusted χ^2 -derived $p < 0.05$, and meeting the directional criteria.

high-candidate and wild-type-query, low-candidate samples were more frequent than expected.

The SLIPT methodology can be performed on expression data, including pathway metagenes (as generated in Section 2.2.3). The application of the SLIPT methodology on public gene expression data was supported with simulation results in Section 3.3 and Chapter 6, including comparison to other statistical methods. SLIPT results for *CDH1* were compared experimental screen results in a breast cell line (Telford *et al.*, 2015): primary screen results are discussed in Section 4.2 and secondary screen results are presented in Section 4.2.4.

3.2 Synthetic Lethal Simulation and Modelling

A statistical model of synthetic lethality was developed to generate simulated data and to evaluate the SLIPT procedure. This section describes the synthetic lethal model and the simulation procedure for generating gene expression data with known synthetic lethal partners. Simulation results, to support usage of the SLIPT methodology throughout this thesis, will be presented in Section 3.3. The simulation procedure will

also be applied in Chapter 6, including in combination with simulations from graph structures (as described in Section 3.4.2).

3.2.1 A Model of Synthetic Lethality in Expression Data

A conceptual model of synthetic lethality was devised (see Figure 3.3), which will be used to build a statistical model of synthetic lethal gene expression and to simulate expression data for assessing various potential synthetic lethal prediction methods, including SLIPT. In the model, synthetic lethality occurs between genes with related functions, as a cell death phenotype, when these functions are inactive.

This model suggests that synthetic lethality is detectable in measures of gene inactivation across a sample population, namely mutation, DNA copy number, DNA methylation, and expression levels. While any of these mechanisms of gene inactivation could lead to synthetic lethality, expression data is readily available and changes in other mechanisms are likely to impact on the amount of expressed RNA that is detectable. Functional relationships between genes could manifest in expression data in several ways, including coexpression, mutual exclusivity and directional shifts. Co-expression is overly simplistic (Lu *et al.*, 2015) and has previously performed poorly as a predictor of synthetic lethality (Jerby-Arnon *et al.*, 2014), although this will still be tested with correlation measures in later simulations. The alternative hypothesis is that synthetic lethality will result in a detectable shift in the number of samples which exhibit low or high expression of either gene. This model does not preclude mutual exclusivity, compensating expression, or co-loss under-representation which may occur between synthetic lethal genes (Lu *et al.*, 2015; Wappett *et al.*, 2016).

The first condition of the synthetic lethal model is that if there are only two synthetic lethal genes (e.g., *CDH1* and one SL partner), then they will not both be non-functional in the same sample (in an ideal model). Gene function is thus determined for each sample in a model of synthetic lethality with the proportion of samples which are functional or non-functional for a gene being arbitrary. Whether a gene is functional can similarly be modelled by an arbitrary threshold of continuous and normally distributed gene expression data to define gene function (as shown in Figure 3.4). For the purposes of modelling synthetic lethality in cancer expression data, a threshold of the 30th percentile of the expression levels was used because approximately 30% of samples analysed had *CDH1* inactivation in breast cancer (TCGA, 2012). This was generalised for a model of the proportion of samples inactivated for each gene. In this ideal case, no samples lowly expressing both of these genes are expected to be observed.

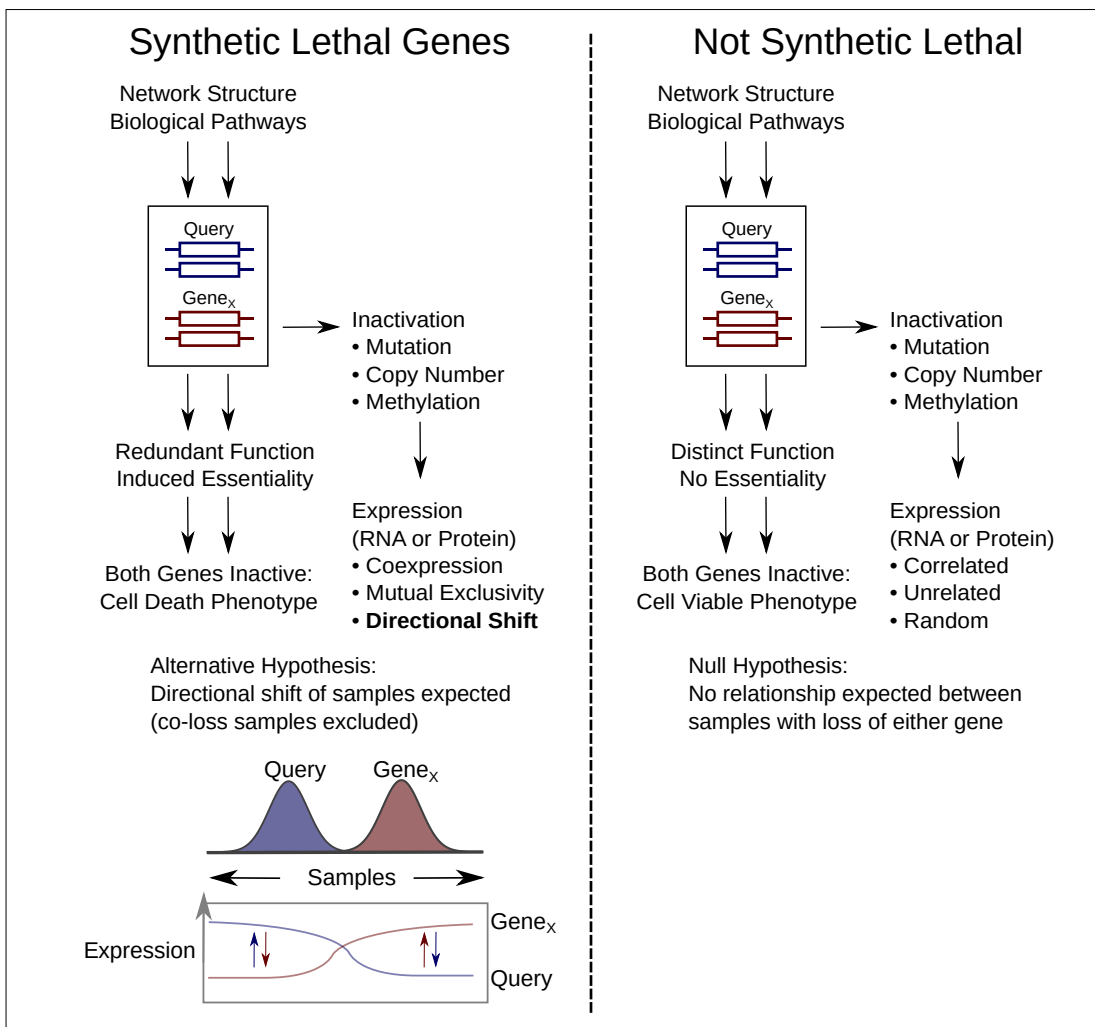


Figure 3.3: **A model of synthetic lethal gene expression.** A conceptual model of synthetic lethal interactions between a Query gene and partner gene (G_X). Genes that are synthetic lethal may not both be non-functional in the same sample without another gene compensating for the loss of function. This is most likely to be detectable as low gene expression, whether they are lost by mutation, deletion, DNA methylation, or suppressing regulatory signals. This could manifest as coexpression, mutual exclusivity, or directional shifts in sample frequency. Thus the alternative hypothesis (H_A) is that synthetic lethal genes will have a reduced frequency of co-loss samples while the null hypothesis (H_0) is that non synthetic lethal gene pairs would show no such relationship, even if they may be correlated for other means such as pathway relationships. In this model synthetic lethal genes may compensate for the loss of each other but this is not assumed, only that loss of both is unfavourable to cell viability and probability of detecting samples with combined gene loss.

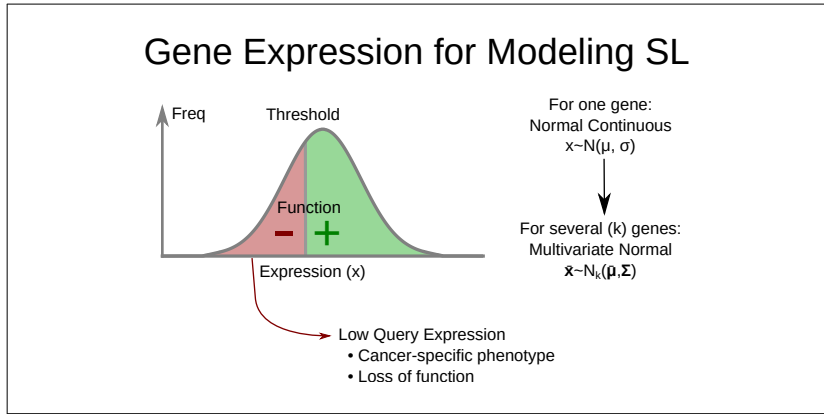


Figure 3.4: **Modelling synthetic lethal gene expression.** When modelling [synthetic lethal](#) interactions between a Query gene and partner genes (G_X and G_Y) above, cellular viability requires that at least of genes is not inactivated. As a model of loss of function, genes are regarded as non-functional with expression below a threshold for the purposes of modelling [synthetic lethality](#). Tumour suppressor genes with loss of function also have cancer specific phenotypes (although these thresholds are not assumed to be the same). Expression is modelled by normally (Gaussian) distributed continuous data, such as (log-scale) data from RNA (microarray or RNA-Seq), protein, or pathway [metagenes](#). This rationale generalises to several genes on a multivariate normal distribution.

While this is not observed, that is to be expected as it is unlikely that only 2 genes will have an exclusive [synthetic lethal](#) partnership. The threshold of the 0.3 quantile was used in simulations dervied from this model throughout this thesis.

A [synthetic lethal](#) pair of genes is unlikely to act in isolation, therefore higher-order [synthetic lethal](#) interactions (i.e., 3 or more genes) must be considered in the model as shown in Figure 3.5. Even when testing pairwise interactions, it is important to model higher level interactions that may interfere. If there are additional [synthetic lethal](#) partners, there are two possibilities for adding these: 1) that they are independent partners of the query genes interacting pairwise (and not with each other) or 2) that an addition partner gene interacts with both of the [synthetic lethal](#) genes already in the system and any of the three (or more) are required to be functional for the cell to survive.

The signal (in terms of [gene expression](#) data) will be weaker for this latter case and this model has the more stringent assumption that all [synthetic lethal](#) partner genes interact with each other: that only one of these must be expressed to satisfy the model of [synthetic lethality](#). In this model, any of the [synthetic lethal](#) genes in a higher-

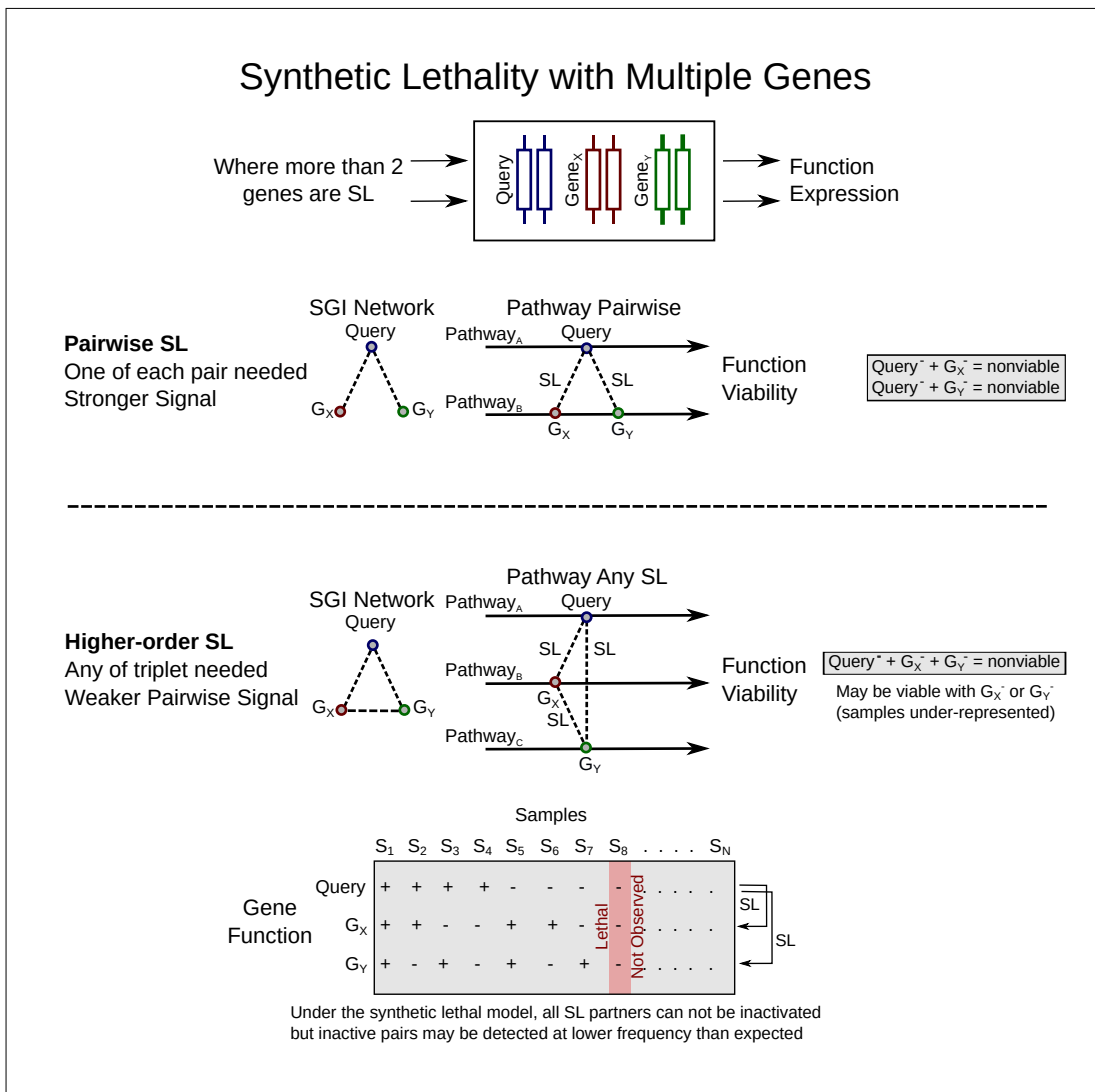


Figure 3.5: **Synthetic lethality with multiple genes.** Higher order synthetic lethal interactions may occur between 3 or more genes, affecting the simulated expression (or synthetic lethal predictions) even if undetected when observed pairwise. Consider interactions between a Query gene and two partner genes (G_X and G_Y). They may interact with the Query pairwise (inviable when either gene pair is lost) or form a higher-order interaction such as the “synthetic lethal triplet” if any of the genes provide an essential function (inviable only when all are lost). Either is plausible with the potential pathway structures. A synthetic lethal triple has 8 potential combinations of gene functional but one is not expected to be observed (due to inviability) but pairwise inactivation may be observed if additional partner genes are functional. The proportion of these combinations varies depending on the functional threshold.

order interaction are able to perform the essential function of the others, allowing for higher-level **synthetic lethal** partners to compensate for loss a **synthetic lethal** gene pair. While samples that express low levels of the **synthetic lethal** gene pairs will be under-represented, they may not be completely absent from the dataset, due to these higher-level interactions. In the example of 3 **synthetic lethal** genes (shown in Figure 3.5), only one of the genes involved in the higher-order **synthetic lethal** interaction is required for cell viability. For **synthetic lethal** pairs, only a subset of these samples will be inviable (i.e., removed from simulated data), leading to an under-representation.

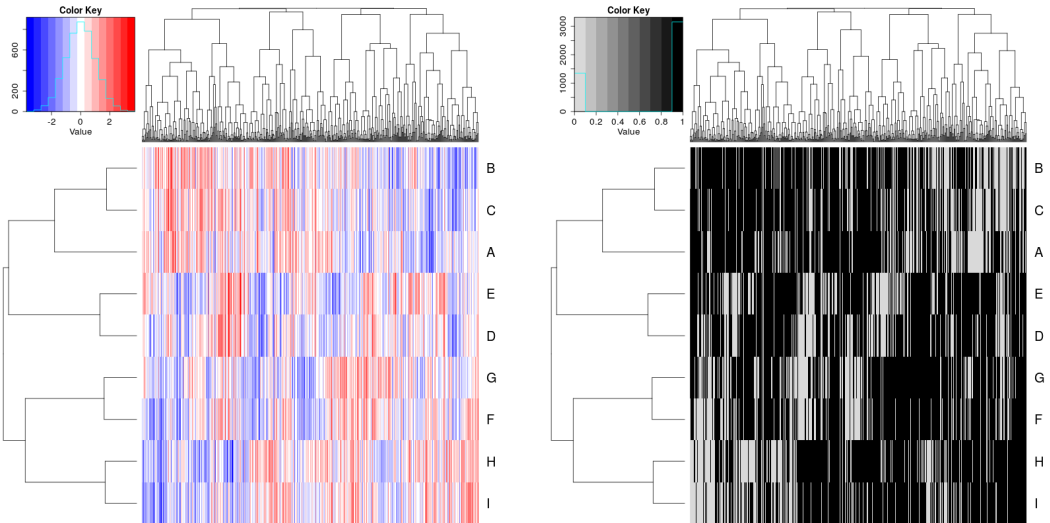
Samples were not actually removed from a simulated dataset, rather the **expression** and function of the query gene is generated across samples separately from the pool of potential partner genes. The query gene data was matched to simulated samples (as shown in Figure 3.7), satisfying the **synthetic lethal** condition with the procedure described in Section 3.2.2. This was performed to maintain a comparable samples size across simulations and the preserve the (multivariate) normal distribution of the data.

3.2.2 Simulation Procedure

Simulations were developed to simulate normal distributions of **expression** data and define gene function with a threshold cut-off. While gene function was used as an intermediary step in modelling **synthetic lethal** genes in **expression** data, the normal distribution was sampled for simulated data to represent normalised empirical **gene expression** data for which **SLIPT** (and other methods) will be applicable.

Sampling a distribution for **expression** profiles has the advantage of enabling simulating correlation structures with the multivariate normal distribution, using the **mvtnorm** R package (Genz and Bretz, 2009; Genz *et al.*, 2016). The parameter Σ is a covariance matrix which defines the correlation structure between the simulated genes being sampled. With a diagonal of one, this Σ matrix simulates genes with a standard deviation of one and the covariance parameters between them are the correlations between each gene. In Figure 3.6, an example of such a simulated multivariate normal dataset is shown with the functional threshold applied.

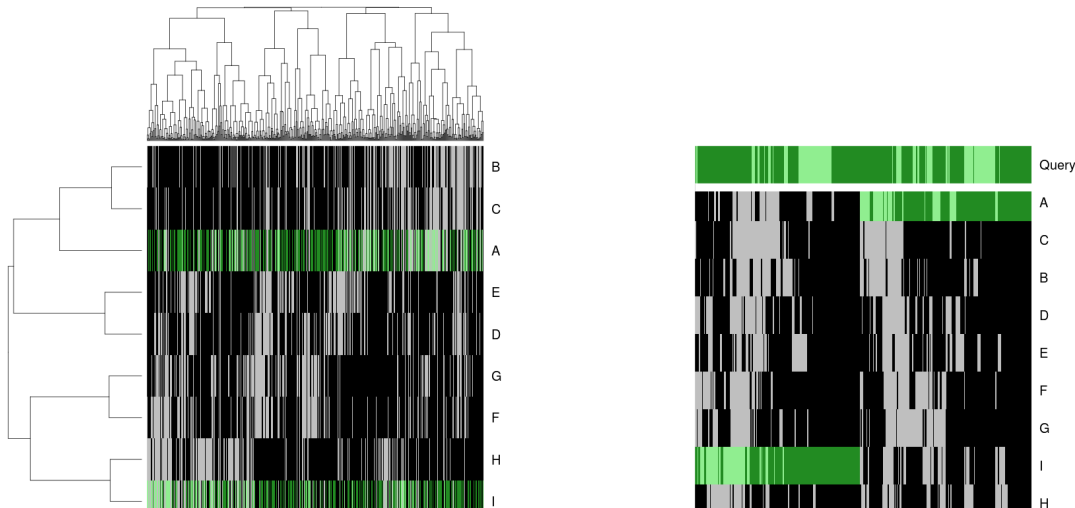
Once a simulated dataset has been generated, the samples were compared by gene function (as derived from a functional threshold). The known underlying **synthetic lethal** partners were selected within the dataset and a query gene was generated by sampling from the normal distribution. These were matched (as shown for 2 **synthetic lethal** partners in Figure 3.7) such that the **synthetic lethal** condition was met: at least one of the synthetic partner genes and the query gene are functional in any particular



(a) Simulated expression matrix

(b) Corresponding gene function calls

Figure 3.6: **Simulating gene function.** A simulated dataset with samples (columns) and genes A–H (rows) was transformed from a continuous (coloured blue–red) scale to a discrete matrix of gene function (black for functional levels and grey for non-functional).



(a) Simulated gene function with SL genes (b) Query gene added with SL condition

Figure 3.7: **Simulating synthetic lethal gene function.** In a discrete simulated gene function dataset (shaded for functional levels and pale otherwise) with samples (columns) and genes (rows), genes A and I are SL partners of a “Query” gene. A partner was selected (highlighted in green) randomly in each sample for simulating synthetic lethality, then ordered such that the query gene or an SL partner were functional in each sample.

cell. The samples are ordered by functional data (without assuming correlation of underlying expression values) with the query gene in one direction and the remaining dataset ordered by the selected synthetic lethal partner.

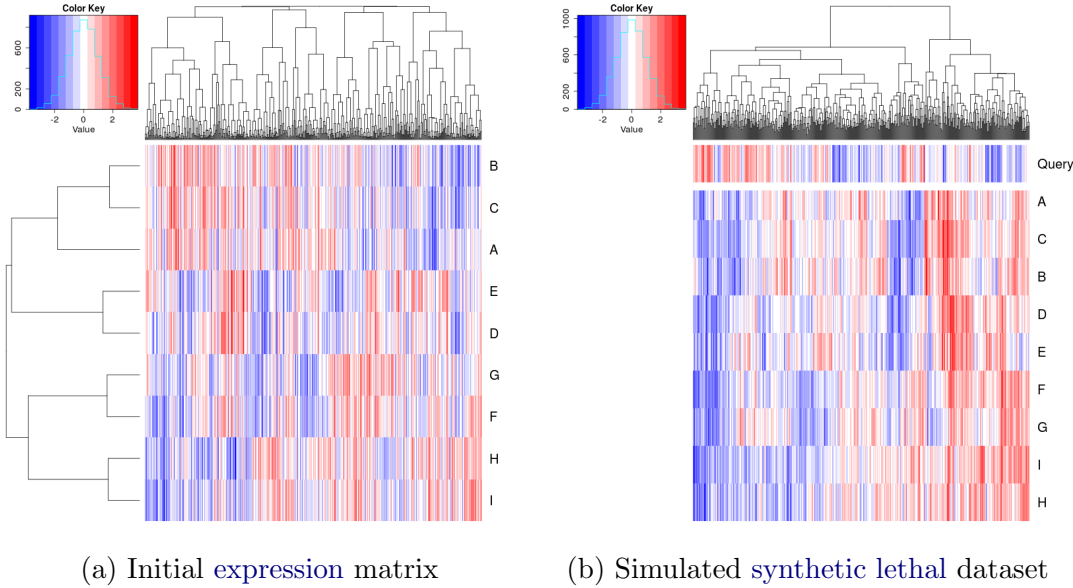


Figure 3.8: **Simulating synthetic lethal gene expression.** A simulated continuous expression dataset (blue–red scale) with samples (columns) and genes (rows) was matched to a query gene such that at least one synthetic lethal partner was above a functional threshold when the query gene was below it which satisfied the synthetic lethal model.

This procedure results in a simulated dataset where samples with non-functional query gene have at least one functional partner gene. Similarly, the query gene is functional in all samples where all of the synthetic lethal partner genes are non-functional. In this procedure, a dataset has been generated with known synthetic lethal partners (see Figure 3.8) with few assumptions about the relationships between the each synthetic lethal pair (allowing compensating functions from higher-order interactions). This procedure has been designed to have the most stringent (least detectable) synthetic lethal relationships, where higher-order interactions are possible for the purposes of testing pairwise detection procedures such as SLIPT.

3.3 Detecting Simulated Synthetic Lethal Partners

The synthetic lethal detection methodology (SLIPT), as described in Section 3.1, was evaluated with simulated data containing known synthetic lethal partners, generated using the procedure described in Section 3.2.2. Simulations were performed to demon-

strate the methodology and support its use throughout this thesis. These simulations were performed by sampling from statistical distributions, including multivariate normal distribution with correlated blocks of genes, generated by Σ matrices such as those shown. A more complex multivariate normal sampling procedure based on pathway graph structures, as described in section 3.4.2, was used for further investigations in Chapter 6.

3.3.1 Binomial Simulation of Synthetic Lethality

The [synthetic lethal](#) simulation procedure (described in Section 3.2.2) initially used gene function, sampled directly from a binomial distribution using the binomial probability of observing functional gene levels ($p = 0.3$) in one observation ($n = 1$) for each samples:

$$X \sim \text{Bin}(n, p)$$

Once a query gene with [synthetic lethal](#) partners has been added, these functional levels were passed directly into [SLIPT](#) as “low” and “high” samples.

The simulation procedure was performed with 20,000 total genes (as occurs in [expression](#) datasets) with a variable number of true [synthetic lethal](#) partners and 500, 1000, 2000, or 5000 samples. Each [ROC](#) curve was derived from the results of 10,000 replicate simulations. The statistical performance (as shown in Figure 3.9) of the χ^2 -derived p-value declined towards random predictions (an [AUROC](#) of 0.5) with an more underlying [synthetic lethal](#) partners to detect. However, increased sample size somewhat mitigated this decline, as expected with a statistical predictor, particularly for moderate numbers of [synthetic lethal](#) partners.

Simulations using this binomial model of [synthetic lethality](#) were limited but informed the development of more complex simulations including [expression](#) and correlation structures. It did not represent the data that [SLIPT](#) will be applied to but the binomial simulations demonstrated that [SLIPT](#) is able to distinguish small numbers of [synthetic lethal](#) partners in a simulated system with behaviours expected with respect to sample size. This supported further development of the [synthetic lethal](#) model and simulation pipeline (as described in Section 3.2) using the multivariate normal distribution.

The multivariate normal simulation procedure more closely recapitulates the (normalised) [expression](#) data that [SLIPT](#) was intended for and enables the methodology procedure to be tested without requiring modifications (in Section 3.3.2). Sampling continuous [expression](#) values from a normal distribution enabled the [expression](#) thresh-

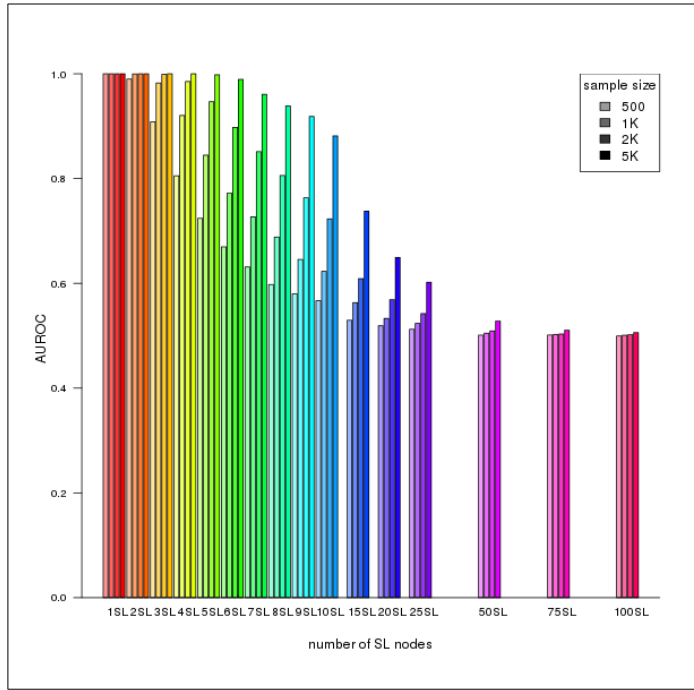


Figure 3.9: **Performance of binomial simulations.** Gene function was simulated by binomial sampling and tested for synthetic lethal genes. Statistical performance declined with additional known synthetic partners but this was mitigated by increased sample sizes.

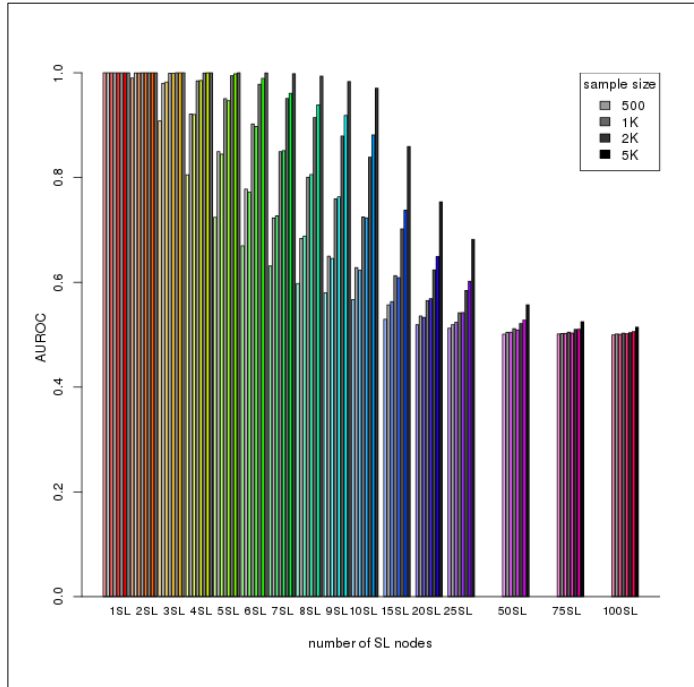


Figure 3.10: **Comparison of statistical performance.** Binomial simulation of synthetic lethality (in colour) in comparison to multivariate normal simulations (in greyscale) which consistently outperformed binomial simulation across parameters.

old for gene function to differ from the categorical “low” and “high” `expression` binning performed by `SLIPT` (as discussed in Section 3.2.1). The `SLIPT` procedure does not assume a known threshold for `expression` and instead uses `expression` as an estimate of gene function which does not compromise the statistical performance of the `SLIPT` in the multivariate normal simulation. The performance was an improvement over the binomial simulation procedure (shown in Figure 3.10) across simulation parameters in an equivalent simulation (without correlation structure). This improvement may be due to how the binomial model defined the `synthetic lethal` condition. While ensuring that at least one `synthetic lethal` partner was active in query-deficient samples, it disrupted the number of samples with functional `synthetic lethal` genes compared to other genes affecting the expected sample proportions of χ^2 test.

3.3.2 Multivariate Normal Simulation of Synthetic Lethality

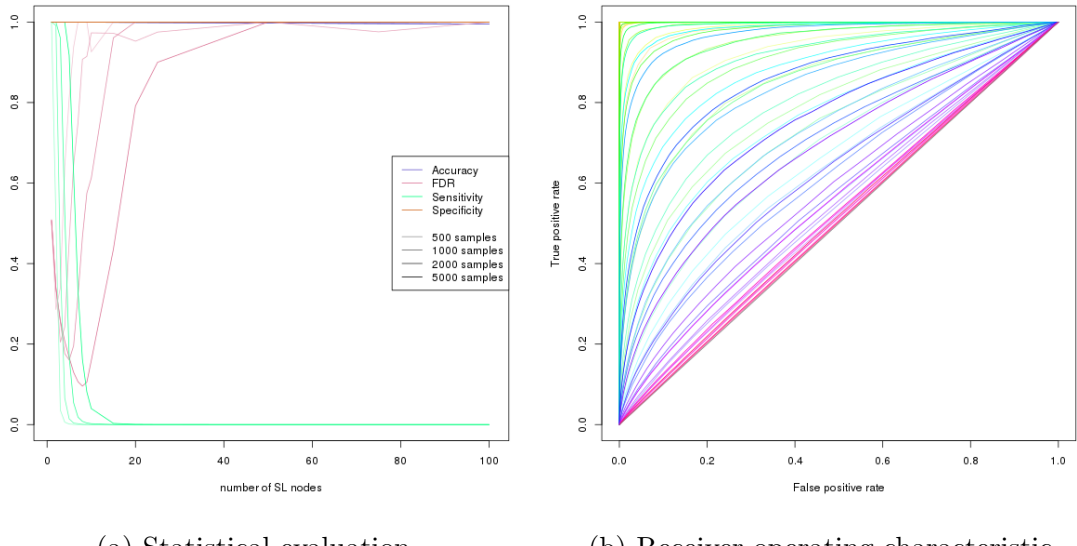
The multivariate normal simulation procedure was initially performed using the `mvtnorm` R package (Genz and Bretz, 2009; Genz *et al.*, 2016) (as described in Section 3.2) without correlation structure. Expression was sampled from multivariate normal distribution with a mean ($\mu = 0$), standard deviation ($\sigma = 1$), and no correlation between genes ($r = 0$):

$$X \sim N(\bar{\mu}, \Sigma)$$

Once a query gene with `synthetic lethal` partners has been added, the simulated `expression` values were tested by `SLIPT`, as described in Section 3.1.

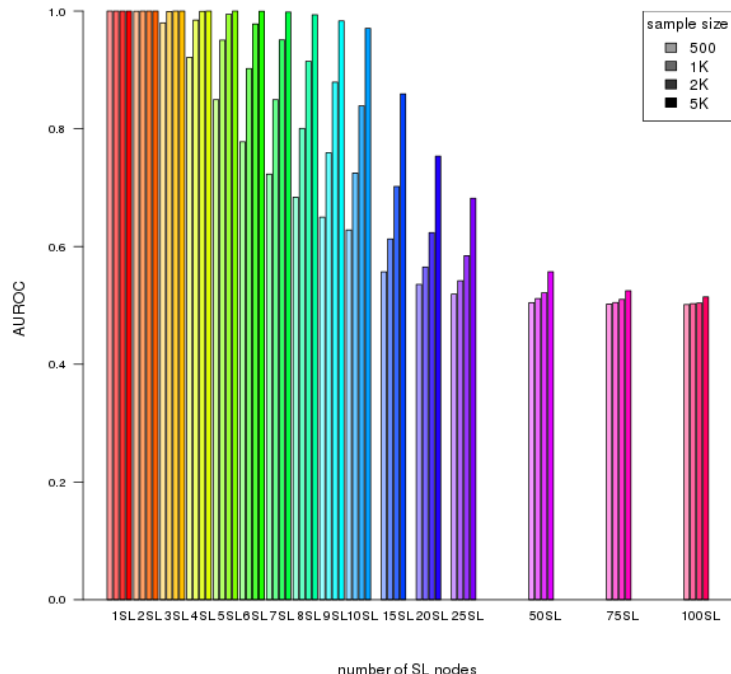
The statistical accuracy of `SLIPT` as a binary classifier was considerably high across simulations of a full dataset of 20,000 genes (shown in Figure 3.11a). Using the χ^2 -derived p-value as a threshold for prediction, this was mostly due to high specificity: the majority of non synthetic lethal genes were distinguished from the underlying `synthetic lethal` genes. Thus the `SLIPT` methodology performed better with larger datasets with more expected negatives and the results of simulations of smaller numbers of genes (e.g., the `graph` structures analysed in Section 6.2.1) can be applied to larger datasets, where they are expected to perform comparably or better with a lower false negative rate (as shown in Sections 6.2.4 and 6.3.2). Accordingly, key results will be supported by replication with larger numbers of non synthetic lethal genes added to the simulations.

The sensitivity of `SLIPT` as a binary classifier of `synthetic lethality` (in Figure 3.11a) declined with higher numbers of `synthetic lethal` genes to detect, although this is somewhat mitigated by higher sample sizes. The minority of true `synthetic lethal` partners are more difficult to distinguish when there are more of them (and a weaker `expression`



(a) Statistical evaluation

(b) Receiver operating characteristic



(c) Statistical performance

Figure 3.11: **Performance of multivariate normal simulations.** Simulation of synthetic lethality was performed sampling from a multivariate normal distribution (without correlation structure). Performance of SLIPT declines for more synthetic partners but this was mitigated by increased sample sizes (in darker colours). This occurred as the sensitivity decreased with a greater number of true positives to detect, which lead to a trade-off in accuracy as seen in a trough for false positive rate and the ROC curves.

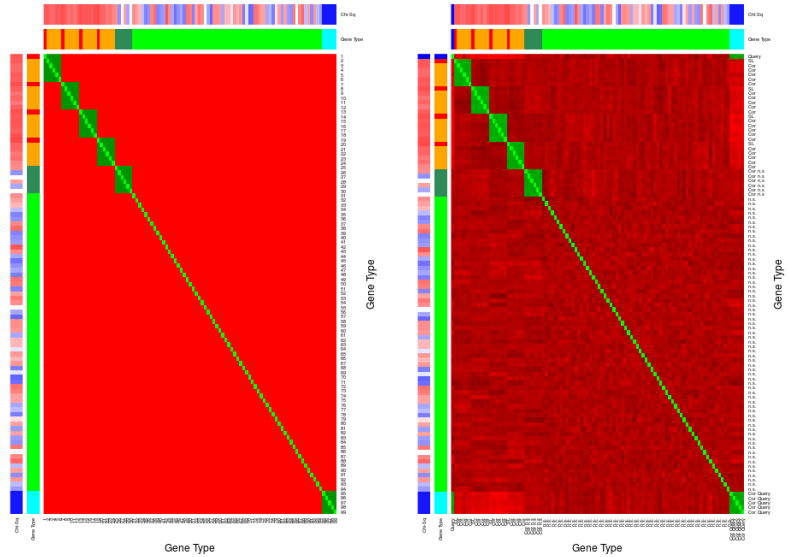
signal from each). While a reduction of the false positive rate could be achieved for moderate numbers of underlying synthetic lethal partners, the number of partners to be detected in analyses of expression data is unknown. However, this simulation procedure is amenable to assessing the performance of SLIPT across simulation parameters, graph structures, and comparisons to other approaches (as presented in Chapter 6).

Not all of the genes detected by SLIPT were true synthetic lethal genes but they were among the strongest candidates and it had higher performance with fewer underlying synthetic lethal genes to detect. These results support a focus on pathway analyses, in particular, the selection of pathways for further investigation. Pathway over-representation analysis was performed to detect functional groups recurrently detected by SLIPT since individually detected gene candidates were not necessarily synthetic lethal. The detection of these functionally related genes (in Chapter 4) supported their role in synthetic lethal relationships. Using pathway metagenes also reduced the number of potential pathways, compared to genes, to identify synthetic lethality. These approaches were both applied in Chapter 4 to identify the synthetic lethal pathways of *CDH1*. Pathways are also more likely to replicate across experimental models, as demonstrated by Dixon *et al.* (2008).

The ROC curves showed that SLIPT has a near equal trade-off between sensitivity and specificity across threshold values (in Figure 3.11b). The lower sensitivity and higher specificity with a binary classification (in Figure 3.11a) results from stringent testing by SLIPT with FDR adjusted p-values. The area under these curves (AUROC) was used to compare statistical performance (in Figure 3.11c), which lower performance for more underlying synthetic lethal partners and higher performance for larger sample size in multivariate normal simulations.

3.3.2.1 Multivariate Normal Simulation with Correlated Genes

Correlation structures were added to the simulation procedure (as discussed in Section 3.2), using correlated blocks of genes with the Σ parameter (in Figure 3.12a). These correlated blocks represent genes with correlated expression, such as co-regulation or biological pathways. The example (in Figure 3.12) shows 4 synthetic lethal genes (out of 100), each with 5 correlated genes that are not themselves synthetic lethal partners of the query gene. These simulations address whether synthetic lethal genes are distinguishable from correlated partners. The Σ matrix produced a similar correlation structure (Figure 3.12b) and expression profiles (Figure 3.12c). Apart from correlated blocks of genes ($r = 0.8$), the remaining genes had small variations due to random sampling. The structure of the dataset, particularly between synthetic lethal genes and



(a) Input Σ matrix parameter (b) Simulated correlation matrix

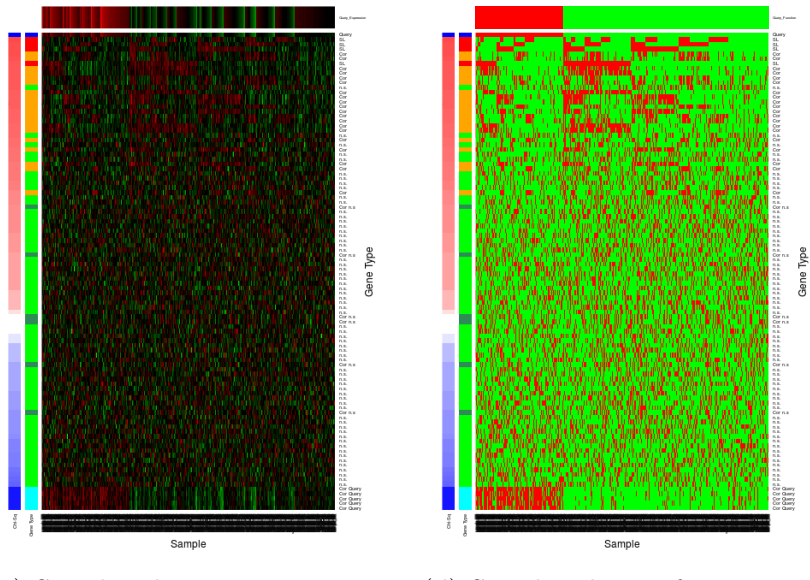


Figure 3.12: Simulating expression with correlated gene blocks. A Σ matrix (a) was used to generate a multivariate normal distribution with 100 genes in correlated blocks of genes (correlated by 0.8) with a comparable structure (b) to the input Σ , as shown by correlation on a red–green scale. The annotation bars for genes show the χ^2 (in blue if the direction of **SLIPT** is met or red otherwise) and the gene category (blue for query, cyan for query-correlated, red for SL, orange for SL-correlated, forest green for non synthetic lethal-correlated, and green for non synthetic lethal). The simulated gene expression (c) and function (d) generated are ordered by χ^2 showing the functional structure of synthetic lethal genes and that they were among the strongest **SLIPT** results.

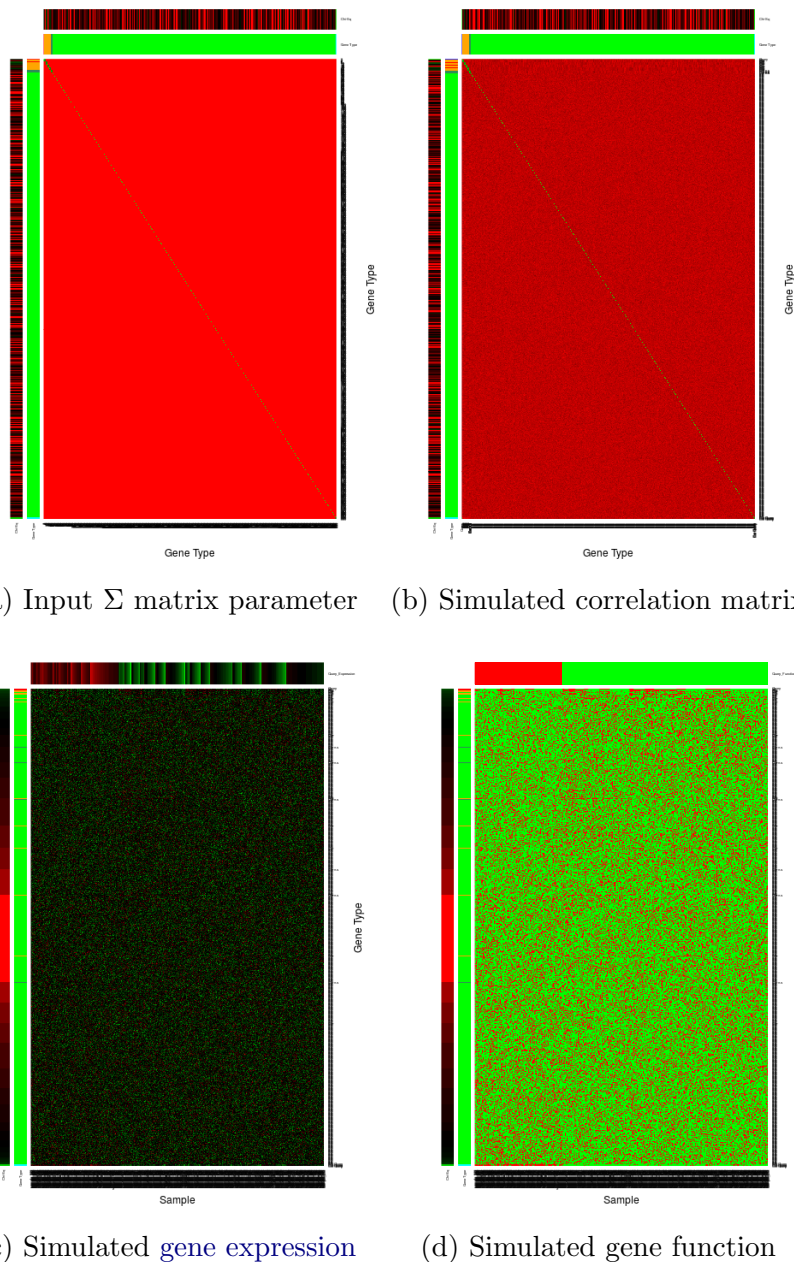


Figure 3.13: **Simulating expression with correlated gene blocks.** Using the (a) Σ matrix, sampling from a multivariate normal distribution with of 1000 genes produced (b) correlated blocks of genes (correlated by 0.8) on a red-green scale. The simulated gene expression (c) and function (d) generated were ordered by χ^2 and **SLIPT** direction show that synthetic lethal genes are among the strongest **SLIPT** results with high specificity against many potential false positives. These are annotated for χ^2 (on a red-green scale) and category (blue for query, cyan for query-correlated, red for SL, orange for SL-correlated, forest green for non synthetic lethal-correlated, and green for non synthetic lethal) for each gene.

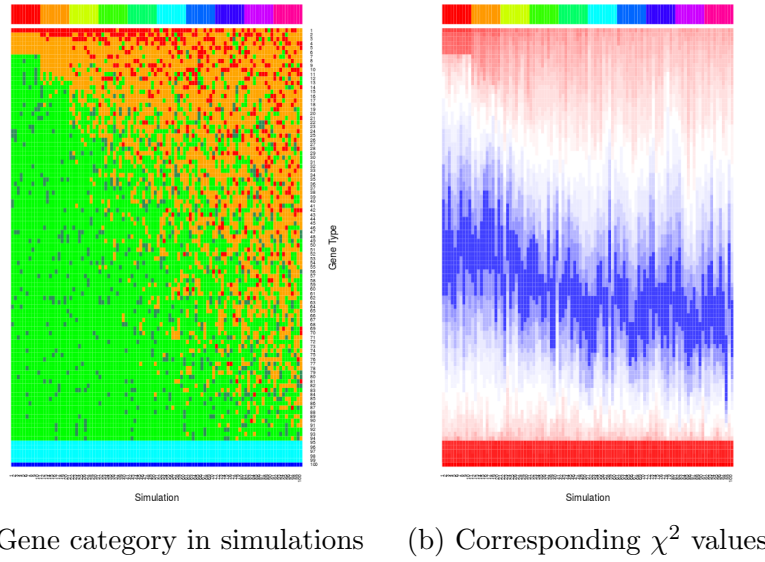
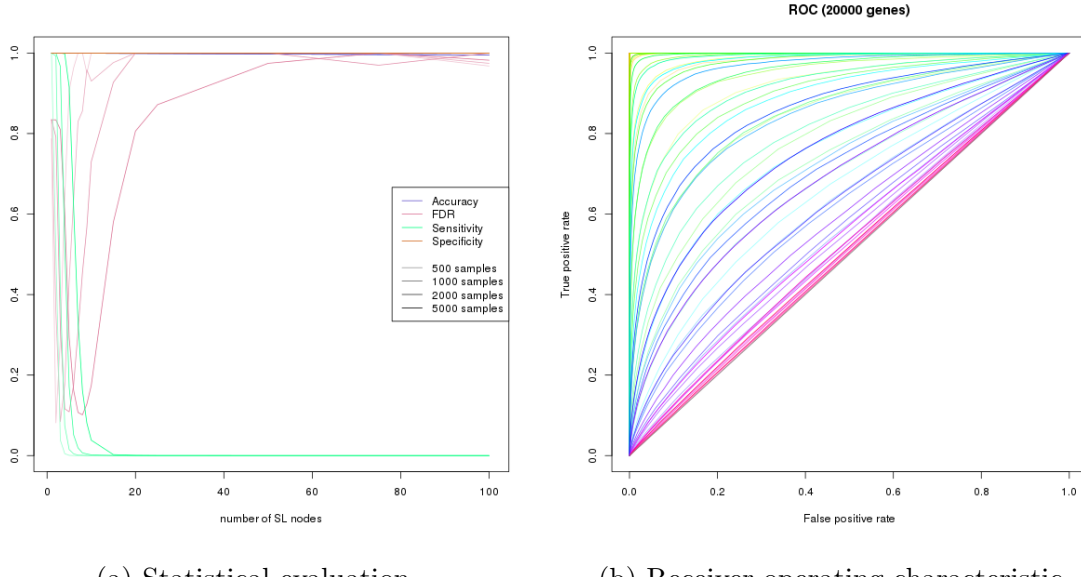


Figure 3.14: Synthetic lethal prediction across simulations. The gene category (blue for query, cyan for query-correlated, red for SL, orange for SL-correlated, forest green for non synthetic lethal-correlated, and green for non synthetic lethal) ordered by χ^2 signed by the **SLIPT** directional condition is shown across simulations. For each of 1–10 SL partners, 10 simulations demonstrate that the increasing numbers of SL partners became harder detect. The χ^2 values showed a threshold for SL and correlated genes when there are fewer of them, distinguishable from correlated genes in this case.

the query, was evident in the simulated gene expression (Figure 3.12c) and function (Figure 3.12d). When these genes were ordered by the **SLIPT** results, the **synthetic lethal** genes were highly ranked, as the majority of them were distinguishable from highly correlated genes.

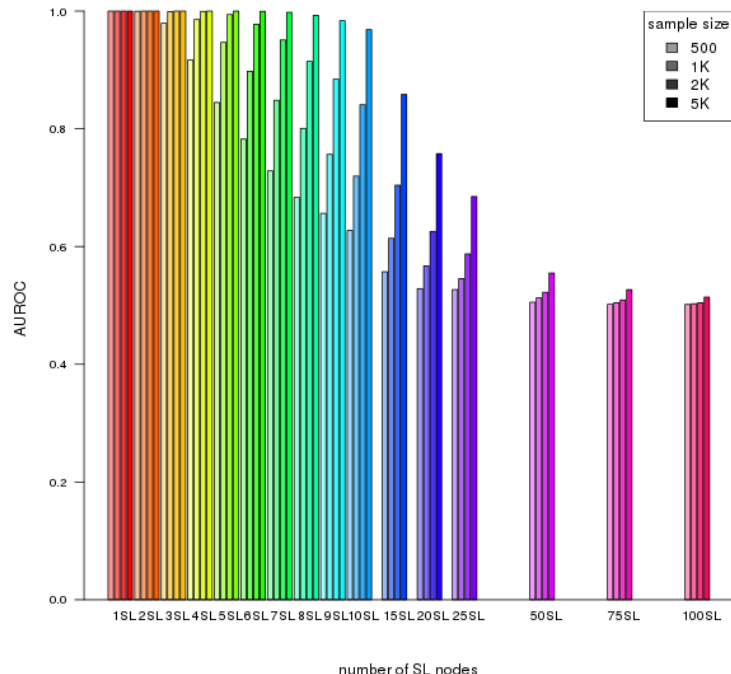
The use of correlation structure was applied to larger datasets, such as 1000 genes shown in Figure 3.13. **Synthetic lethal** genes were highly ranked by **SLIPT** and were often distinguishable from correlated genes. As previously discussed in Section 3.3.2, these **synthetic lethal** genes were still detectable among a larger number of non synthetic lethal genes and the **SLIPT** methodology performed better on large datasets.

These plots (Figures 3.12 and 3.13) used similar correlated blocks with a non synthetic lethal gene (true negative) and the query gene (which is not **synthetic lethal** with itself). Neither of these were **synthetic lethal** but they could potentially affect performance methodology, particularly the specificity, as correlated non synthetic lethal genes may be distinguishable from **synthetic lethal** genes. The non synthetic lethal correlated



(a) Statistical evaluation

(b) Receiver operating characteristic



(c) Statistical performance

Figure 3.15: Performance with correlations. Simulation of synthetic lethality was performed sampling from a multivariate normal distribution (with correlation structure). Performance of **SLIPT** declines for more synthetic partners but this is mitigated by increased sample sizes (darker colours). This generally occurs as the sensitivity decreases for a greater number of true positives to detect, leading to a trade-off in accuracy as seen in a trough for false positive rate and the **ROC** curves.

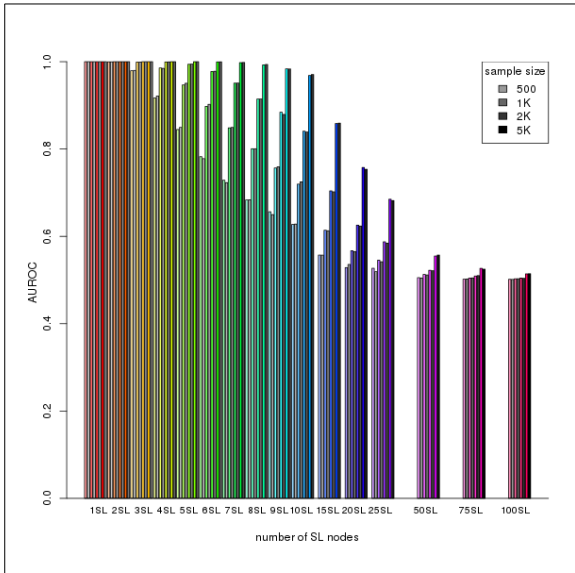
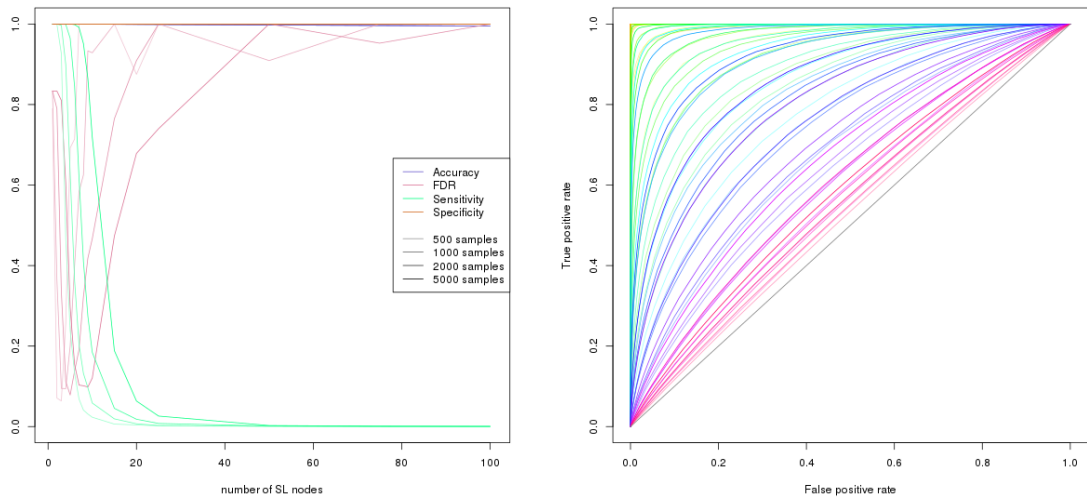


Figure 3.16: **Comparison of statistical performance with correlation structure.** Multivariate simulation of synthetic lethality with correlation structure (in colour) has comparable performance to simulation without correlations (in greyscale) with known synthetic partners across parameters.

block of genes had no impact on synthetic lethal detection but the query correlated genes were important (as shown in Sections 3.3.2.2 and 6.1.1.1).

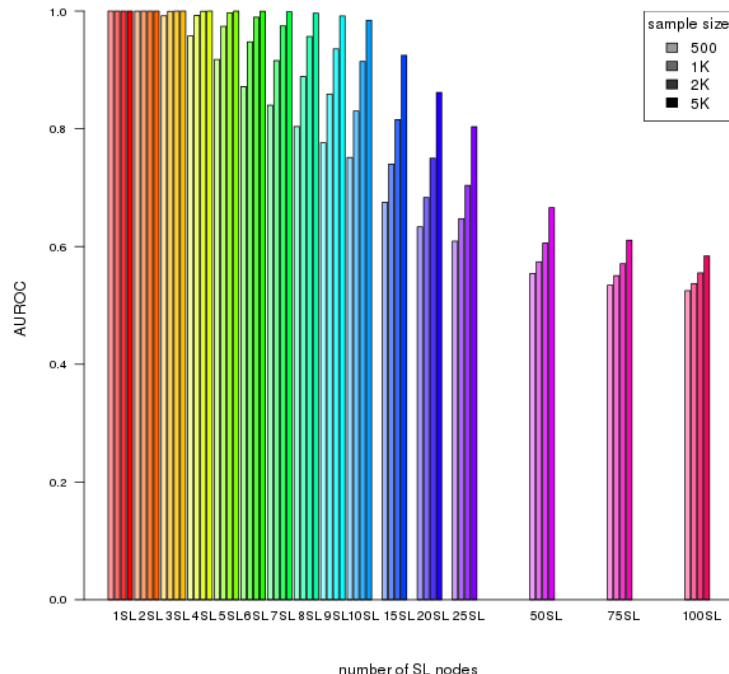
The simulations of gene expression data (with 100 genes) with correlations structure were used to examine the variation between detection in different samples and varying the number of underlying synthetic lethal partners. A small number of simulations (10 for each) are shown to demonstrate the variation between replicate simulations from iterative sampling from the same multivariate normal distribution (in Figure 3.14). These simulations showed that synthetic lethal genes were highly ranked by SLIPT when there are few of them and these were consistent across replicate simulations. However, they were less consistent for higher numbers of synthetic lethal partners to detect and were more difficult to distinguish from other genes, particularly those correlated with them. Similarly, the χ^2 values showed clear thresholds for synthetic lethal and correlated genes in simple simulations but these were more gradual for higher numbers of synthetic lethal partners.

While the synthetic lethal genes were detected in simple simulations (in Figure 3.14), ROC analysis was performed to determine whether they were robustly detectable and to make further comparisons. These results (in Figure 3.15) were similar to simulations without correlation structure. As a binary classifier, SLIPT had low sensitivity



(a) Statistical evaluation

(b) Receiver operating characteristic



(c) Statistical performance

Figure 3.17: Performance with query correlations. Simulation of synthetic lethality was performed sampling from a multivariate normal distribution (with correlation structure including correlated genes with non synthetic lethal and query genes). Performance of **SLIPT** declined for more synthetic partners and is mitigated by increased sample sizes (darker colours) but the sensitivity remains higher for a greater number of true positives with corresponding improvements in **ROC** curves.

for higher numbers of **synthetic lethal** partners to detect and high specificity with the vast majority of non synthetic lethal genes (for 20,000 genes). This was reflected in a similar reduction in statistical performance for higher numbers of **synthetic lethal** partners and a higher performance with higher sample size. Overall, the statistical performance was no different to simulations without correlation structure (as shown in Figure 3.16).

SLIPT was robust across correlation structures and applicable to gene expression data, with **pathway** structures and correlations. These correlation structures were not intended to model specific biological pathways or represent them but showed potential impact of correlation structure on the performance of **SLIPT** using highly correlated ($r = 0.8$) gene blocks. More complex correlation structures, such as genes positively correlated with the query gene and derived from pathway **graph** structures (as described in 3.4.2) were examined further in Sections 3.3.2.2 and 6.2.1 respectively.

In particular, genes correlated with true **synthetic lethal** genes had little impact on the performance of **SLIPT** detection: **synthetic lethal** genes were as distinguishable from true negative genes as without correlated genes. Genes correlated with **synthetic lethal** partners did not interfere with the detection of true **synthetic lethal** genes, although they were often ranked next below them and may still be biologically informative with related gene functions.

3.3.2.2 Specificity with Query-Correlated Pathways

Correlation structures were also considered for non synthetic lethal genes that were (positively) correlated genes with the query gene. Specifically, 5 highly correlated ($r = 0.8$) with the query gene were added (as described in Section 3.3.2.1). These simulations had similar performance (in Figure 3.17) to those without these correlations with a higher specificity and a lower false positive rate (shown in Figure 3.17a).

The directional criteria of the **SLIPT** procedure was important in this case, enhancing its performance, particularly in distinguishing positively correlated non synthetic lethal genes. The multivariate normal simulations were performed, with 20,000 genes, including all of the correlation structures discussed (SL, non synthetic lethal, and query correlated genes). These simulations were compared for the direction **SLIPT** and the χ^2 testing. There was a considerably higher statistical performance with **SLIPT**, particularly increased sensitivity and lower false positive rate (as shown in Figure 3.18).

These results show that the performance of **SLIPT** is appropriate for the analysis of **expression** datasets, where positively correlated genes are commonly occur, with the directional condition robustly improving the performance of **SLIPT** across simulation

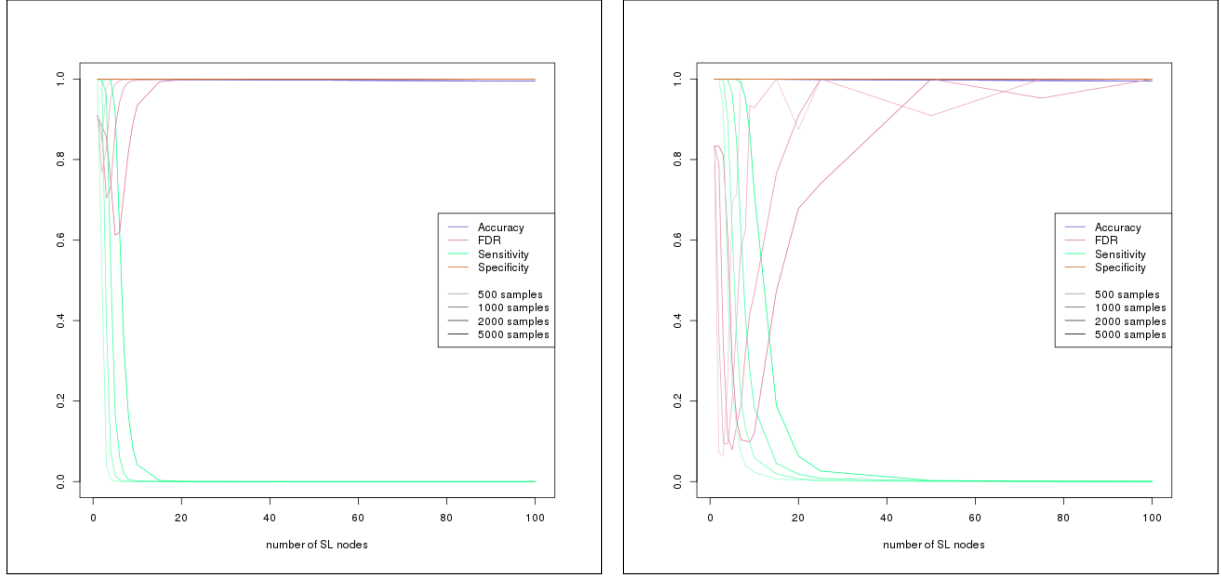
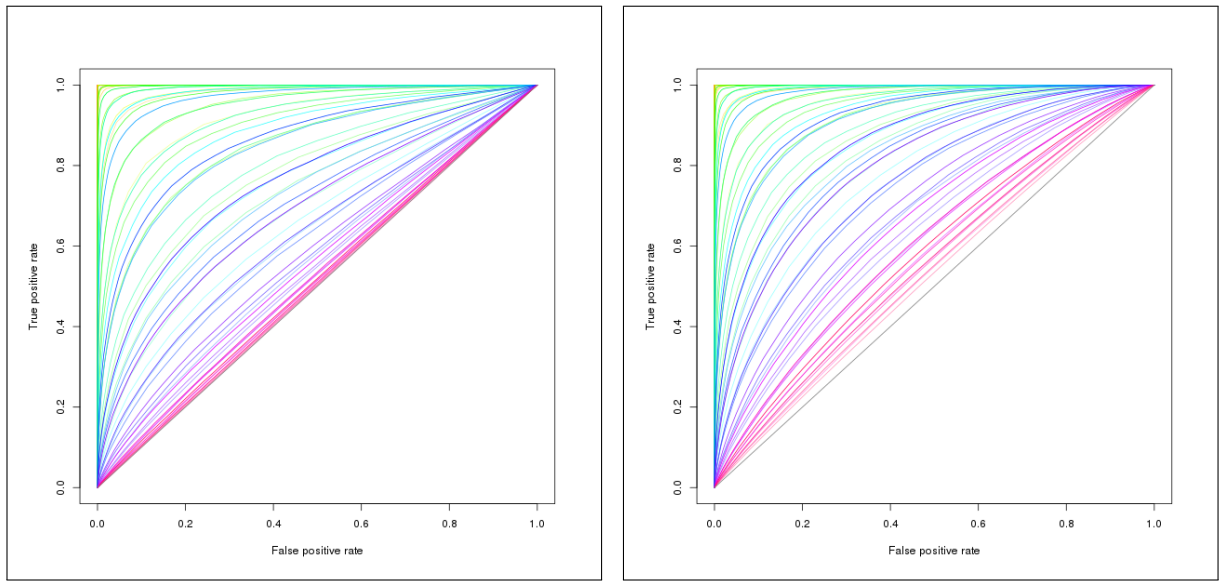


Figure 3.18: **Statistical evaluation of directional criteria.** A simulated multivariate normal dataset of 20,000 genes with correlation structures was tested by **SLIPT** with the directional condition and the χ^2 test. **SLIPT** exhibited a consistently higher sensitivity and lower false positive rate.

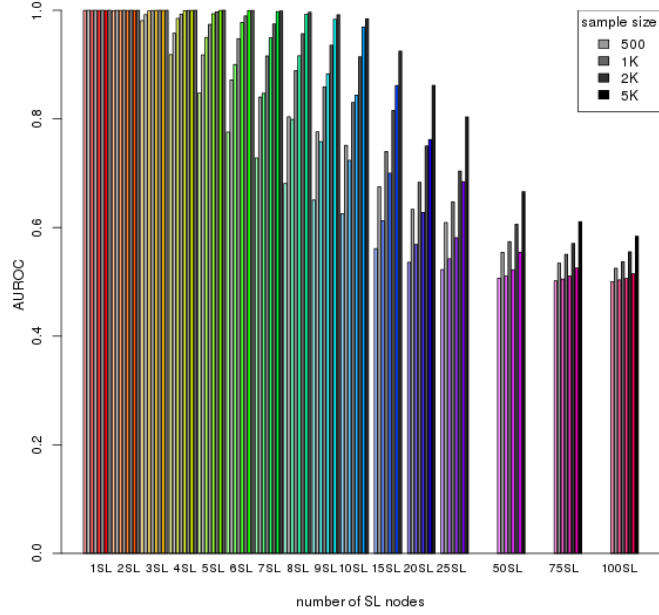
parameters (compared to the χ^2 test). Without assuming the underlying number of synthetic lethal genes, **SLIPT** will perform better than the χ^2 test alone, irrespective of significance threshold as shown by ROC analysis (in Figure 3.19). The directional **SLIPT** methodology outperformed the χ^2 test at detecting synthetic lethal partners with even up to 100 synthetic lethal genes.

Together these simulation results support the application of the **SLIPT** methodology as it has been performed throughout Chapters 4 and 5. The methodology and simulation procedure were explored further in Chapter 6, with comparison to other synthetic lethal detection approaches and the inclusion of graph structures.



(a) χ^2 testing without direction

(b) SLIPT with directional criteria



(c) Statistical performance

Figure 3.19: **Performance with directional criteria.** A simulated multivariate normal dataset of 20,000 genes with correlation structures was tested by **SLIPT** and χ^2 test. **SLIPT** had higher performance across simulation parameters, clearly differing from random (grey diagonal) in ROC curves up to 100 SL genes (b). The performance (c) of **SLIPT** (in greyscale) was consistently higher than the χ^2 test (in color).

3.4 Graph Structure Methods

Graph structures have been used in several ways in this project, including novel approaches to analysis and simulations. Procedures were developed for statistical and network analysis of gene states in [pathway](#) structures. Specifically, the relationships between siRNA and [SLIPT](#) genes were tested within biological pathways in Chapter 5. These [graph](#) structures were also used in Chapter 6 to derive correlation structure between simulated [gene expression](#) profiles to represent biological pathways.

3.4.1 Upstream and Downstream Gene Detection

Comparison of experimental and computational candidate [synthetic lethal](#) partner genes within [pathway](#) structures was performed to determine whether these sets of genes were related by [pathway](#) structure. Considering the differences in how these candidates were generated, it was unsurprising that they did not detect some identical genes within the candidate biological pathways. However, they could still be related by being upstream or downstream of each other.

Using the Reactome version 52 ([Croft et al., 2014](#)), as described in Section 2.4.2, genes detected by each [synthetic lethal](#) discovery approach were mapped to the [graph](#) structure for each candidate pathway identified in Chapter 4 (with graphs defined as described in Section 2.4.3). To test whether [siRNA](#) candidate genes were upstream of [SLIPT](#) candidate genes, [shortest paths](#) were traced between each pair of these genes in a directed network. The number of genes where the [siRNA](#) candidate was upstream were scored “up” and where the [siRNA](#) candidate was downstream were scored “down”. This procedure yielded the total number of [shortest paths](#) which indicated that [siRNA](#) genes were upstream or downstream of the [SLIPT](#) genes. The difference between these scores was used to determine if there was an imbalance in a particular direction. While this difference was indicative of the number of paths between the gene candidate groups in either direction, it was not sufficient to statistically verify structure or relationships between [siRNA](#) and [SLIPT](#) genes. It was combined with a permutation resampling procedure (as described in Section 3.4.1.1) to test for directional relationships in either direction.

Initially, this procedure excluded genes that were detected by both approaches since they would count in both directions. Upon further consideration, these genes were restored to account for since they may contribute unequally to each gene set if there are unequal numbers of genes above or below them in the [pathway](#) structure.

3.4.1.1 Permutation Analysis for Statistical Significance

A permutation procedure was developed to randomly assign members of the pathway to **siRNA** and/or **SLIPT** groups, with the same number of each candidate partner gene set as observed in the pathway. These permuted genes were measured for **pathway** structure between the permuted gene groups as performed for the observed candidates (as performed in Section 3.4.1). A distribution of **pathway** structure relationships expected by chance was generated by permuting iteratively over these pathways. The resulting null distribution was compared to the observed counts of relationships (in either direction). This procedure yielded a permutation p-value as the proportion of permutations in which had a value greater than the observed value. The null hypothesis was that there was no relationship between these gene groups compared to genes that had been selected at random. Thus both the alternate hypotheses that the **siRNA** genes were either upstream of the **SLIPT** genes or that they are downstream of them were testable.

The permutation procedure does not assume the underlying distribution of the data under the null hypothesis and accounts for the total number of **nodes**, **edges**, **siRNA**, and **SLIPT** genes in each **graph** or **network** pathway structure. The number of genes detected by both **siRNA** and **SLIPT** was not accounted for under the initial **shortest path** counts procedure that excluded them. Once they were included, it was ensured that the number of intersecting genes was equal to the number observed to test for **pathway** structure without changing the intersection size, the subject of prior analyses.

3.4.1.2 Hierarchy Based on Biological Context

An alternative approach to **pathway** structure was based on the biological context, given that genes at the upstream and downstream ends of a pathway perform different functions, such as a kinase signalling cascade receiving signals from external stimuli and passes these on ribosomes or the nucleus. Genes were assigned to a hierarchy to determine if genes of either candidate group disproportionately performed upstream or downstream functions.

A network-based approach was used to generate the pathway hierarchy of genes in a computationally rational way when applied to different biological pathways with a directed **graph** structure, G (without loops). The diameter of the network (i.e., the length of longest possible **shortest path** between the most distant genes) was used to identify a gene (z) at the downstream end of the pathway (at the end of a diameter

spanning [shortest path](#)), which was assigned a hierarchy of:

$$\text{hierarchy}(z) = 1 + \text{diameter}(G)$$

Having identified the downstream end of the pathway, genes upstream (e.g., gene i) of this were assigned a hierarchy by the length of their [shortest path](#) (d) to this gene, z .

$$\text{hierarchy}(i) = \text{hierarchy}(z) - d_{iz}$$

The remaining unassigned genes (e.g., gene j) gained the hierarchy of the length of the [shortest path](#) downstream from the nearest assigned gene if possible.

$$\text{hierarchy}(j) = \text{hierarchy}(i) + d_{ij}$$

This process could be performed iteratively to fill in pathway hierarchy but it was not necessary to perform further iterations for the candidate [synthetic lethal](#) pathways investigated which exhibited strong directional structure and the [small world](#) property (i.e., had a low diameter). Using this procedure, genes in a pathway [graph](#) structure were assigned to an integer valued hierarchy upstream to downstream by this procedure:

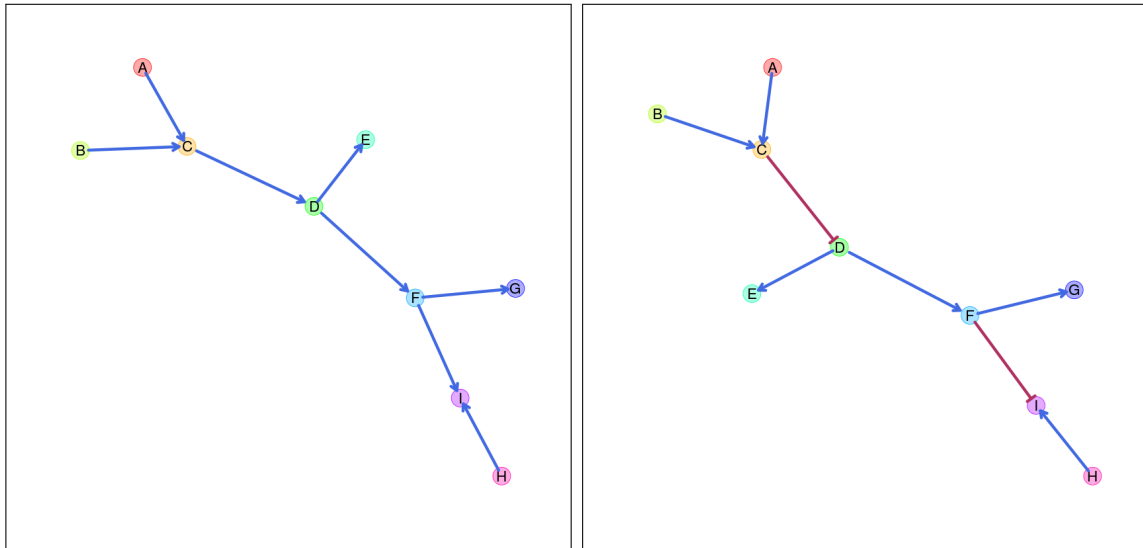
$$\text{hierarchy} \in \{1, 2, 3, \dots, 1 + \text{diameter}(G)\}$$

This hierarchy of pathway directionality (e.g., that shown in Figure 5.7) was used for comparison with measures of the number of [synthetic lethal](#) partners detected by either approach.

3.4.2 Simulating Gene Expression from Graph Structures

A further refinement of the simulation procedure generated [expression](#) data with correlation structure, derived from a known [graph](#) structure. This enables modelling of [synthetic lethal](#) partners within a biological pathway and the investigation of impact of [pathway](#) structure on [synthetic lethal](#) prediction. A simulated pathway is first constructed as a [graph](#) structure, with the `igraph` R package [Csardi and Nepusz \(2006\)](#), with the added annotation of the state of the [edges](#) (i.e, whether they activate or inhibit downstream pathway members). This simulation procedure was intended for biological pathway members with correlated [gene expression](#) (higher than the background of genes in other pathways) but it may also be applicable to modelling protein levels (in a kinase regulation cascade) or substrates and products (in a metabolic pathway).

First, the [graph](#) structure is constructed for simulated data to be generated from (by sampling from a multivariate normal distribution using the `mvtnorm` R package



(a) Activating `pathway` structure (b) Pathway structure including inhibitions

Figure 3.20: **Simulated graph structures.** A constructed `graph` structure used as an example to demonstrate the simulation procedure. Activating `links` are denoted by blue arrows and inhibiting `links` by red edges.

(Genz and Bretz, 2009; Genz *et al.*, 2016)). Throughout this section, the simulation procedure will be demonstrated with the relatively simple constructed `graph` structure shown in Figure 3.20. This `graph` structure visualisation was specifically developed for (directed) iGraph objects in R and has been released in the `plot.igraph` package and `igraph.extensions` library (see Table 2.6 and Section 3.5.3). The `plot_directed` function allows customisation of plot parameters for each `node` or `edge` and mixed (directed) `edge` types for indicating activation or inhibition. These inhibition `links` (which often occur in biological pathways) are demonstrated in Figure 3.20b.

The simulation procedure is designed to use such `graph` structures to inform development of a “Sigma” variance-covariance matrix (Σ) for sampling from a multivariate normal distribution (using the `mvtnorm` R package). Given a `graph` structure (or adjacency matrix), such as Figure 3.21a, a relation matrix is calculated based on distance such that nearer `nodes` are given higher weight than farther `nodes`. For the purposes of this thesis a geometrically decreasing (relative) distance weighting was used, with each more distant `node` being related by $1/2$ compared to the next nearest as shown in Figure 3.21b. However, an arithmetically decreasing (absolute) distance weighting is also available in the `graphsim` R package release of this procedure.

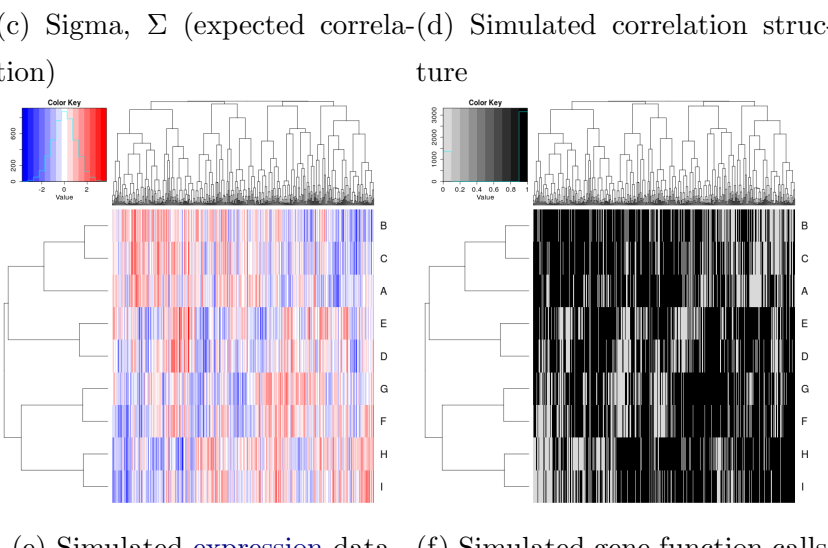
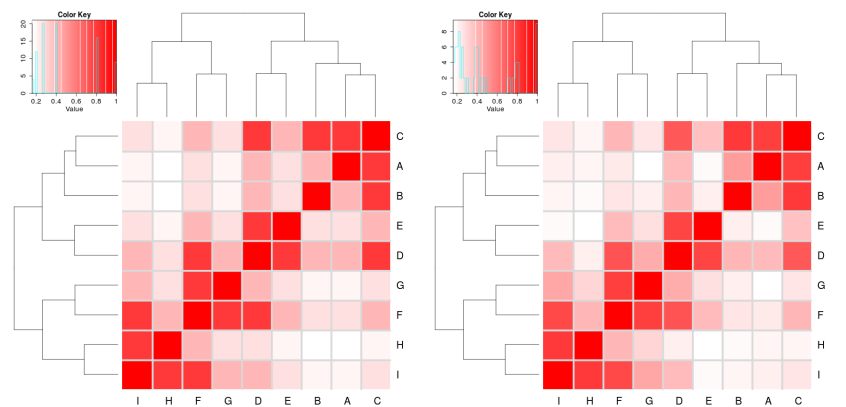
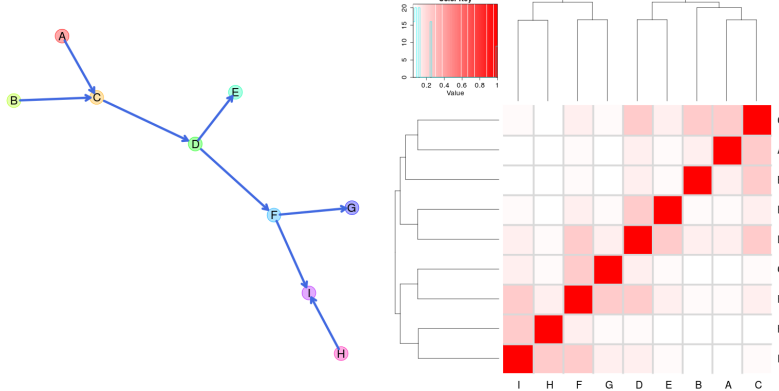


Figure 3.21: **Simulating expression from a graph structure.** An example graph structure was used to derive a correlation structure from the relative distances between nodes and simulate continuous gene expression with sampling from the multivariate normal distribution.

A Σ matrix is derived from this distance weighting matrix, creating a matrix (with a diagonal of 1) where each **node** has a variance and standard deviation of 1. Thus covariances between adjacent **nodes** are assigned by a correlation parameter and the remaining matrix based on weighting these correlations with by the distance matrix (or the nearest “positive definite” matrix). For the purposes of this thesis, the correlation parameter is 0.8 unless otherwise specified (as used for the example in Figure 3.21c). This Σ matrix was used to sample from a multivariate normal distribution with each gene having a mean of 0, standard deviation 1, and covariance within the range [0, 1] such that they are correlations. This procedure generates a simulated (continuous normally distributed) **expression** profile for each **node** (as shown in Figure 3.21e) with corresponding correlation structure (Figure 3.21d). The simulated correlation structure closely resembles the expected correlation structure (Sigma in 3.21c) even for the relatively modest sample size ($N = 100$) illustrated in 3.21. Once a simulated **gene expression** dataset has been generated (as in Figure 3.21e), then a discrete matrix of gene function can be constructed with a functional threshold quantile to simulate functional relationships of **synthetic lethality** (as shown in Figure 3.4). For the purposes of this thesis, this threshold is the 0.3 quantile (as discussed in Section 3.2.1) which generates functional discrete matrices such as those used for **synthetic lethal** simulation in Section 3.2.2 (as shown Figure 3.21f)

The simulation procedure (depicted in Figure 3.21) is amenable to pathways containing inhibition **links** (as shown in Figure 3.22) with several refinements. With the inhibition **links** (as shown in Figure 3.22a), distances are calculated in the same manner as before (Figure 3.22b) with inhibitions accounted for by iteratively multiplying downstream **nodes** by -1 to form blocks of negative correlations (as shown in Figures 3.22c and 3.22d). As before, a multivariate normal distribution with these negative correlations can be sampled to generate simulated data (as shown in Figures 3.22e and 3.22f).

These simulated datasets are amenable to simulating **synthetic lethal** partners of a query gene within a graph network. The query gene is assumed to be separate from the graph network pathway and is added to the dataset using the procedure in Section 3.2.2. Thus we can simulate known **synthetic lethal** partner genes within a **synthetic lethal** partner pathway structure.

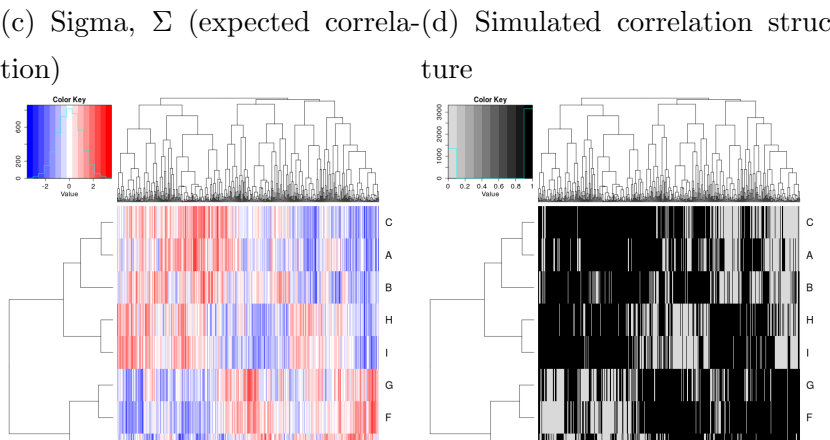
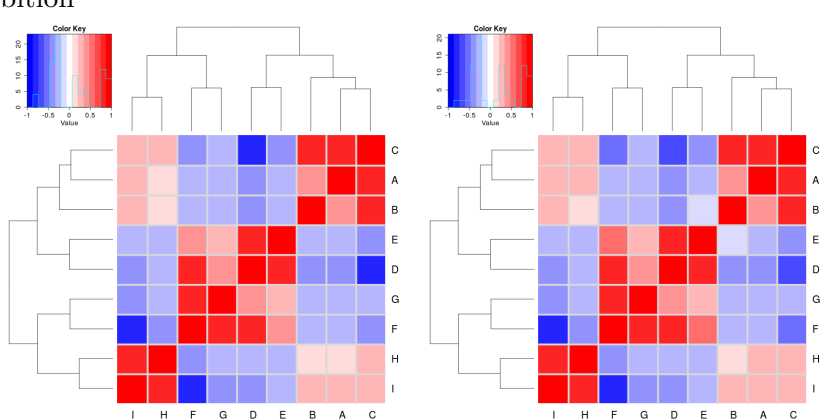
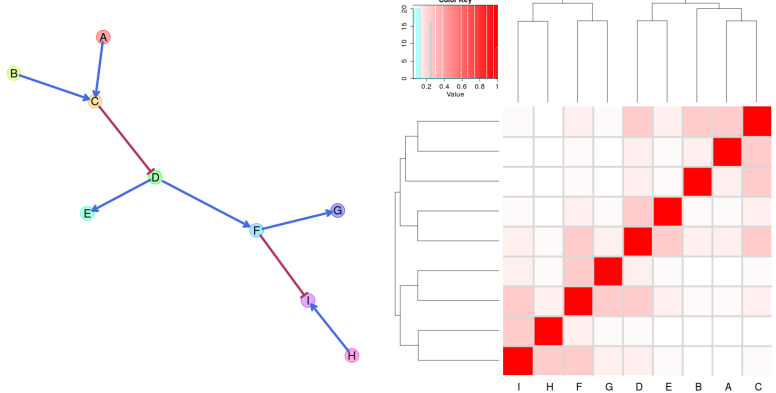


Figure 3.22: **Simulating expression from graph structure with inhibitions.** An example graph structure was used to derive a correlation structure from the relative distances between nodes and simulate continuous gene expression with sampling from the multivariate normal distribution.

3.5 Customised Functions and Packages Developed

[Move to Appendix?]

Various R packages have been developed throughout this thesis using `devtools` (Wickham and Chang, 2016) and `roxygen` (Wickham *et al.*, 2017) to enable reproducibility of customised analysis and visualisation. Many of these have the added benefit of the functions being documented, demonstrated in example vignettes, and released on GitHub to enable the research community to access utilise them in their own analysis. These are summarised in Table 2.6, along with the corresponding urls for their GitHub repository which contains a README file with instructions for installation with the `devtools` R package (Wickham and Chang, 2016) and `links` to the relevant vignette(s) where available.

3.5.1 Synthetic Lethal Interaction Prediction Tool

The statistical methodology for detection of synthetic lethality in gene expression data (**SLIPT**) is one of the main novel procedures developed in this thesis, as described in Section 3.1. The `slipt` R package has been prepared for release to accompany a publication demonstrating the applications of the methodology for identifying candidate interacting genes and pathways with *CDH1* in breast cancer (TCGA, 2012).

SLIPT is amenable to analysis of any effectively continuous measure of gene activity (e.g., microarray, RNA-Seq, protein abundance, or pathway metagenes). Executing `slipt` is straightforward: the `prep_data_for_SL` function scores samples as “low”, “medium”, or “high” for each gene, then the `detect_SL` function tests a given query gene against all potential partners by performing the chi-squared test and directional conditions. This function returns a table summarising the observed and expected sample numbers used for the directional criteria, the χ^2 values, and corresponding p-values including adjusting for multiple comparisons. The `count_of_SL` and `table_of_SL` functions serve to facilitate summary and extraction of the positive **SLIPT** hits, respectively, from the table of predictions of synthetic lethal partners.

The **SLIPT** methodology in this package release has been used in later analyses rather than the corresponding source R code, including use on remote machines and upon simulated data. In particular, the functions in the package facilitate alterations to parameters, such as the proportion of samples called as exhibiting low or high gene activity. This release support reproducibility and enables wider use of **SLIPT** in future investigations into other disease genes.

3.5.2 Data Visualisation

Customisations to existing data visualisations in R have been developed to present data throughout this thesis. The `vioplotx` and `heatmap.2x` packages are enhancements of the `vioplot` package (Adler, 2005) and `heatmap.2` provided by the `gplots` package (Warnes *et al.*, 2015).

The `vioplotx` package provides an alternative visualisation (of continuous variables against categories) to the more familiar boxplot, showing variability of the data by the width of the plots. As demonstrated in Figure 3.23, the customised version enables separate plotting parameters for each violin with vector inputs for colour, shape, and size of various elements of the median point, central boxplot, borders, and fill colour for the violin. Scaling violin width to adjust violin area and splitting data by a second categorical variable is also enabled. This function is intended to be backwards compatible with the inputs of `vioplot` (applying scalar inputs across all violins) and `boxplot` (by enabling formula inputs as an S3 method). Each of these features is demonstrated with examples in respective vignettes on the package [GitHub repository](#).

The `heatmap.2x` provides extensions for annotation colour bars for both the rows and columns (as shown in Figure 3.24). Multiple bars are enabled on both axes with matrix inputs (rather than single vector for `heatmap.2`) which facilitates additional plotting of gene and sample characteristics for comparison with correlation matrices, `expression` profiles, or pathway `metagenes`. Annotation bar inputs correspond to their orientation on the plot, each colour bar is provided as a column for the row annotation on the left of the heatmap and as a row for the column annotation on top of the heatmap. Row and column annotation bars are labelled with the column or row names respectively. Additional parameters enable resizing of these annotation bar labels and control of reordering columns for if samples are ordered in advance (e.g., ranked by a `metagene` or split into groups clustered separately). These features were used through this thesis and are provided in a package [GitHub repository](#).



Figure 3.23: **Demonstration of violin plots with custom features.** An example of the *iris* dataset is plotted to show the custom features of the `vioplotx` package including a) individual colour, shape and size parameters of each violin, scaling violin widths by area, and b) splitting violins to compare subsets of data.

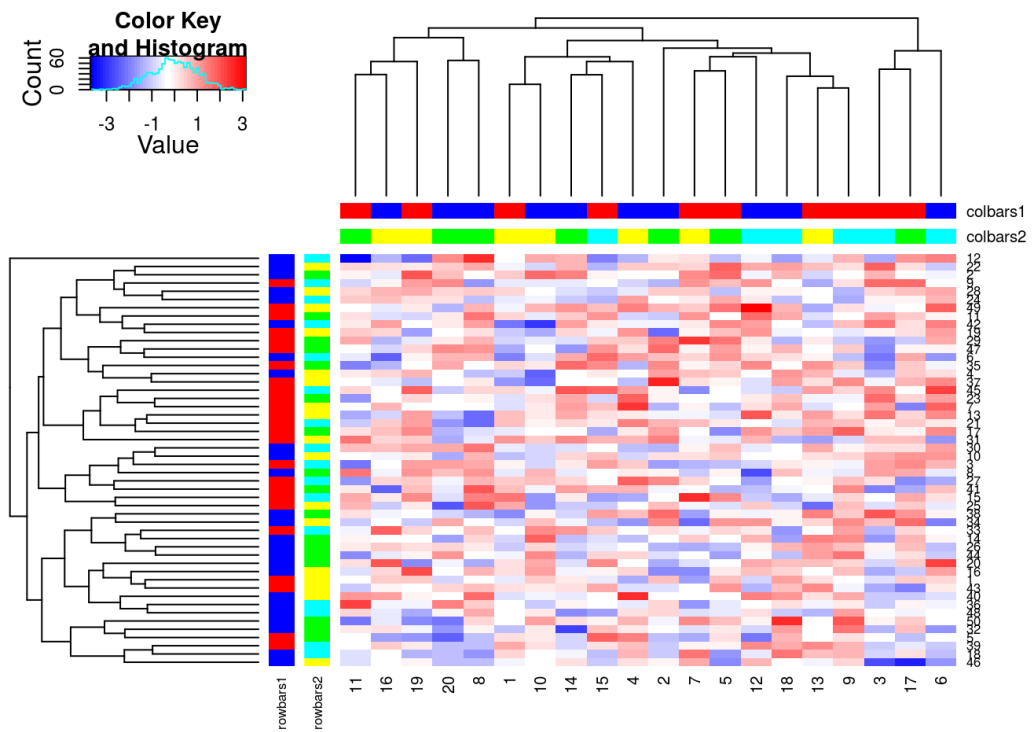


Figure 3.24: **Demonstration of annotated heatmap.** The example heatmap depicts the additional row and column annotation bars enabled by `heatmap.2x`, extending the features of `gplots` with backwards compatible inputs.

3.5.3 Extensions to the iGraph Package

The following features were developed during this thesis using “iGraph” data objects, building upon the `igraph` package (Csardi and Nepusz, 2006). These have been released as separate packages for each respective procedure and can be installed together as a collection of extensions to the `igraph` package.

3.5.3.1 Sampling Simulated Data from Graph Structures

The `graphsim` package implements the procedure for simulating gene expression from `graph` structures (as described in Section 3.4.2). By default, this derives a matrix with a geometrically decreasing weighting by distance (by `shortest paths`) between each pair of `nodes` with. An absolute decreasing weighting is also available with the option of to derive correlation structures from adjacency matrices or the number of `links` common partners (i.e., size of the shared “neighbourhood” (Hell, 1976)) between each pair of `nodes`. Functions to compute these are called directly by passing parameters to them when running the `generate_expression` or `make_sigma_mat` commands. This package enables simulating `expression` data directly from a `graph` structure (with the intermediate steps automated) or generating Σ parameters for `mvtnorm` from `graph` structures or matrices derived from them. These functions support assigning activating or inhibiting to each `edge` (with a `state` parameter).

3.5.3.2 Plotting Directed Graph Structures

The `plot.igraph` package provides the `plot_directed` function specifically developed for directed `graph` structures and to plot activating or inhibiting for each `edge` (as described in Section 3.4.2). As shown in Figure 3.25, this function supports separate plotting parameters for each `node`, `node` label, and `edge`. This includes colours of `node` fill, border, label text, and `edges` and size of `nodes`, `edge` widths, arrowhead lengths, and font size of labels. The `state` parameter for assigning activating or inhibiting to each `edge` determines whether `edges` are depicted with 30° or 90° arrowheads. Colours are assigned separately and so they may be customised. Vectorised parameters are applied across each `node` or `edge`, whereas scalar parameters apply the same plotting parameters across them. The default layout function is `layout.fruchterman.reingold` but any layout function supported by `plot` function in `igraph` (Csardi and Nepusz, 2006) is compatible such as `layout.kamada.kawai` used to implement the Kamada–Kawai algorithm (Kamada and Kawai, 1989) for graph plots throughout this thesis.

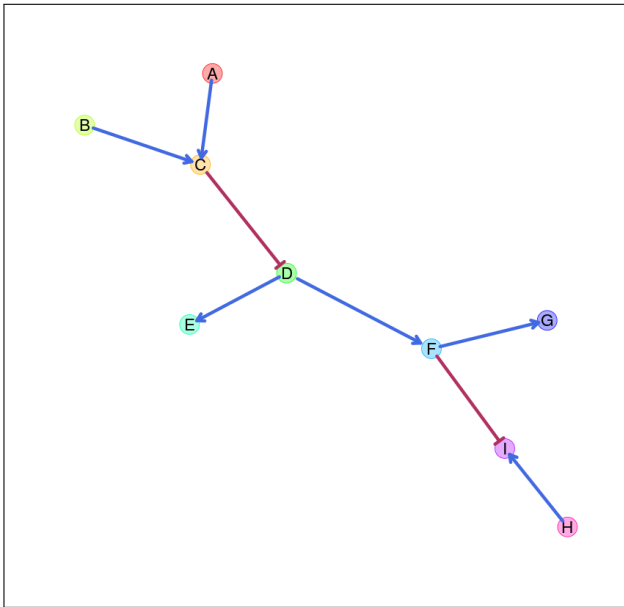


Figure 3.25: **Simulating graph structures.** An example graph structure which will be used throughout demonstrating the simulation procedure from graph structures. Here activating links are denoted by blue arrows and inhibiting links by red edges.

3.5.3.3 Computing Information Centrality

The shortest paths of a network are computed by the `igraph` package Csardi and Nepusz (2006) which can be extended to calculate the network efficiency but is not provided by the package itself (as described in Section 2.4.4). The “information centrality” of a vertex is computed as the relative change in the network efficiency when the vertex is removed. Information centrality is calculated iteratively for each node and the sum of information centrality for each vertex is the information centrality for the network. These metrics are provided by the `info.centrality` package.

3.5.3.4 Testing Pathway Structure with Permutation Testing

A network-based procedure developed was used for comparison of siRNA and SLIPT candidate genes in a pathway structure. Such pathway structure relationships were tested by computing the number of shortest paths between two different groups of nodes in either direction within a graph. This pathway relationship metric was implemented in the `pathway.structure.permutation` package with permutation testing (as described in sections 3.4.1 and 3.4.1.1).

3.5.3.5 Metapackage to Install iGraph Functions

These features may be installed together with `igraph.extensions` which can be accessed from a [GitHub repository](#). This meta-package installs `igraph` ([Csardi and Nepusz, 2006](#)) and the packages described in Section 3.5.3 including their dependencies for matrix operations and statistical procedures: `Matrix`, `matrixcalc`, and `mvtnorm` ([Bates and Maechler, 2016](#); [Genz and Bretz, 2009](#); [Genz *et al.*, 2016](#); [Novomestky, 2012](#)).

Bibliography

- Aarts, M., Bajrami, I., Herrera-Abreu, M.T., Elliott, R., Brough, R., Ashworth, A., Lord, C.J., and Turner, N.C. (2015) Functional genetic screen identifies increased sensitivity to wee1 inhibition in cells with defects in fanconi anemia and hr pathways. *Mol Cancer Ther*, **14**(4): 865–76.
- Abeshouse, A., Ahn, J., Akbani, R., Ally, A., Amin, S., Andry, C.D., Annala, M., Aprikian, A., Armenia, J., Arora, A., *et al.* (2015) The Molecular Taxonomy of Primary Prostate Cancer. *Cell*, **163**(4): 1011–1025.
- Adler, D. (2005) *vioplot: Violin plot*. R package version 0.2.
- Akbani, R., Akdemir, K.C., Aksoy, B.A., Albert, M., Ally, A., Amin, S.B., Arachchi, H., Arora, A., Auman, J.T., Ayala, B., *et al.* (2015) Genomic Classification of Cutaneous Melanoma. *Cell*, **161**(7): 1681–1696.
- Akobeng, A.K. (2007) Understanding diagnostic tests 3: receiver operating characteristic curves. *Acta Pdiatrica*, **96**(5): 644–647.
- American Cancer Society (2017) Genetics and cancer. <https://www.cancer.org/cancer/cancer-causes/genetics.html>. Accessed: 22/03/2017.
- Anjomshoaa, A., Lin, Y.H., Black, M.A., McCall, J.L., Humar, B., Song, S., Fukuzawa, R., Yoon, H.S., Holzmann, B., Friederichs, J., *et al.* (2008) Reduced expression of a gene proliferation signature is associated with enhanced malignancy in colon cancer. *Br J Cancer*, **99**(6): 966–973.
- Araki, H., Knapp, C., Tsai, P., and Print, C. (2012) GeneSetDB: A comprehensive meta-database, statistical and visualisation framework for gene set analysis. *FEBS Open Bio*, **2**: 76–82.

- Ashburner, M., Ball, C.A., Blake, J.A., Botstein, D., Butler, H., Cherry, J.M., Davis, A.P., Dolinski, K., Dwight, S.S., Eppig, J.T., *et al.* (2000) Gene ontology: tool for the unification of biology. The Gene Ontology Consortium. *Nat Genet*, **25**(1): 25–29.
- Ashworth, A. (2008) A synthetic lethal therapeutic approach: poly(adp) ribose polymerase inhibitors for the treatment of cancers deficient in dna double-strand break repair. *J Clin Oncol*, **26**(22): 3785–90.
- Audeh, M.W., Carmichael, J., Penson, R.T., Friedlander, M., Powell, B., Bell-McGuinn, K.M., Scott, C., Weitzel, J.N., Oaknin, A., Loman, N., *et al.* (2010) Oral poly(adp-ribose) polymerase inhibitor olaparib in patients with *BRCA1* or *BRCA2* mutations and recurrent ovarian cancer: a proof-of-concept trial. *Lancet*, **376**(9737): 245–51.
- Babyak, M.A. (2004) What you see may not be what you get: a brief, nontechnical introduction to overfitting in regression-type models. *Psychosom Med*, **66**(3): 411–21.
- Bamford, S., Dawson, E., Forbes, S., Clements, J., Pettett, R., Dogan, A., Flanagan, A., Teague, J., Futreal, P.A., Stratton, M.R., *et al.* (2004) The COSMIC (Catalogue of Somatic Mutations in Cancer) database and website. *Br J Cancer*, **91**(2): 355–358.
- Barabási, A.L. and Albert, R. (1999) Emergence of scaling in random networks. *Science*, **286**(5439): 509–12.
- Barabási, A.L., Gulbahce, N., and Loscalzo, J. (2011) Network medicine: a network-based approach to human disease. *Nat Rev Genet*, **12**(1): 56–68.
- Barabási, A.L. and Oltvai, Z.N. (2004) Network biology: understanding the cell's functional organization. *Nat Rev Genet*, **5**(2): 101–13.
- Barrat, A. and Weigt, M. (2000) On the properties of small-world network models. *The European Physical Journal B - Condensed Matter and Complex Systems*, **13**(3): 547–560.
- Barretina, J., Caponigro, G., Stransky, N., Venkatesan, K., Margolin, A.A., Kim, S., Wilson, C.J., Lehar, J., Kryukov, G.V., Sonkin, D., *et al.* (2012) The Cancer Cell Line Encyclopedia enables predictive modelling of anticancer drug sensitivity. *Nature*, **483**(7391): 603–607.

Barry, W.T. (2016) *safe: Significance Analysis of Function and Expression*. R package version 3.14.0.

Baryshnikova, A., Costanzo, M., Dixon, S., Vizeacoumar, F.J., Myers, C.L., Andrews, B., and Boone, C. (2010a) Synthetic genetic array (sga) analysis in *saccharomyces cerevisiae* and *schizosaccharomyces pombe*. *Methods Enzymol*, **470**: 145–79.

Baryshnikova, A., Costanzo, M., Kim, Y., Ding, H., Koh, J., Toufighi, K., Youn, J.Y., Ou, J., San Luis, B.J., Bandyopadhyay, S., et al. (2010b) Quantitative analysis of fitness and genetic interactions in yeast on a genome scale. *Nat Meth*, **7**(12): 1017–1024.

Bass, A.J., Thorsson, V., Shmulevich, I., Reynolds, S.M., Miller, M., Bernard, B., Hinoue, T., Laird, P.W., Curtis, C., Shen, H., et al. (2014) Comprehensive molecular characterization of gastric adenocarcinoma. *Nature*, **513**(7517): 202–209.

Bates, D. and Maechler, M. (2016) *Matrix: Sparse and Dense Matrix Classes and Methods*. R package version 1.2-7.1.

Bateson, W. and Mendel, G. (1909) *Mendel's principles of heredity, by W. Bateson*. University Press, Cambridge [Eng.].

Becker, K.F., Atkinson, M.J., Reich, U., Becker, I., Nekarda, H., Siewert, J.R., and Hfler, H. (1994) E-cadherin gene mutations provide clues to diffuse type gastric carcinomas. *Cancer Research*, **54**(14): 3845–3852.

Bell, D., Berchuck, A., Birrer, M., Chien, J., Cramer, D., Dao, F., Dhir, R., DiSaia, P., Gabra, H., Glenn, P., et al. (2011) Integrated genomic analyses of ovarian carcinoma. *Nature*, **474**(7353): 609–615.

Benjamini, Y. and Hochberg, Y. (1995) Controlling the false discovery rate: A practical and powerful approach to multiple testing. *Journal of the Royal Statistical Society Series B (Methodological)*, **57**(1): 289–300.

Berx, G., Cleton-Jansen, A.M., Nollet, F., de Leeuw, W.J., van de Vijver, M., Cornelisse, C., and van Roy, F. (1995) E-cadherin is a tumour/invasion suppressor gene mutated in human lobular breast cancers. *EMBO J*, **14**(24): 6107–15.

Berx, G., Cleton-Jansen, A.M., Strumane, K., de Leeuw, W.J., Nollet, F., van Roy, F., and Cornelisse, C. (1996) E-cadherin is inactivated in a majority of invasive human

- lobular breast cancers by truncation mutations throughout its extracellular domain. *Oncogene*, **13**(9): 1919–25.
- Berx, G. and van Roy, F. (2009) Involvement of members of the cadherin superfamily in cancer. *Cold Spring Harb Perspect Biol*, **1**: a003129.
- Bitler, B.G., Aird, K.M., Garipov, A., Li, H., Amatangelo, M., Kossenkov, A.V., Schultz, D.C., Liu, Q., Shih Ie, M., Conejo-Garcia, J.R., *et al.* (2015) Synthetic lethality by targeting ezh2 methyltransferase activity in arid1a-mutated cancers. *Nat Med*, **21**(3): 231–8.
- Blake, J.A., Christie, K.R., Dolan, M.E., Drabkin, H.J., Hill, D.P., Ni, L., Sitnikov, D., Burgess, S., Buza, T., Gresham, C., *et al.* (2015) Gene Ontology Consortium: going forward. *Nucleic Acids Res*, **43**(Database issue): D1049–1056.
- Boettcher, M., Lawson, A., Ladenburger, V., Fredebohm, J., Wolf, J., Hoheisel, J.D., Frezza, C., and Shlomi, T. (2014) High throughput synthetic lethality screen reveals a tumorigenic role of adenylate cyclase in fumarate hydratase-deficient cancer cells. *BMC Genomics*, **15**: 158.
- Boone, C., Bussey, H., and Andrews, B.J. (2007) Exploring genetic interactions and networks with yeast. *Nat Rev Genet*, **8**(6): 437–49.
- Borgatti, S.P. (2005) Centrality and network flow. *Social Networks*, **27**(1): 55 – 71.
- Boucher, B. and Jenna, S. (2013) Genetic interaction networks: better understand to better predict. *Front Genet*, **4**: 290.
- Bozovic-Spasojevic, I., Azambuja, E., McCaskill-Stevens, W., Dinh, P., and Cardoso, F. (2012) Chemoprevention for breast cancer. *Cancer treatment reviews*, **38**(5): 329–339.
- Breiman, L. (2001) Random forests. *Machine Learning*, **45**(1): 5–32.
- Brin, S. and Page, L. (1998) The anatomy of a large-scale hypertextual web search engine. *Computer Networks and ISDN Systems*, **30**(1): 107 – 117.
- Broulxhon, S.M., Kyrkanides, S., Teng, X., Athar, M., Ghazizadeh, S., Simon, M., O'Banion, M.K., and Ma, L. (2014) Soluble E-cadherin: a critical oncogene modulating receptor tyrosine kinases, MAPK and PI3K/Akt/mTOR signaling. *Oncogene*, **33**(2): 225–235.

- Bryant, H.E., Schultz, N., Thomas, H.D., Parker, K.M., Flower, D., Lopez, E., Kyle, S., Meuth, M., Curtin, N.J., and Helleday, T. (2005) Specific killing of *BRCA2*-deficient tumours with inhibitors of polyadribose polymerase. *Nature*, **434**(7035): 913–7.
- Bussey, H., Andrews, B., and Boone, C. (2006) From worm genetic networks to complex human diseases. *Nat Genet*, **38**(8): 862–3.
- Butland, G., Babu, M., Diaz-Mejia, J.J., Bohdana, F., Phanse, S., Gold, B., Yang, W., Li, J., Gagarinova, A.G., Pogoutse, O., *et al.* (2008) esga: *E. coli* synthetic genetic array analysis. *Nat Methods*, **5**(9): 789–95.
- cBioPortal for Cancer Genomics (cBioPortal) (2017) cBioPortal for Cancer Genomics. <http://www.cbioportal.org/>. Accessed: 26/03/2017.
- Cerami, E.G., Gross, B.E., Demir, E., Rodchenkov, I., Babur, O., Anwar, N., Schultz, N., Bader, G.D., and Sander, C. (2011) Pathway Commons, a web resource for biological pathway data. *Nucleic Acids Res*, **39**(Database issue): D685–690.
- Chen, A., Beetham, H., Black, M.A., Priya, R., Telford, B.J., Guest, J., Wiggins, G.A.R., Godwin, T.D., Yap, A.S., and Guilford, P.J. (2014) E-cadherin loss alters cytoskeletal organization and adhesion in non-malignant breast cells but is insufficient to induce an epithelial-mesenchymal transition. *BMC Cancer*, **14**(1): 552.
- Chen, S. and Parmigiani, G. (2007) Meta-analysis of BRCA1 and BRCA2 penetrance. *J Clin Oncol*, **25**(11): 1329–1333.
- Chen, X. and Tompa, M. (2010) Comparative assessment of methods for aligning multiple genome sequences. *Nat Biotechnol*, **28**(6): 567–572.
- Chipman, K. and Singh, A. (2009) Predicting genetic interactions with random walks on biological networks. *BMC Bioinformatics*, **10**(1): 17.
- Christofori, G. and Semb, H. (1999) The role of the cell-adhesion molecule E-cadherin as a tumour-suppressor gene. *Trends in Biochemical Sciences*, **24**(2): 73 – 76.
- Ciriello, G., Gatza, M.L., Beck, A.H., Wilkerson, M.D., Rhie, S.K., Pastore, A., Zhang, H., McLellan, M., Yau, C., Kandoth, C., *et al.* (2015) Comprehensive Molecular Portraits of Invasive Lobular Breast Cancer. *Cell*, **163**(2): 506–519.

- Clark, M.J. (2004) Endogenous Regulator of G Protein Signaling Proteins Suppress G_o-Dependent -Opioid Agonist-Mediated Adenylyl Cyclase Supersensitization. *Journal of Pharmacology and Experimental Therapeutics*, **310**(1): 215–222.
- Clough, E. and Barrett, T. (2016) The Gene Expression Omnibus Database. *Methods Mol Biol*, **1418**: 93–110.
- Collingridge, D.S. (2013) A primer on quantitized data analysis and permutation testing. *Journal of Mixed Methods Research*, **7**(1): 81–97.
- Collins, F.S. and Barker, A.D. (2007) Mapping the cancer genome. Pinpointing the genes involved in cancer will help chart a new course across the complex landscape of human malignancies. *Sci Am*, **296**(3): 50–57.
- Collisson, E., Campbell, J., Brooks, A., Berger, A., Lee, W., Chmielecki, J., Beer, D., Cope, L., Creighton, C., Danilova, L., et al. (2014) Comprehensive molecular profiling of lung adenocarcinoma. *Nature*, **511**(7511): 543–550.
- Corcoran, R.B., Ebi, H., Turke, A.B., Coffee, E.M., Nishino, M., Cogdill, A.P., Brown, R.D., Della Pelle, P., Dias-Santagata, D., Hung, K.E., et al. (2012) Egfr-mediated reactivation of mapk signaling contributes to insensitivity of BRAF-mutant colorectal cancers to raf inhibition with vemurafenib. *Cancer Discovery*, **2**(3): 227–235.
- Costanzo, M., Baryshnikova, A., Bellay, J., Kim, Y., Spear, E.D., Sevier, C.S., Ding, H., Koh, J.L., Toufighi, K., Mostafavi, S., et al. (2010) The genetic landscape of a cell. *Science*, **327**(5964): 425–31.
- Costanzo, M., Baryshnikova, A., Myers, C.L., Andrews, B., and Boone, C. (2011) Charting the genetic interaction map of a cell. *Curr Opin Biotechnol*, **22**(1): 66–74.
- Courtney, K.D., Corcoran, R.B., and Engelman, J.A. (2010) The PI3K pathway as drug target in human cancer. *J Clin Oncol*, **28**(6): 1075–1083.
- Creighton, C.J., Morgan, M., Gunaratne, P.H., Wheeler, D.A., Gibbs, R.A., Robertson, A., Chu, A., Beroukhim, R., Cibulskis, K., Signoretti, S., et al. (2013) Comprehensive molecular characterization of clear cell renal cell carcinoma. *Nature*, **499**(7456): 43–49.
- Croft, D., Mundo, A.F., Haw, R., Milacic, M., Weiser, J., Wu, G., Caudy, M., Garapati, P., Gillespie, M., Kamdar, M.R., et al. (2014) The Reactome pathway knowledgebase. *Nucleic Acids Res*, **42**(database issue): D472D477.

- Crunkhorn, S. (2014) Cancer: Predicting synthetic lethal interactions. *Nat Rev Drug Discov*, **13**(11): 812.
- Csardi, G. and Nepusz, T. (2006) The igraph software package for complex network research. *InterJournal, Complex Systems*: 1695.
- Dai, X., Li, T., Bai, Z., Yang, Y., Liu, X., Zhan, J., and Shi, B. (2015) Breast cancer intrinsic subtype classification, clinical use and future trends. *Am J Cancer Res*, **5**(10): 2929–2943.
- Davierwala, A.P., Haynes, J., Li, Z., Brost, R.L., Robinson, M.D., Yu, L., Mnaimneh, S., Ding, H., Zhu, H., Chen, Y., *et al.* (2005) The synthetic genetic interaction spectrum of essential genes. *Nat Genet*, **37**(10): 1147–1152.
- De Leeuw, W.J., Berx, G., Vos, C.B., Peterse, J.L., Van de Vijver, M.J., Litvinov, S., Van Roy, F., Cornelisse, C.J., and Cleton-Jansen, A.M. (1997) Simultaneous loss of E-cadherin and catenins in invasive lobular breast cancer and lobular carcinoma in situ. *J Pathol*, **183**(4): 404–11.
- De Santis, G., Miotti, S., Mazzi, M., Canevari, S., and Tomassetti, A. (2009) E-cadherin directly contributes to PI3K/AKT activation by engaging the PI3K-p85 regulatory subunit to adherens junctions of ovarian carcinoma cells. *Oncogene*, **28**(9): 1206–1217.
- Demir, E., Babur, O., Rodchenkov, I., Aksoy, B.A., Fukuda, K.I., Gross, B., Sumer, O.S., Bader, G.D., and Sander, C. (2013) Using biological pathway data with Paxtools. *PLoS Comput Biol*, **9**(9): e1003194.
- Deshpande, R., Asiedu, M.K., Klebig, M., Sutor, S., Kuzmin, E., Nelson, J., Piotrowski, J., Shin, S.H., Yoshida, M., Costanzo, M., *et al.* (2013) A comparative genomic approach for identifying synthetic lethal interactions in human cancer. *Cancer Res*, **73**(20): 6128–36.
- Dickson, D. (1999) Wellcome funds cancer database. *Nature*, **401**(6755): 729.
- Dienstmann, R. and Tabernero, J. (2011) BRAF as a target for cancer therapy. *Anti-cancer Agents Med Chem*, **11**(3): 285–95.
- Dijkstra, E.W. (1959) A note on two problems in connexion with graphs. *Numerische Mathematik*, **1**(1): 269–271.

- Dixon, S.J., Andrews, B.J., and Boone, C. (2009) Exploring the conservation of synthetic lethal genetic interaction networks. *Commun Integr Biol*, **2**(2): 78–81.
- Dixon, S.J., Fedyshyn, Y., Koh, J.L., Prasad, T.S., Chahwan, C., Chua, G., Toufighi, K., Baryshnikova, A., Hayles, J., Hoe, K.L., et al. (2008) Significant conservation of synthetic lethal genetic interaction networks between distantly related eukaryotes. *Proc Natl Acad Sci U S A*, **105**(43): 16653–8.
- Dong, L.L., Liu, L., Ma, C.H., Li, J.S., Du, C., Xu, S., Han, L.H., Li, L., and Wang, X.W. (2012) E-cadherin promotes proliferation of human ovarian cancer cells in vitro via activating MEK/ERK pathway. *Acta Pharmacol Sin*, **33**(6): 817–822.
- Dorogovtsev, S.N. and Mendes, J.F. (2003) *Evolution of networks: From biological nets to the Internet and WWW*. Oxford University Press, USA.
- Dorsam, R.T. and Gutkind, J.S. (2007) G-protein-coupled receptors and cancer. *Nat Rev Cancer*, **7**(2): 79–94.
- Erdős, P. and Rényi, A. (1959) On random graphs I. *Publ Math Debrecen*, **6**: 290–297.
- Erdős, P. and Rényi, A. (1960) On the evolution of random graphs. In *Publ. Math. Inst. Hung. Acad. Sci*, volume 5, 17–61.
- Eroles, P., Bosch, A., Perez-Fidalgo, J.A., and Lluch, A. (2012) Molecular biology in breast cancer: intrinsic subtypes and signaling pathways. *Cancer Treat Rev*, **38**(6): 698–707.
- Farmer, H., McCabe, N., Lord, C.J., Tutt, A.N., Johnson, D.A., Richardson, T.B., Santarosa, M., Dillon, K.J., Hickson, I., Knights, C., et al. (2005) Targeting the dna repair defect in BRCA mutant cells as a therapeutic strategy. *Nature*, **434**(7035): 917–21.
- Fawcett, T. (2006) An introduction to ROC analysis. *Pattern Recognition Letters*, **27**(8): 861 – 874. {ROC} Analysis in Pattern Recognition.
- Fece de la Cruz, F., Gapp, B.V., and Nijman, S.M. (2015) Synthetic lethal vulnerabilities of cancer. *Annu Rev Pharmacol Toxicol*, **55**: 513–531.
- Ferlay, J., Soerjomataram, I., Dikshit, R., Eser, S., Mathers, C., Rebelo, M., Parkin, D.M., Forman, D., and Bray, F. (2015) Cancer incidence and mortality worldwide:

sources, methods and major patterns in GLOBOCAN 2012. *Int J Cancer*, **136**(5): E359–386.

Fisher, R.A. (1919) Xv.the correlation between relatives on the supposition of mendelian inheritance. *Earth and Environmental Science Transactions of the Royal Society of Edinburgh*, **52**(02): 399–433.

Fong, P.C., Boss, D.S., Yap, T.A., Tutt, A., Wu, P., Mergui-Roelvink, M., Mortimer, P., Swaisland, H., Lau, A., O'Connor, M.J., et al. (2009) Inhibition of poly(adp-ribose) polymerase in tumors from BRCA mutation carriers. *N Engl J Med*, **361**(2): 123–34.

Fong, P.C., Yap, T.A., Boss, D.S., Carden, C.P., Mergui-Roelvink, M., Gourley, C., De Greve, J., Lubinski, J., Shanley, S., Messiou, C., et al. (2010) Poly(adp)-ribose polymerase inhibition: frequent durable responses in BRCA carrier ovarian cancer correlating with platinum-free interval. *J Clin Oncol*, **28**(15): 2512–9.

Forbes, S.A., Beare, D., Gunasekaran, P., Leung, K., Bindal, N., Boutselakis, H., Ding, M., Bamford, S., Cole, C., Ward, S., et al. (2015) COSMIC: exploring the world's knowledge of somatic mutations in human cancer. *Nucleic Acids Res*, **43**(Database issue): D805–811.

Fraser, A. (2004) Towards full employment: using RNAi to find roles for the redundant. *Oncogene*, **23**(51): 8346–52.

Fromental-Ramain, C., Warot, X., Lakkaraju, S., Favier, B., Haack, H., Birling, C., Dierich, A., Doll e, P., and Chambon, P. (1996) Specific and redundant functions of the paralogous Hoxa-9 and Hoxd-9 genes in forelimb and axial skeleton patterning. *Development*, **122**(2): 461–472.

Futreal, P.A., Coin, L., Marshall, M., Down, T., Hubbard, T., Wooster, R., Rahman, N., and Stratton, M.R. (2004) A census of human cancer genes. *Nat Rev Cancer*, **4**(3): 177–183.

Futreal, P.A., Kasprzyk, A., Birney, E., Mullikin, J.C., Wooster, R., and Stratton, M.R. (2001) Cancer and genomics. *Nature*, **409**(6822): 850–852.

Gao, B. and Roux, P.P. (2015) Translational control by oncogenic signaling pathways. *Biochimica et Biophysica Acta*, **1849**(7): 753–65.

- Gatza, M.L., Kung, H.N., Blackwell, K.L., Dewhirst, M.W., Marks, J.R., and Chi, J.T. (2011) Analysis of tumor environmental response and oncogenic pathway activation identifies distinct basal and luminal features in HER2-related breast tumor subtypes. *Breast Cancer Res*, **13**(3): R62.
- Gatza, M.L., Lucas, J.E., Barry, W.T., Kim, J.W., Wang, Q., Crawford, M.D., Datto, M.B., Kelley, M., Mathey-Prevot, B., Potti, A., *et al.* (2010) A pathway-based classification of human breast cancer. *Proc Natl Acad Sci USA*, **107**(15): 6994–6999.
- Gatza, M.L., Silva, G.O., Parker, J.S., Fan, C., and Perou, C.M. (2014) An integrated genomics approach identifies drivers of proliferation in luminal-subtype human breast cancer. *Nat Genet*, **46**(10): 1051–1059.
- Gentleman, R.C., Carey, V.J., Bates, D.M., Bolstad, B., Dettling, M., Dudoit, S., Ellis, B., Gautier, L., Ge, Y., Gentry, J., *et al.* (2004) Bioconductor: open software development for computational biology and bioinformatics. *Genome Biol*, **5**(10): R80.
- Genz, A. and Bretz, F. (2009) Computation of multivariate normal and t probabilities. In *Lecture Notes in Statistics*, volume 195. Springer-Verlag, Heidelberg.
- Genz, A., Bretz, F., Miwa, T., Mi, X., Leisch, F., Scheipl, F., and Hothorn, T. (2016) *mvtnorm: Multivariate Normal and t Distributions*. R package version 1.0-5. URL.
- Glaire, M.A., Brown, M., Church, D.N., and Tomlinson, I. (2017) Cancer predisposition syndromes: lessons for truly precision medicine. *J Pathol*, **241**(2): 226–235.
- Globus (Globus) (2017) Research data management simplified. <https://www.globus.org/>. Accessed: 25/03/2017.
- Goodwin, S., McPherson, J.D., and McCombie, W.R. (2016) Coming of age: ten years of next-generation sequencing technologies. *Nat Rev Genet*, **17**(6): 333–351.
- Grady, W.M., Willis, J., Guilford, P.J., Dunbier, A.K., Toro, T.T., Lynch, H., Wiesner, G., Ferguson, K., Eng, C., Park, J.G., *et al.* (2000) Methylation of the CDH1 promoter as the second genetic hit in hereditary diffuse gastric cancer. *Nat Genet*, **26**(1): 16–17.
- Graziano, F., Humar, B., and Guilford, P. (2003) The role of the E-cadherin gene (*CDH1*) in diffuse gastric cancer susceptibility: from the laboratory to clinical practice. *Annals of Oncology*, **14**(12): 1705–1713.

- Güell, O., Sagus, F., and Serrano, M. (2014) Essential plasticity and redundancy of metabolism unveiled by synthetic lethality analysis. *PLoS Comput Biol*, **10**(5): e1003637.
- Guilford, P. (1999) E-cadherin downregulation in cancer: fuel on the fire? *Molecular Medicine Today*, **5**(4): 172 – 177.
- Guilford, P., Hopkins, J., Harraway, J., McLeod, M., McLeod, N., Harawira, P., Taite, H., Scouler, R., Miller, A., and Reeve, A.E. (1998) E-cadherin germline mutations in familial gastric cancer. *Nature*, **392**(6674): 402–5.
- Guilford, P., Humar, B., and Blair, V. (2010) Hereditary diffuse gastric cancer: translation of *CDH1* germline mutations into clinical practice. *Gastric Cancer*, **13**(1): 1–10.
- Guilford, P.J., Hopkins, J.B., Grady, W.M., Markowitz, S.D., Willis, J., Lynch, H., Rajput, A., Wiesner, G.L., Lindor, N.M., Burgart, L.J., *et al.* (1999) E-cadherin germline mutations define an inherited cancer syndrome dominated by diffuse gastric cancer. *Hum Mutat*, **14**(3): 249–55.
- Guo, J., Liu, H., and Zheng, J. (2016) SynLethDB: synthetic lethality database toward discovery of selective and sensitive anticancer drug targets. *Nucleic Acids Res*, **44**(D1): D1011–1017.
- Hajian-Tilaki, K. (2013) Receiver Operating Characteristic (ROC) Curve Analysis for Medical Diagnostic Test Evaluation. *Caspian J Intern Med*, **4**(2): 627–635.
- Hall, M., Frank, E., Holmes, G., Pfahringer, B., Reutemann, P., and Witten, I.H. (2009) The weka data mining software: an update. *SIGKDD Explor Newsl*, **11**(1): 10–18.
- Hamerman, P.S., Lawrence, M.S., Voet, D., Jing, R., Cibulskis, K., Sivachenko, A., Stojanov, P., McKenna, A., Lander, E.S., Gabriel, S., *et al.* (2012) Comprehensive genomic characterization of squamous cell lung cancers. *Nature*, **489**(7417): 519–525.
- Hanahan, D. and Weinberg, R.A. (2000) The hallmarks of cancer. *Cell*, **100**(1): 57–70.
- Hanahan, D. and Weinberg, R.A. (2011) Hallmarks of cancer: the next generation. *Cell*, **144**(5): 646–674.

- Hanna, S. (2003) Cancer incidence in new zealand (2003-2007). In D. Forman, D. Bray F Brewster, C. Gombe Mbalawa, B. Kohler, M. Piñeros, E. Steliarova-Foucher, R. Swaminathan, and J. Ferlay (editors), *Cancer Incidence in Five Continents*, volume X, 902–907. International Agency for Research on Cancer, Lyon, France. Electronic version <http://ci5.iarc.fr> Accessed 22/03/2017.
- Hansford, S., Kaurah, P., Li-Chang, H., Woo, M., Senz, J., Pinheiro, H., Schrader, K.A., Schaeffer, D.F., Shumansky, K., Zogopoulos, G., *et al.* (2015) Hereditary Diffuse Gastric Cancer Syndrome: CDH1 Mutations and Beyond. *JAMA Oncol*, **1**(1): 23–32.
- Heiskanen, M., Bian, X., Swan, D., and Basu, A. (2014) caArray microarray database in the cancer biomedical informatics gridTM (caBIGTM). *Cancer Research*, **67**(9 Supplement): 3712–3712.
- Heiskanen, M.A. and Aittokallio, T. (2012) Mining high-throughput screens for cancer drug targets—lessons from yeast chemical-genomic profiling and synthetic lethality. *Wiley Interdisciplinary Reviews: Data Mining and Knowledge Discovery*, **2**(3): 263–272.
- Hell, P. (1976) Graphs with given neighbourhoods i. problèmes combinatoires at theorie des graphes. *Proc Coll Int CNRS, Orsay*, **260**: 219–223.
- Hillenmeyer, M.E. (2008) The chemical genomic portrait of yeast: uncovering a phenotype for all genes. *Science*, **320**: 362–365.
- Hoadley, K.A., Yau, C., Wolf, D.M., Cherniack, A.D., Tamborero, D., Ng, S., Leiserson, M.D., Niu, B., McLellan, M.D., Uzunangelov, V., *et al.* (2014) Multiplatform analysis of 12 cancer types reveals molecular classification within and across tissues of origin. *Cell*, **158**(4): 929–944.
- Hoehndorf, R., Hardy, N.W., Osumi-Sutherland, D., Tweedie, S., Schofield, P.N., and Gkoutos, G.V. (2013) Systematic analysis of experimental phenotype data reveals gene functions. *PLoS ONE*, **8**(4): e60847.
- Holm, S. (1979) A simple sequentially rejective multiple test procedure. *Scandinavian Journal of Statistics*, **6**(2): 65–70.
- Holme, P. and Kim, B.J. (2002) Growing scale-free networks with tunable clustering. *Physical Review E*, **65**(2): 026107.

- Hopkins, A.L. (2008) Network pharmacology: the next paradigm in drug discovery. *Nat Chem Biol*, **4**(11): 682–690.
- Hu, Z., Fan, C., Oh, D.S., Marron, J.S., He, X., Qaqish, B.F., Livasy, C., Carey, L.A., Reynolds, E., Dressler, L., et al. (2006) The molecular portraits of breast tumors are conserved across microarray platforms. *BMC Genomics*, **7**: 96.
- Huang, E., Cheng, S., Dressman, H., Pittman, J., Tsou, M., Horng, C., Bild, A., Iversen, E., Liao, M., Chen, C., et al. (2003) Gene expression predictors of breast cancer outcomes. *Lancet*, **361**: 1590–1596.
- Hutchison, C.A., Chuang, R.Y., Noskov, V.N., Assad-Garcia, N., Deering, T.J., Ellsman, M.H., Gill, J., Kannan, K., Karas, B.J., Ma, L., et al. (2016) Design and synthesis of a minimal bacterial genome. *Science*, **351**(6280): aad6253.
- International HapMap 3 Consortium (HapMap) (2003) The International HapMap Project. *Nature*, **426**(6968): 789–796.
- Jeanes, A., Gottardi, C.J., and Yap, A.S. (2008) Cadherins and cancer: how does cadherin dysfunction promote tumor progression? *Oncogene*, **27**(55): 6920–6929.
- Jerby-Arnon, L., Pfeffer, N., Waldman, Y., McGarry, L., James, D., Shanks, E., Seashore-Ludlow, B., Weinstock, A., Geiger, T., Clemons, P., et al. (2014) Predicting cancer-specific vulnerability via data-driven detection of synthetic lethality. *Cell*, **158**(5): 1199–1209.
- Joachims, T. (1999) Making large-scale support vector machine learning practical. In S. Bernhard, lkopf, J.C.B. Christopher, and J.S. Alexander (editors), *Advances in kernel methods*, 169–184. MIT Press.
- Ju, Z., Liu, W., Roebuck, P.L., Siwak, D.R., Zhang, N., Lu, Y., Davies, M.A., Akbani, R., Weinstein, J.N., Mills, G.B., et al. (2015) Development of a robust classifier for quality control of reverse-phase protein arrays. *Bioinformatics*, **31**(6): 912.
- Kaelin, Jr, W. (2005) The concept of synthetic lethality in the context of anticancer therapy. *Nat Rev Cancer*, **5**(9): 689–98.
- Kaelin, Jr, W. (2009) Synthetic lethality: a framework for the development of wiser cancer therapeutics. *Genome Med*, **1**: 99.

- Kamada, T. and Kawai, S. (1989) An algorithm for drawing general undirected graphs. *Information Processing Letters*, **31**(1): 7–15.
- Kawai, J., Shinagawa, A., Shibata, K., Yoshino, M., Itoh, M., Ishii, Y., Arakawa, T., Hara, A., Fukunishi, Y., Konno, H., et al. (2001) Functional annotation of a full-length mouse cDNA collection. *Nature*, **409**(6821): 685–690.
- Kelley, R. and Ideker, T. (2005) Systematic interpretation of genetic interactions using protein networks. *Nat Biotech*, **23**(5): 561–566.
- Kelly, S.T. (2013) *Statistical Predictions of Synthetic Lethal Interactions in Cancer*. Dissertation, University of Otago.
- Kelly, S.T., Single, A.B., Telford, B.J., Beetham, H.G., Godwin, T.D., Chen, A., Black, M.A., and Guilford, P.J. (unpublished) Towards HDGC chemoprevention: vulnerabilities in E-cadherin-negative cells identified by genome-wide interrogation of isogenic cell lines and whole tumors. Submitted to *Cancer Prev Res*.
- Kim, N.G., Koh, E., Chen, X., and Gumbiner, B.M. (2011) E-cadherin mediates contact inhibition of proliferation through Hippo signaling-pathway components. *Proc Natl Acad Sci USA*, **108**(29): 11930–11935.
- Kockel, L., Zeitlinger, J., Staszewski, L.M., Mlodzik, M., and Bohmann, D. (1997) Jun in drosophila development: redundant and nonredundant functions and regulation by two mapk signal transduction pathways. *Genes & Development*, **11**(13): 1748–1758.
- Kozlov, K.N., Gursky, V.V., Kulakovskiy, I.V., and Samsonova, M.G. (2015) Sequence-based model of gap gene regulation network. *BMC Genomics*, **15**(Suppl 12): S6.
- Kranthi, S., Rao, S., and Manimaran, P. (2013) Identification of synthetic lethal pairs in biological systems through network information centrality. *Mol BioSyst*, **9**(8): 2163–2167.
- Kroepil, F., Fluegen, G., Totikov, Z., Baldus, S.E., Vay, C., Schauer, M., Topp, S.A., Esch, J.S., Knoefel, W.T., and Stoecklein, N.H. (2012) Down-regulation of CDH1 is associated with expression of SNAI1 in colorectal adenomas. *PLoS ONE*, **7**(9): e46665.
- Lander, E.S. (2011) Initial impact of the sequencing of the human genome. *Nature*, **470**(7333): 187–197.

- Lander, E.S., Linton, L.M., Birren, B., Nusbaum, C., Zody, M.C., Baldwin, J., Devon, K., Dewar, K., Doyle, M., FitzHugh, W., *et al.* (2001) Initial sequencing and analysis of the human genome. *Nature*, **409**(6822): 860–921.
- Langmead, B., Trapnell, C., Pop, M., and Salzberg, S.L. (2009) Ultrafast and memory-efficient alignment of short DNA sequences to the human genome. *Genome Biol*, **10**(3): R25.
- Latora, V. and Marchiori, M. (2001) Efficient behavior of small-world networks. *Phys Rev Lett*, **87**: 198701.
- Laufer, C., Fischer, B., Billmann, M., Huber, W., and Boutros, M. (2013) Mapping genetic interactions in human cancer cells with RNAi and multiparametric phenotyping. *Nat Methods*, **10**(5): 427–31.
- Law, C.W., Chen, Y., Shi, W., and Smyth, G.K. (2014) voom: precision weights unlock linear model analysis tools for RNA-seq read counts. *Genome Biol*, **15**(2): R29.
- Le Meur, N. and Gentleman, R. (2008) Modeling synthetic lethality. *Genome Biol*, **9**(9): R135.
- Le Meur, N., Jiang, Z., Liu, T., Mar, J., and Gentleman, R.C. (2014) Slgi: Synthetic lethal genetic interaction. r package version 1.26.0.
- Lee, A.Y., Perreault, R., Harel, S., Boulier, E.L., Suderman, M., Hallett, M., and Jenna, S. (2010a) Searching for signaling balance through the identification of genetic interactors of the rab guanine-nucleotide dissociation inhibitor gdi-1. *PLoS ONE*, **5**(5): e10624.
- Lee, I., Lehner, B., Vavouri, T., Shin, J., Fraser, A.G., and Marcotte, E.M. (2010b) Predicting genetic modifier loci using functional gene networks. *Genome Research*, **20**(8): 1143–1153.
- Lee, I. and Marcotte, E.M. (2009) Effects of functional bias on supervised learning of a gene network model. *Methods Mol Biol*, **541**: 463–75.
- Lee, M.J., Ye, A.S., Gardino, A.K., Heijink, A.M., Sorger, P.K., MacBeath, G., and Yaffe, M.B. (2012) Sequential application of anticancer drugs enhances cell death by rewiring apoptotic signaling networks. *Cell*, **149**(4): 780–94.

- Lehner, B., Crombie, C., Tischler, J., Fortunato, A., and Fraser, A.G. (2006) Systematic mapping of genetic interactions in *caenorhabditis elegans* identifies common modifiers of diverse signaling pathways. *Nat Genet*, **38**(8): 896–903.
- Li, X.J., Mishra, S.K., Wu, M., Zhang, F., and Zheng, J. (2014) Syn-lethality: An integrative knowledge base of synthetic lethality towards discovery of selective anticancer therapies. *Biomed Res Int*, **2014**: 196034.
- Linehan, W.M., Spellman, P.T., Ricketts, C.J., Creighton, C.J., Fei, S.S., Davis, C., Wheeler, D.A., Murray, B.A., Schmidt, L., Vocke, C.D., *et al.* (2016) Comprehensive Molecular Characterization of Papillary Renal-Cell Carcinoma. *N Engl J Med*, **374**(2): 135–145.
- Lokody, I. (2014) Computational modelling: A computational crystal ball. *Nature Reviews Cancer*, **14**(10): 649–649.
- Lord, C.J., Tutt, A.N., and Ashworth, A. (2015) Synthetic lethality and cancer therapy: lessons learned from the development of PARP inhibitors. *Annu Rev Med*, **66**: 455–470.
- Lu, X., Kensche, P.R., Huynen, M.A., and Notebaart, R.A. (2013) Genome evolution predicts genetic interactions in protein complexes and reveals cancer drug targets. *Nat Commun*, **4**: 2124.
- Lu, X., Megchelenbrink, W., Notebaart, R.A., and Huynen, M.A. (2015) Predicting human genetic interactions from cancer genome evolution. *PLoS One*, **10**(5): e0125795.
- Lum, P.Y., Armour, C.D., Stepaniants, S.B., Cavet, G., Wolf, M.K., Butler, J.S., Hinchshaw, J.C., Garnier, P., Prestwich, G.D., Leonardson, A., *et al.* (2004) Discovering modes of action for therapeutic compounds using a genome-wide screen of yeast heterozygotes. *Cell*, **116**(1): 121–137.
- Luo, J., Solimini, N.L., and Elledge, S.J. (2009) Principles of Cancer Therapy: Oncogene and Non-oncogene Addiction. *Cell*, **136**(5): 823–837.
- Machado, J., Olivera, C., Carvalh, R., Soares, P., Berx, G., Caldas, C., Sercuca, R., Carneiro, F., and Sorbrinho-Simoes, M. (2001) E-cadherin gene (*CDH1*) promoter methylation as the second hit in sporadic diffuse gastric carcinoma. *Oncogene*, **20**: 1525–1528.

- Markowetz, F. (2017) All biology is computational biology. *PLoS Biol*, **15**(3): e2002050.
- Masciari, S., Larsson, N., Senz, J., Boyd, N., Kaurah, P., Kandel, M.J., Harris, L.N., Pinheiro, H.C., Troussard, A., Miron, P., *et al.* (2007) Germline E-cadherin mutations in familial lobular breast cancer. *J Med Genet*, **44**(11): 726–31.
- Mattison, J., van der Weyden, L., Hubbard, T., and Adams, D.J. (2009) Cancer gene discovery in mouse and man. *Biochim Biophys Acta*, **1796**(2): 140–161.
- McLachlan, J., George, A., and Banerjee, S. (2016) The current status of parp inhibitors in ovarian cancer. *Tumori*, **102**(5): 433–440.
- McLendon, R., Friedman, A., Bigner, D., Van Meir, E.G., Brat, D.J., Mastrogiannakis, G.M., Olson, J.J., Mikkelsen, T., Lehman, N., Aldape, K., *et al.* (2008) Comprehensive genomic characterization defines human glioblastoma genes and core pathways. *Nature*, **455**(7216): 1061–1068.
- Miles, D.W. (2001) Update on HER-2 as a target for cancer therapy: herceptin in the clinical setting. *Breast Cancer Res*, **3**(6): 380–384.
- Mortazavi, A., Williams, B.A., McCue, K., Schaeffer, L., and Wold, B. (2008) Mapping and quantifying mammalian transcriptomes by RNA-Seq. *Nat Methods*, **5**(7): 621–628.
- Muzny, D.M., Bainbridge, M.N., Chang, K., Dinh, H.H., Drummond, J.A., Fowler, G., Kovar, C.L., Lewis, L.R., Morgan, M.B., Newsham, I.F., *et al.* (2012) Comprehensive molecular characterization of human colon and rectal cancer. *Nature*, **487**(7407): 330–337.
- Nagalla, S., Chou, J.W., Willingham, M.C., Ruiz, J., Vaughn, J.P., Dubey, P., Lash, T.L., Hamilton-Dutoit, S.J., Bergh, J., Sotiriou, C., *et al.* (2013) Interactions between immunity, proliferation and molecular subtype in breast cancer prognosis. *Genome Biol*, **14**(4): R34.
- Neeley, E.S., Kornblau, S.M., Coombes, K.R., and Baggerly, K.A. (2009) Variable slope normalization of reverse phase protein arrays. *Bioinformatics*, **25**(11): 1384.
- Novomestky, F. (2012) *matrixcalc: Collection of functions for matrix calculations*. R package version 1.0-3.

- Nowak, M.A., Boerlijst, M.C., Cooke, J., and Smith, J.M. (1997) Evolution of genetic redundancy. *Nature*, **388**(6638): 167–171.
- Oliveira, C., Senz, J., Kaurah, P., Pinheiro, H., Sanges, R., Haegert, A., Corso, G., Schouten, J., Fitzgerald, R., Vogelsang, H., et al. (2009) Germline *CDH1* deletions in hereditary diffuse gastric cancer families. *Human Molecular Genetics*, **18**(9): 1545–1555.
- Oliveira, C., Seruca, R., Hoogerbrugge, N., Ligtenberg, M., and Carneiro, F. (2013) Clinical utility gene card for: Hereditary diffuse gastric cancer (HDGC). *Eur J Hum Genet*, **21**(8).
- Pandey, G., Zhang, B., Chang, A.N., Myers, C.L., Zhu, J., Kumar, V., and Schadt, E.E. (2010) An integrative multi-network and multi-classifier approach to predict genetic interactions. *PLoS Comput Biol*, **6**(9).
- Parker, J., Mullins, M., Cheung, M., Leung, S., Voduc, D., Vickery, T., Davies, S., Fauron, C., He, X., Hu, Z., et al. (2009) Supervised risk predictor of breast cancer based on intrinsic subtypes. *Journal of Clinical Oncology*, **27**(8): 1160–1167.
- Pereira, B., Chin, S.F., Rueda, O.M., Vollan, H.K., Provenzano, E., Bardwell, H.A., Pugh, M., Jones, L., Russell, R., Sammut, S.J., et al. (2016) Erratum: The somatic mutation profiles of 2,433 breast cancers refine their genomic and transcriptomic landscapes. *Nat Commun*, **7**: 11908.
- Perou, C.M., Sørlie, T., Eisen, M.B., van de Rijn, M., Jeffrey, S.S., Rees, C.A., Pollack, J.R., Ross, D.T., Johnsen, H., Akslen, L.A., et al. (2000) Molecular portraits of human breast tumours. *Nature*, **406**(6797): 747–752.
- Polyak, K. and Weinberg, R.A. (2009) Transitions between epithelial and mesenchymal states: acquisition of malignant and stem cell traits. *Nat Rev Cancer*, **9**(4): 265–73.
- Prahallas, A., Sun, C., Huang, S., Di Nicolantonio, F., Salazar, R., Zecchin, D., Beijersbergen, R.L., Bardelli, A., and Bernards, R. (2012) Unresponsiveness of colon cancer to *BRAF*(v600e) inhibition through feedback activation of egfr. *Nature*, **483**(7387): 100–3.
- R Core Team (2016) *R: A Language and Environment for Statistical Computing*. R Foundation for Statistical Computing, Vienna, Austria. R version 3.3.2.

- Ravnan, M.C. and Matalka, M.S. (2012) Vemurafenib in patients with *BRAF* v600e mutation-positive advanced melanoma. *Clin Ther*, **34**(7): 1474–86.
- Ritchie, M.E., Phipson, B., Wu, D., Hu, Y., Law, C.W., Shi, W., and Smyth, G.K. (2015) limma powers differential expression analyses for RNA-sequencing and microarray studies. *Nucleic Acids Research*, **43**(7): e47.
- Robinson, M.D. and Oshlack, A. (2010) A scaling normalization method for differential expression analysis of RNA-seq data. *Genome Biol*, **11**(3): R25.
- Roguev, A., Bandyopadhyay, S., Zofall, M., Zhang, K., Fischer, T., Collins, S.R., Qu, H., Shales, M., Park, H.O., Hayles, J., et al. (2008) Conservation and rewiring of functional modules revealed by an epistasis map in fission yeast. *Science*, **322**(5900): 405–10.
- Roychowdhury, S. and Chinnaiyan, A.M. (2016) Translating cancer genomes and transcriptomes for precision oncology. *CA Cancer J Clin*, **66**(1): 75–88.
- Rung, J. and Brazma, A. (2013) Reuse of public genome-wide gene expression data. *Nat Rev Genet*, **14**(2): 89–99.
- Rustici, G., Kolesnikov, N., Brandizi, M., Burdett, T., Dylag, M., Emam, I., Farne, A., Hastings, E., Ison, J., Keays, M., et al. (2013) ArrayExpress update—trends in database growth and links to data analysis tools. *Nucleic Acids Res*, **41**(Database issue): D987–990.
- Ryan, C., Lord, C., and Ashworth, A. (2014) Daisy: Picking synthetic lethals from cancer genomes. *Cancer Cell*, **26**(3): 306–308.
- Schena, M. (1996) Genome analysis with gene expression microarrays. *Bioessays*, **18**(5): 427–431.
- Scheuer, L., Kauff, N., Robson, M., Kelly, B., Barakat, R., Satagopan, J., Ellis, N., Hensley, M., Boyd, J., Borgen, P., et al. (2002) Outcome of preventive surgery and screening for breast and ovarian cancer in BRCA mutation carriers. *J Clin Oncol*, **20**(5): 1260–1268.
- Semb, H. and Christofori, G. (1998) The tumor-suppressor function of E-cadherin. *Am J Hum Genet*, **63**(6): 1588–93.

Sing, T., Sander, O., Beerenwinkel, N., and Lengauer, T. (2005) Rocr: visualizing classifier performance in r. *Bioinformatics*, **21**(20): 7881.

Slurm development team (Slurm) (2017) Slurm workload manager. <https://slurm.schedmd.com/>. Accessed: 25/03/2017.

Sørlie, T., Perou, C.M., Tibshirani, R., Aas, T., Geisler, S., Johnsen, H., Hastie, T., Eisen, M.B., van de Rijn, M., Jeffrey, S.S., *et al.* (2001) Gene expression patterns of breast carcinomas distinguish tumor subclasses with clinical implications. *Proc Natl Acad Sci USA*, **98**(19): 10869–10874.

Stajich, J.E. and Lapp, H. (2006) Open source tools and toolkits for bioinformatics: significance, and where are we? *Brief Bioinformatics*, **7**(3): 287–296.

Stratton, M.R., Campbell, P.J., and Futreal, P.A. (2009) The cancer genome. *Nature*, **458**(7239): 719–724.

Ström, C. and Helleday, T. (2012) Strategies for the use of poly(adenosine diphosphate ribose) polymerase (parp) inhibitors in cancer therapy. *Biomolecules*, **2**(4): 635–649.

Sun, C., Wang, L., Huang, S., Heynen, G.J.J.E., Prahallad, A., Robert, C., Haanen, J., Blank, C., Wesseling, J., Willems, S.M., *et al.* (2014) Reversible and adaptive resistance to *BRAF*(v600e) inhibition in melanoma. *Nature*, **508**(7494): 118–122.

Telford, B.J., Chen, A., Beetham, H., Frick, J., Brew, T.P., Gould, C.M., Single, A., Godwin, T., Simpson, K.J., and Guilford, P. (2015) Synthetic lethal screens identify vulnerabilities in gpcr signalling and cytoskeletal organization in E-cadherin-deficient cells. *Mol Cancer Ther*, **14**(5): 1213–1223.

The 1000 Genomes Project Consortium (1000 Genomes) (2010) A map of human genome variation from population-scale sequencing. *Nature*, **467**(7319): 1061–1073.

The Cancer Genome Atlas Research Network (TCGA) (2012) Comprehensive molecular portraits of human breast tumours. *Nature*, **490**(7418): 61–70.

The Cancer Genome Atlas Research Network (TCGA) (2017) The Cancer Genome Atlas Project. <https://cancergenome.nih.gov/>. Accessed: 26/03/2017.

The Catalogue Of Somatic Mutations In Cancer (COSMIC) (2016) Cosmic: The catalogue of somatic mutations in cancer. <http://cancer.sanger.ac.uk/cosmic>. Release 79 (23/08/2016), Accessed: 05/02/2017.

The Comprehensive R Archive Network (CRAN) (2017) Cran. <https://cran.r-project.org/>. Accessed: 24/03/2017.

The ENCODE Project Consortium (ENCODE) (2004) The ENCODE (ENCyclopedia Of DNA Elements) Project. *Science*, **306**(5696): 636–640.

The National Cancer Institute (NCI) (2015) The genetics of cancer. <https://www.cancer.gov/about-cancer/causes-prevention/genetics>. Published: 22/04/2015, Accessed: 22/03/2017.

The New Zealand eScience Infrastructure (NeSI) (2017) NeSI. <https://www.nesi.org.nz/>. Accessed: 25/03/2017.

Tierney, L., Rossini, A.J., Li, N., and Sevcikova, H. (2015) *snow: Simple Network of Workstations*. R package version 0.4-2.

Tiong, K.L., Chang, K.C., Yeh, K.T., Liu, T.Y., Wu, J.H., Hsieh, P.H., Lin, S.H., Lai, W.Y., Hsu, Y.C., Chen, J.Y., *et al.* (2014) Csnk1e/ctnnb1 are synthetic lethal to tp53 in colorectal cancer and are markers for prognosis. *Neoplasia*, **16**(5): 441–50.

Tischler, J., Lehner, B., and Fraser, A.G. (2008) Evolutionary plasticity of genetic interaction networks. *Nat Genet*, **40**(4): 390–391.

Tomasetti, C. and Vogelstein, B. (2015) Cancer etiology. Variation in cancer risk among tissues can be explained by the number of stem cell divisions. *Science*, **347**(6217): 78–81.

Tong, A.H., Evangelista, M., Parsons, A.B., Xu, H., Bader, G.D., Page, N., Robinson, M., Raghibizadeh, S., Hogue, C.W., Bussey, H., *et al.* (2001) Systematic genetic analysis with ordered arrays of yeast deletion mutants. *Science*, **294**(5550): 2364–8.

Tong, A.H., Lesage, G., Bader, G.D., Ding, H., Xu, H., Xin, X., Young, J., Berriz, G.F., Brost, R.L., Chang, M., *et al.* (2004) Global mapping of the yeast genetic interaction network. *Science*, **303**(5659): 808–13.

Tran, B., Dancey, J.E., Kamel-Reid, S., McPherson, J.D., Bedard, P.L., Brown, A.M., Zhang, T., Shaw, P., Onetto, N., Stein, L., *et al.* (2012) Cancer genomics: technology, discovery, and translation. *J Clin Oncol*, **30**(6): 647–660.

Travers, J. and Milgram, S. (1969) An experimental study of the small world problem. *Sociometry*, **32**(4): 425–443.

- Tsai, H.C., Li, H., Van Neste, L., Cai, Y., Robert, C., Rassool, F.V., Shin, J.J., Harbom, K.M., Beaty, R., Pappou, E., *et al.* (2012) Transient low doses of dna-demethylating agents exert durable antitumor effects on hematological and epithelial tumor cells. *Cancer Cell*, **21**(3): 430–46.
- Tunggal, J.A., Helfrich, I., Schmitz, A., Schwarz, H., Gunzel, D., Fromm, M., Kemler, R., Krieg, T., and Niessen, C.M. (2005) E-cadherin is essential for in vivo epidermal barrier function by regulating tight junctions. *EMBO J*, **24**(6): 1146–1156.
- Tutt, A., Robson, M., Garber, J.E., Domchek, S.M., Audeh, M.W., Weitzel, J.N., Friedlander, M., Arun, B., Loman, N., Schmutzler, R.K., *et al.* (2010) Oral poly(adt-ribose) polymerase inhibitor olaparib in patients with *BRCA1* or *BRCA2* mutations and advanced breast cancer: a proof-of-concept trial. *Lancet*, **376**(9737): 235–44.
- University of California, Santa Cruz (UCSC) (2012) Ucsc cancer browser. Accessed 29/03/2012.
- van der Meer, R., Song, H.Y., Park, S.H., Abdulkadir, S.A., and Roh, M. (2014) RNAi screen identifies a synthetic lethal interaction between PIM1 overexpression and PLK1 inhibition. *Clinical Cancer Research*, **20**(12): 3211–3221.
- van der Post, R.S., Vogelaar, I.P., Carneiro, F., Guilford, P., Huntsman, D., Hoogerbrugge, N., Caldas, C., Schreiber, K.E., Hardwick, R.H., Ausems, M.G., *et al.* (2015) Hereditary diffuse gastric cancer: updated clinical guidelines with an emphasis on germline CDH1 mutation carriers. *J Med Genet*, **52**(6): 361–374.
- van Steen, K. (2012) Travelling the world of genegene interactions. *Briefings in Bioinformatics*, **13**(1): 1–19.
- van Steen, M. (2010) *Graph Theory and Complex Networks: An Introduction*. Maarten van Steen, VU Amsterdam.
- Vapnik, V.N. (1995) *The nature of statistical learning theory*. Springer-Verlag New York, Inc.
- Vizeacoumar, F.J., Arnold, R., Vizeacoumar, F.S., Chandrashekhar, M., Buzina, A., Young, J.T., Kwan, J.H., Sayad, A., Mero, P., Lawo, S., *et al.* (2013) A negative genetic interaction map in isogenic cancer cell lines reveals cancer cell vulnerabilities. *Mol Syst Biol*, **9**: 696.

- Vogelstein, B., Papadopoulos, N., Velculescu, V.E., Zhou, S., Diaz, L.A., and Kinzler, K.W. (2013) Cancer genome landscapes. *Science*, **339**(6127): 1546–1558.
- Vos, C.B., Cleton-Jansen, A.M., Berx, G., de Leeuw, W.J., ter Haar, N.T., van Roy, F., Cornelisse, C.J., Peterse, J.L., and van de Vijver, M.J. (1997) E-cadherin inactivation in lobular carcinoma in situ of the breast: an early event in tumorigenesis. *Br J Cancer*, **76**(9): 1131–3.
- Waldron, D. (2016) Cancer genomics: A multi-layer omics approach to cancer. *Nat Rev Genet*, **17**(8): 436–437.
- Wang, K., Singh, D., Zeng, Z., Coleman, S.J., Huang, Y., Savich, G.L., He, X., Mieczkowski, P., Grimm, S.A., Perou, C.M., *et al.* (2010) MapSplice: accurate mapping of RNA-seq reads for splice junction discovery. *Nucleic Acids Res*, **38**(18): e178.
- Wang, X. and Simon, R. (2013) Identification of potential synthetic lethal genes to p53 using a computational biology approach. *BMC Medical Genomics*, **6**(1): 30.
- Wappett, M. (2014) Bisep: Toolkit to identify candidate synthetic lethality. r package version 2.0.
- Wappett, M., Dulak, A., Yang, Z.R., Al-Watban, A., Bradford, J.R., and Dry, J.R. (2016) Multi-omic measurement of mutually exclusive loss-of-function enriches for candidate synthetic lethal gene pairs. *BMC Genomics*, **17**: 65.
- Warnes, G.R., Bolker, B., Bonebakker, L., Gentleman, R., Liaw, W.H.A., Lumley, T., Maechler, M., Magnusson, A., Moeller, S., Schwartz, M., *et al.* (2015) *gplots: Various R Programming Tools for Plotting Data*. R package version 2.17.0.
- Watts, D.J. and Strogatz, S.H. (1998) Collective dynamics of 'small-world' networks. *Nature*, **393**(6684): 440–2.
- Weinstein, I.B. (2000) Disorders in cell circuitry during multistage carcinogenesis: the role of homeostasis. *Carcinogenesis*, **21**(5): 857–864.
- Weinstein, J.N., Akbani, R., Broom, B.M., Wang, W., Verhaak, R.G., McConkey, D., Lerner, S., Morgan, M., Creighton, C.J., Smith, C., *et al.* (2014) Comprehensive molecular characterization of urothelial bladder carcinoma. *Nature*, **507**(7492): 315–322.

- Weinstein, J.N., Collisson, E.A., Mills, G.B., Shaw, K.R., Ozenberger, B.A., Ellrott, K., Shmulevich, I., Sander, C., Stuart, J.M., Chang, K., *et al.* (2013) The Cancer Genome Atlas Pan-Cancer analysis project. *Nat Genet*, **45**(10): 1113–1120.
- Wickham, H. and Chang, W. (2016) *devtools: Tools to Make Developing R Packages Easier*. R package version 1.12.0.
- Wickham, H., Danenberg, P., and Eugster, M. (2017) *roxygen2: In-Line Documentation for R*. R package version 6.0.1.
- Wong, S.L., Zhang, L.V., Tong, A.H.Y., Li, Z., Goldberg, D.S., King, O.D., Lesage, G., Vidal, M., Andrews, B., Bussey, H., *et al.* (2004) Combining biological networks to predict genetic interactions. *Proceedings of the National Academy of Sciences of the United States of America*, **101**(44): 15682–15687.
- World Health Organization (WHO) (2017) Fact sheet: Cancer. <http://www.who.int/mediacentre/factsheets/fs297/en/>. Updated February 2017, Accessed: 22/03/2017.
- Wu, M., Li, X., Zhang, F., Li, X., Kwoh, C.K., and Zheng, J. (2014) In silico prediction of synthetic lethality by meta-analysis of genetic interactions, functions, and pathways in yeast and human cancer. *Cancer Inform*, **13**(Suppl 3): 71–80.
- Yu, H. (2002) Rmpi: Parallel statistical computing in r. *R News*, **2**(2): 10–14.
- Zhang, F., Wu, M., Li, X.J., Li, X.L., Kwoh, C.K., and Zheng, J. (2015) Predicting essential genes and synthetic lethality via influence propagation in signaling pathways of cancer cell fates. *J Bioinform Comput Biol*, **13**(3): 1541002.
- Zhang, J., Baran, J., Cros, A., Guberman, J.M., Haider, S., Hsu, J., Liang, Y., Rivkin, E., Wang, J., Whitty, B., *et al.* (2011) International cancer genome consortium data portal a one-stop shop for cancer genomics data. *Database: The Journal of Biological Databases and Curation*, **2011**: bar026.
- Zhong, W. and Sternberg, P.W. (2006) Genome-wide prediction of c. elegans genetic interactions. *Science*, **311**(5766): 1481–1484.
- Zweig, M.H. and Campbell, G. (1993) Receiver-operating characteristic (roc) plots: a fundamental evaluation tool in clinical medicine. *Clinical Chemistry*, **39**(4): 561–577.